

# **The specific role of iron in promoting adventitious root formation in petunia cuttings**

**Dissertation**

**zur Erlangung des Doktorgrades  
der Naturwissenschaften (Dr. rer. nat.)**

der  
Naturwissenschaftlichen Fakultät I  
– Biowissenschaften –  
der Martin Luther Universität  
Halle-Wittenberg

vorgelegt  
von Herrn **Alexander Hilo**  
geb. am 17.02.1986 in Molodechno

verteidigt am  
11.07.2017

begutachtet von:

**Prof. Dr. Nicolaus von Wirén (IPK, Gatersleben)**

**Prof. Dr. Klaus Humbeck (MLU, Halle)**

**Prof. Dr. Philipp Franken (IGZ, Großbeeren)**

HALLE (SAALE), GERMANY, 2017

## Acknowledgments

First of all I would like to express my sincere gratitude to my supervisors, Dr. Mohammad-Reza Hajirezaei and Prof. Nicolaus von Wirén, for giving me the opportunity to do this project and for all their patient guidance, encouragement and support throughout my research.

Furthermore, I wish to thank Prof. Klaus Humbeck and Prof. Philipp Franken for agreeing to evaluate this thesis.

Special thanks should be given to Dr. Uwe Droege and Prof. Philipp Franken, for their advice and fruitful discussions during my research.

I wish to acknowledge the effort of Dr. Fahimeh Shahinnia in establishing the hydroponic system and substantial help with initial experiments.

I would like to offer my special thanks to Dr. Michael Melzer and his colleagues, Dr. Twan Rutten, Dr. Marek Marzec, Aleksandra Muszyńska, Sybille Freist and Kirsten Hoffie for their support and assistance in histological analysis.

I would like to thank Dr. Goetz Hensel and Dr. Jochen Kumlehn for kindly providing a pGH183 vector and his support in developing a p9Ndoi-TOCS vector.

I wish to acknowledge excellent assistance in mineral analysis by Susanne Reiner and Dr. Yudelsy Antonia Tandron Moya.

I am particularly grateful for the assistance with the tissue culture given by Heike Nierig and Andrea Knospe.

My acknowledgments are extended to Enk Geyer and his colleagues for taking care of the glasshouse plants.

My special thanks and appreciation go to all of my former and current colleagues from the Molecular Plant Nutrition group for their lively discussions and useful suggestions.

I also wish to thank Dr. Britt Leps for her great support and personal effort in solving problems that chase every foreign student.

Finally, I would like to send my love and gratitude to my mother Larisa Hilo and my dearest friends, Enrico Nickel, Aleksandra Muszyńska, Alexandra Lešková, Pavel Grinkevich and Siarhei Sitnik for their support and all the sparkles of joy in my everyday life.

*To my first biology teacher, Natalia L. Pozdniakova  
I am infinitely grateful to her for showing me the mysterious and amazing  
world of Life Science*

*Прысвячаецца маёй першай настаўніцы біялогіі  
Наталлі Леанідаўне Паздняковай  
Я бясконца ўдзячны Вам за тое, што Вы адкрылі для мяне  
загадковы і цудоўны сусвет навукі пра жыццё*

## Table of contents

Abbreviations.....	1
List of Figures and Tables .....	3
1. Introduction.....	6
1.1 Adventitious roots as a part of the root system .....	6
1.2 Stages of AR formation .....	8
1.3 Essential factors involved in AR formation .....	10
1.3.1 Hormonal regulation of AR formation .....	10
1.3.1.1 Auxin .....	11
1.3.1.2 Cytokinins.....	12
1.3.1.3 Stress-related phytohormones .....	13
1.3.1.4 Other hormones and signaling molecules .....	14
1.3.2 Role of photosynthesis and carbohydrate metabolism in AR formation.....	15
1.3.3 Possible involvement of mineral nutrition in AR formation .....	19
1.4 Commercial importance of adventitious rooting.....	23
1.5 Petunia as a model.....	24
1.6 Aims and approaches of the current work .....	26
2. Materials and methods .....	28
2.1 Plant material, growth conditions and sampling .....	28
2.1.1 Plant growth conditions .....	28
2.1.2 Sample collection .....	28
2.1.3 Application of auxin regulators .....	29
2.2 Morphological assessment of AR formation.....	29
2.3 Histological and histochemical analyses .....	29
2.3.1 Histological examination .....	29
2.3.2 Quantitative analysis of AR formation .....	30
2.3.3 Histochemical detection of Fe.....	30
2.3.4 Confocal microscopy .....	31
2.4 Biochemical analyses .....	31

## Table of contents

---

2.4.1 Analysis of chlorophyll concentration in leaves .....	31
2.4.2 Quantitative measurement of GUS activity .....	32
2.4.3 Measurement of phytohormones .....	33
2.4.4 Carbohydrate and amino acid analysis .....	34
2.4.5 Analysis of primary metabolites .....	35
2.4.6 Mineral element analysis .....	36
2.5 Analysis of transcript abundance .....	36
2.5.1 RNA isolation and cDNA synthesis .....	36
2.5.2 q(RT)-PCR.....	36
2.6 Generation of DR5::GFP/GUS auxin reporter petunia plants .....	37
2.6.1 Standard molecular techniques and bacterial strains.....	37
2.6.2 Generation of p9N-DR5-GFP-GUSi construct .....	37
2.6.3 Plant transformation .....	38
2.7 Statistical analyses.....	38
3. Results .....	39
3.1 The role of individual nutrients in AR formation.....	39
3.1.1 Determination of mineral nutrients essential for AR formation.....	39
3.1.2 Anatomy of AR formation in response to nutrient application.....	43
3.2 The effect of iron and ammonium on mineral homeostasis and metabolic activity during AR formation.....	46
3.2.1 Mineral status during AR formation in response to nutrient application.....	46
3.2.2 Effect of nutrient application on iron acquisition and homeostasis genes.....	48
3.2.3 The impact of nutrient application on carbohydrate distribution .....	50
3.2.4 The effect of nutrient application on primary metabolites and organic acids .....	51
3.2.5 The impact of nutrient application on concentrations of amino acids .....	53
3.2.6 Impact of nutrients on the expression of genes involved in nitrogen metabolism .....	55
3.3 Involvement of phytohormones in nutrient-mediated AR formation .....	57
3.3.1 Effect of iron and ammonium application on the phytohormonal balance .....	57
3.3.2 Impact of iron and ammonium supply on the activity of the auxin reporter DR5::GFP/GUS .....	58

---

3.3.3 Effect of nutrients application on the expression of genes for auxin transport and biosynthesis.....	62
3.3.4 Impact of nutrient application on the expression of mitotic cyclins .....	64
3.3.5 Effect of auxin inhibitors on AR formation in response to nutrient application.....	64
3.3.6 Impact of auxin application on nutrient-mediated AR formation .....	66
3.4 The role of Fe distribution and allocation during AR formation .....	68
3.4.1 Effect of foliar Fe application on AR formation and chlorophyll concentration .....	68
3.4.2 Cellular localization of iron during AR formation.....	69
3.4.3 Effect of the medium pH on AR formation .....	71
3.5 Genotypic differences in Fe-dependant promotion of AR formation.....	72
4. Discussion.....	75
4.1 Promotion of AR formation by iron and ammonium .....	75
4.1.1 Ammonium and iron promote different root traits in LR and AR formation.....	75
4.1.2 Promotion of AR formation by iron and ammonium is not primarily related to the shoot nutritional status.....	76
4.2 Phytohormone homeostasis and metabolic activity in nutrient-dependent AR formation... ..	77
4.2.1 Phytohormone homeostasis is not a primary cause of nutrient-dependent stimulation of AR formation .....	77
4.2.2 Nutrient-dependent AR formation does not involve changes in primary metabolism ... ..	79
4.3 A local function of iron in the development of AR primordia.....	79
4.3.1 Developing AR meristems create a sink for Fe .....	79
4.3.2 Proposed mechanism for Fe-mediated stimulation of meristematic growth .....	80
4.3.3 Ammonium facilitates iron-mediated AR formation .....	83
4.3.4 Genotypic variability in Fe-mediated improvement of AR formation in petunia .....	84
5. Summary .....	86
6. Zusammenfassung.....	87
7. Literature.....	89
8. Appendix.....	101
9. Publications and proceedings related to the submitted thesis .....	109
10. Declaration .....	110
11. Curriculum vitae .....	111

## Abbreviations

ABA	Abscisic acid
ANOVA	Analysis of variance
AQC	6-Aminoquinolyl-N-hydroxysuccinimidyl carbamate
AR(s)	Adventitious root(s)
ATP	Adenosine tri-phosphate
ATPase	Adenosine triphosphatase
Aux	Auxins
bp	Base pairs
cDNA	Complementary deoxyribonucleic acid
CKs	Cytokinins
cZ	<i>cis</i> -Zeatin
cZR	<i>cis</i> -Zeatin riboside
d	Day(s)
DAB	3,3'-Diaminobenzidine
DAPI	4'6-Diamidino-2-phenylindole
DNA	Deoxyribonucleic acid
DNAse	Deoxyribonuclease enzyme
DPA	Dihydrophaseic acid
dpe	Days post excision
DW	Dry weight
DZR	Dihydrozeatin riboside
EDTA	Ethylenediaminetetraacetic acid
<i>EGFP</i>	Enhanced green fluorescent protein
EPA	Environmental protection agency
ER	Endoplasmic reticulum
EST	Expressed sequence tag
Et	Ethylene
FeEDDHA	Fe-ethylenediamine-NN'-bis(2-hydroxyphenylacetic acid)
FeEDTA	Ethylenediaminetetraacetic acid iron(III) sodium salt
FW	Fresh weight
GA	Gibberellins
GFP	Green fluorescent protein
GUS	$\beta$ - Glucuronidase
h	Hour(s)
H <sup>+</sup> -ATPase	Proton-translocating adenosine triphosphatase
HPLC	High-performance liquid chromatography
(HR)-ICP-MS	High resolution ion chromatography - mass spectrometry
IAA	Indole-3-acetic acid
IBA	Indole-3-butyric acid
IC-MS/MS	Ion chromatography – tandem mass spectrometry

---

ICP-MS	Inductively coupled plasma - mass spectrometry
iP	Isopentenyladenine
JA	Jasmonic acid
Kyn	L-Kynurenine
LR(s)	Lateral root(s)
LC-MS/MS	Liquid chromatography – tandem mass spectrometry
LSD Fisher's	Fisher's least significant difference method
MES	2-(N-morpholino)-ethanesulfonic acid
ml	Milliliter
mM	Millimolar (concentration)
MRM	Multiple reaction monitoring
mRNA	Messenger ribonucleic acid
MU	4-Methylumbelliferone
NAA	1-Naphthaleneacetic acid
nmol	Nanomole
NPA	N-1-Naphthylphthalamic acid
°C	Centigrade
OD <sub>600</sub>	Optical density at 600 nm
OES	Optical emission spectroscopy technique
oxIAA	2-Oxindole-3-acetic acid
P	Probability
PAT	Polar auxin transport
PCR	Polymerase chain reaction
PI	Propidium iodide
PR	Primary root
qPCR	Quantitative real-time polymerase chain reaction
qRT-PCR	Reverse transcription - quantitative real-time polymerase chain reaction
RNA	Ribonucleic acid
RNase	Ribonuclease enzyme
ROS	Reactive oxygen species
rpm	Revolutions per minute
rRNA	Ribosomal ribonucleic acid
(RT)-PCR	Reverse transcription - polymerase chain reaction
SE	Standard Error
Str	Strigolactones
<i>tZ</i>	<i>trans</i> -Zeatin
<i>tZR</i>	<i>trans</i> -Zeatin riboside
UDP	Uridine di-phosphate
UPLC	Ultra performance liquid chromatography
µg	Microgram
µl	Microlitre
µM	Micromolar (concentration)



## List of Figures and Tables

<b>Fig. 1</b> Anatomical and morphological structure of the root and apical meristem of <i>Arabidopsis</i> .	6
<b>Fig. 2</b> Types of the root systems.	7
<b>Fig. 3</b> Successive stages of adventitious root formation in leafy shoot cuttings.	9
<b>Fig. 4</b> Mechanisms for the involvement of major phytohormones in the regulation of adventitious root formation.	11
<b>Fig. 5</b> Mechanisms for the involvement of carbohydrates and their interaction with major phytohormones in regulation of adventitious root formation.	15
<b>Fig. 6</b> Potential mechanisms for the involvement of mineral nutrients in the regulation of adventitious root formation.	19
<b>Fig. 7</b> Wholesale value for operations with more than \$10,000 sales, in category “annual bedding/garden plants”, USA, 2015	24
<b>Fig. 8</b> Effect of the withdrawal of components from full mineral solution on adventitious root formation in <i>Petunia hybrida</i> .	39
<b>Fig. 9</b> Effect of the application of individual elements and their combinations on rooting performance of leafy cuttings of <i>Petunia hybrida</i> .	41
<b>Fig. 10</b> Effect of a “pulse application” of individual nutrients on adventitious root formation in <i>Petunia hybrida</i> .	42
<b>Fig. 11</b> Anatomy of adventitious root formation in <i>Petunia hybrida</i> cuttings in response to nutrient application.	44
<b>Fig. 12</b> Quantitative assessment of the dynamics of adventitious root formation in <i>Petunia hybrida</i> cuttings in response to nutrient application.	45
<b>Fig. 13</b> Mineral balance in the stem base and mature leaves of <i>Petunia hybrida</i> cuttings during adventitious root formation in response to nutrient application.	47
<b>Fig. 14</b> Transcript abundance of key Fe-related genes in the stem base of <i>Petunia hybrida</i> cuttings during adventitious root formation in response to nutrient application.	49

---

<b>Fig. 15</b> Concentrations of soluble carbohydrates in the stem base, mature leaves and phloem exudates of <i>Petunia hybrida</i> cuttings during adventitious formation in response to nutrient application.	50
<b>Fig. 16</b> Concentrations of primary intermediates of sugar metabolism in the stem base of <i>Petunia hybrida</i> cuttings during adventitious root formation in response to nutrient application.	52
<b>Fig. 17</b> Concentrations of proteinogenic amino acids in the stem base and in mature leaves of <i>Petunia hybrida</i> cuttings during adventitious root formation in response to nutrient application.	54
<b>Fig. 18</b> Transcript abundance of genes for N transport and metabolism in the stem and mature leaves of <i>Petunia hybrida</i> cuttings during adventitious root formation in response to nutrient application.	56
<b>Fig. 19</b> Concentrations of major phytohormones and their intermediates in the stem base of <i>Petunia hybrida</i> cuttings during adventitious root formation in response to nutrient application.	57
<b>Fig. 20</b> Auxin-induced GFP fluorescence in the stem base of <i>Petunia hybrida</i> DR5::GUS/GFP reporter line cuttings during adventitious root formation in response to nutrient application.	59
<b>Fig. 21</b> GUS activity in the stem base of a <i>Petunia hybrida</i> DR5::GUS/GFP reporter line cuttings during adventitious root formation in response to nutrient application.	61
<b>Fig. 22</b> Influence of nutrient application on transcript abundance of auxin-related genes in the stem base of <i>Petunia hybrida</i> cuttings during adventitious root formation.	63
<b>Fig. 23</b> Influence of nutrient application on transcript abundance of mitotic cyclins in the stem base of <i>Petunia hybrida</i> cuttings during adventitious root formation.	64
<b>Fig. 24</b> Effect of auxin inhibitors on adventitious root formation in <i>Petunia hybrida</i> in response to nutrient application.	65
<b>Fig. 25</b> Effect of the application of NAA to the cuttings of <i>Petunia hybrida</i> , supplied with Fe, full mineral or nutrient-free medium.	67

<b>Fig. 26</b> Effect of foliar or basal application of iron on adventitious root formation in <i>Petunia hybrida</i> .	68
<b>Fig. 27</b> Localization of Fe by Perls'/DAB method in the stem base of <i>Petunia hybrida</i> cuttings during adventitious root formation in response to Fe supply.	70
<b>Fig. 28</b> Effect of the medium pH on adventitious root formation in <i>Petunia hybrida</i> in comparison to the average rooting performance under ammonium and nitrate supply.	71
<b>Fig. 29</b> Effect of application of Fe on adventitious root formation in commercial cultivars of <i>Petunia hybrida</i> compared to average rooting performance of <i>P. hybrida</i> "Mitchell".	73
<b>Fig. 30</b> Working model for the stimulation of adventitious root formation by iron and ammonium in <i>Petunia hybrida</i> .	82
<b>Table 1</b> Effect of different concentrations of Fe and of N supply on adventitious root formation in <i>Petunia hybrida</i> cuttings	40

# 1. Introduction

## 1.1 Adventitious roots as a part of the root system

Roots are axial multicellular organs that evolved in the sporophytes of vascular plants as an adaptation to the terrestrial environment, enabling the anchorage of the plant body and deeper exploration of the substrate for more efficient acquisition of water and nutrients (Raven & Edwards, 2001; Seago & Fernando, 2013; Kenrick & Strullu-Derrien, 2014).

In modern seed plants, the root is initiated during the early embryogenesis and therefore referred to as embryonic or primary root (PR). The growth of the root occurs at the tip due to the activity of the root apical meristem, which divides in two directions with the centrally localized quiescent center that maintains the stem cells niche (Dolan et al., 1993). Outer meristem of the root apex forms the root cap that lubricates the penetrating root through the substrate and acts as a gravity sensor (Chen et al., 1999). The inner meristem, localized above the quiescent center, consists of actively dividing cells, which are organized into five concentric layers:

epidermis, cortex, endodermis, pericycle and stele (Fig. 1; Dolan et al., 1993). Above the meristem zone, cells elongate and proceed into differentiation. The differentiation zone is characterized by the formation of root hairs that increase the surface area of the root for better contact with the substrate (Bennett & Scheres, 2010). Formation of the Casparian strip in the endodermis at the differentiation zone isolates the stele from the apoplastic flow of water and dissolved nutrients, while lignification of the vasculature in the stele ensures the delivery of water and nutrients toward the aerial parts of the plants.

A distinctive characteristic of the differentiation zone is the formation of lateral roots (LRs, Fig. 1), considered post-embryonic and serving to increase the ability of the plant to

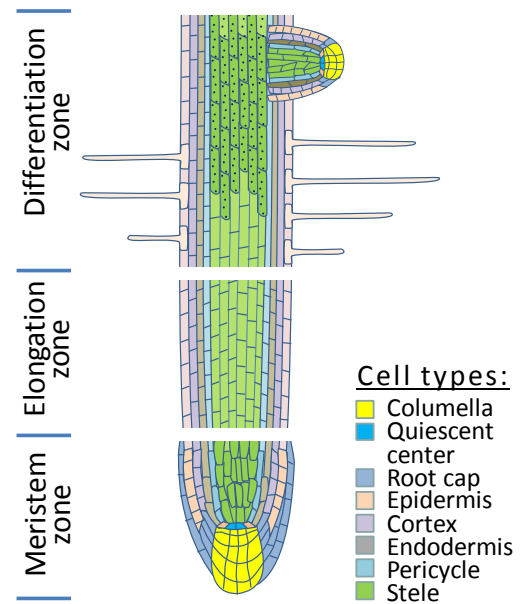


**Fig. 1** Anatomical and morphological structure of the root and apical meristem of Arabidopsis.

better explore the substrate. Unlike shoot branching, where the lateral meristems are formed on the surface of the apical meristem (Benková *et al.*, 2003), initiation of LRs occurs endogenously in the pericycle layer (Dolan *et al.*, 1993; Bennett & Scheres, 2010). Formation of secondary and higher-order LRs is a key mechanism for root branching that leads to the establishment of a primary root system, which prevails among dicotyledonous plant species (Fig. 2b).

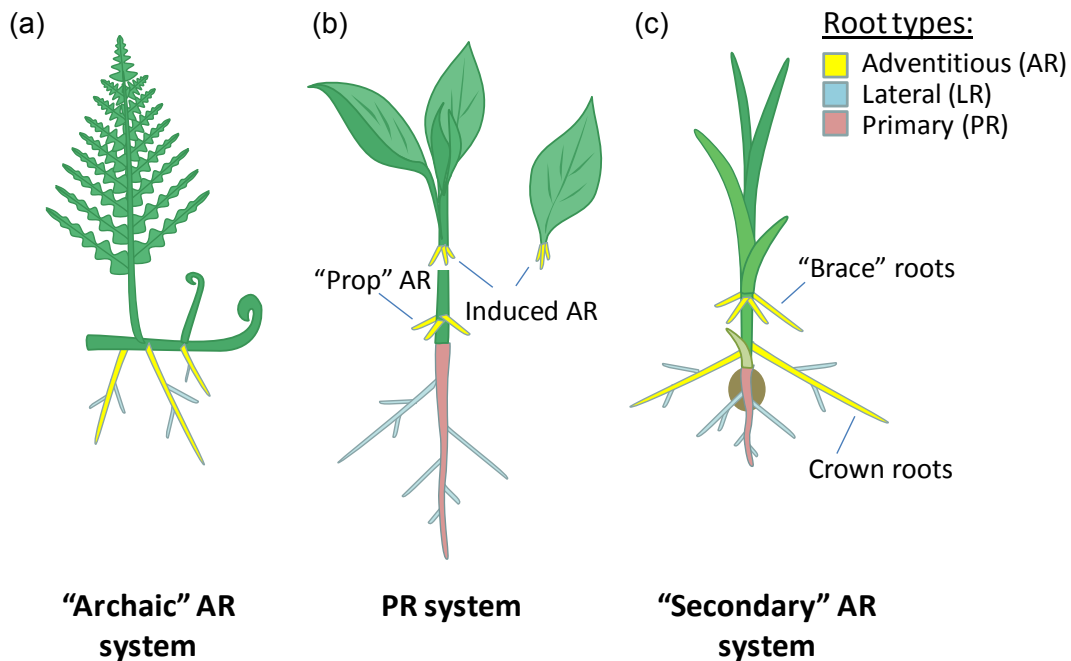


**Fig. 2** Types of the root systems. (a) "Archaic" root system of primitive non-seed plants, built by AR; (b) tap root system of dicotyledonous plants with dominant central primary root and (c) fibrous root system of the monocot plants with prevailing adventitious crown roots.

Another type of post-embryonic roots developing outside of the root system i.e. on shoots or leaves is designated as adventitious roots (AR). Although the term "adventitious" implies accidental or unusual anatomical position, from the evolutionary perspective, the most "archaic" root system typical for the primitive non-seed plants, members of *Pteridophyta* (Fig. 2a), is build up exclusively by ARs, suggesting that the first roots evolved in vascular plants were, in fact, adventitious (Raven & Edwards, 2001; Seago & Fernando, 2013; Kenrick & Strullu-Derrien, 2014).

Among the flowering plants ARs can form as a result of a developmental program, for instance, nodal roots of strawberry (*Fragaria vesca* L.) runners or non-nodal "prop" roots supporting the stem of certain vines and mangroves (Fig. 2,b; Steffens & Rasmussen, 2016). However, the most remarkable example of the dominance of

developmentally predefined ARs is the fibrous root system of monocots, where the embryonic root system, composed of primary and seminal roots, is eventually replaced by post-embryonic adventitious roots, i.e. crown roots, developing from belowground nodes and brace roots, forming on aboveground nodes (Hochholdinger *et al.*, 2004; Atkinson *et al.*, 2014). Therefore, such fibrous root system could be considered as a “secondary” AR system that developed as a result of specialization of monocots into herbaceous grass-like life forms.

Various members of the seed plants retained the ability to develop ARs in response to different environmental signals. ARs can emerge as a response to submergence of existing root systems, allowing plants to survive a flood or burial (Steffens & Rasmussen, 2016). On the other hand, formation of ARs on severed plant organs demonstrates the adaptation of several species to recovery into a new organism even upon extreme injuries. The latter phenomenon of so-called wound-induced AR formation is utilized in vegetative plant propagation by shoot and leaf cuttings that has found an intense application in modern propagation industry.

## 1.2 Stages of AR formation

Wound-induced AR formation is an example of the *de novo* organogenesis that principally resembles the process of LR formation, however the anatomical origin and initial signals that start the developmental program of formation of both root types may differ and will be considered throughout this work. Whereas LRs form almost exclusively in the pericycle, studies on different plants indicate that ARs can arise from several types of cells, however, frequently in proximity to the vascular tissues (De Klerk *et al.*, 1999). Such close positioning to the vasculature is vital for connection of the forming roots with the main stele. ARs were shown to originate from hypocotyl pericycle (*Arabidopsis thaliana* (L.) Heynh., *Coleus sp.*), phloem parenchyma (*Solanum lycopersicum* Lam., *Cucurbita pepo* L., *Vigna radiata* (L.) R.Wilczek, *Dianthus sp.*), cambium (*Malus domestica* L., *Acanthus sp.*, *Lonicera sp.*) or via formation of callus tissue (*Picea sp.*, *Pinus sp.*, *Ginkgo biloba* L.; Hartmann *et al.*, 2011; Bellini *et al.*, 2014)

Traditionally, the process of AR formation in the shoot cuttings is divided into three successive stages (1) induction, (2) initiation and (3) expression (Fig. 3; Kevers *et al.*, 1997; Li *et al.*, 2009).

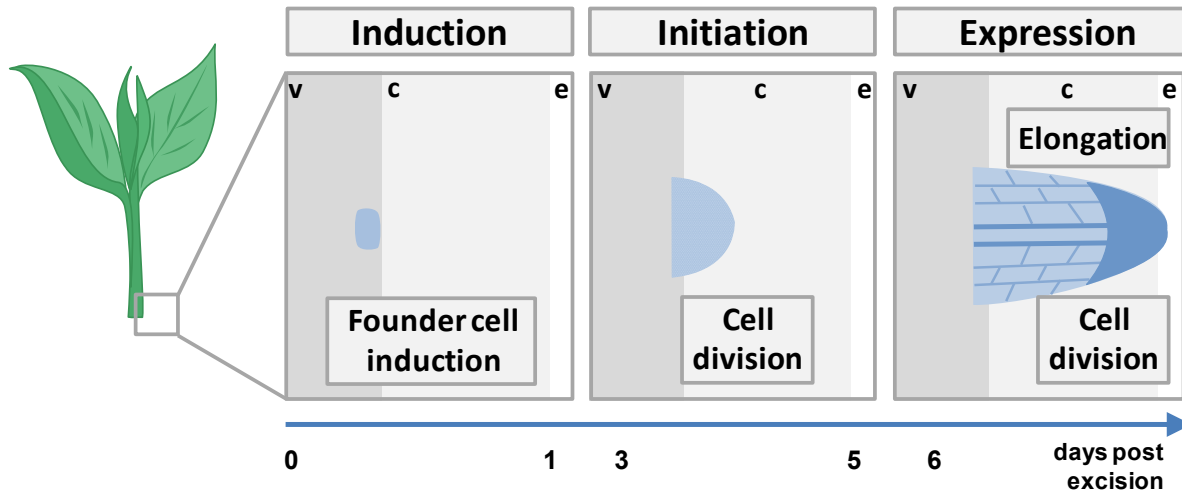


**Fig. 3** Successive stages of adventitious root formation in leafy shoot cuttings. v, vasculature; c, cortex; e, epidermis.

The first stage is devoid of any histological changes and is associated with the physical separation of the cutting from the stock plant that stimulates certain cells to become founder cells that are competent to eventually form ARs. Accumulating auxin in the stem base of the cutting is suggested to be the major player in induction of the founder cells and will be discussed together with the other phytohormones in the Subchapter 1.3.1. The period of auxin-mediated induction in microcuttings of apple tree (*Malus domestica* L.) and oak (*Quercus robur* L.) was reported to continue for up to two days post excision (dpe) of the cutting (De Klerk *et al.*, 1999; Vidal *et al.*, 2003), whereas in leafy cuttings of carnation (*Dianthus caryophyllus* L.) and petunia (*Petunia hybrida* Vilm.) this period lasted only for one day (Ahkami *et al.*, 2009, 2013; Agulló-Antón *et al.*, 2014).

Similar to initiation of LRs, induced founder cells undergo first anticlinal divisions followed by a series of mitotic divisions leading to the formation of meristematic cell clusters, characterized by dense cytoplasm and large nuclei. First mitotic events were observed in 2 dpe in microcuttings of apple tree and oak and in leafy cuttings of carnation, however in petunia and *Ficus pumila* L. first cell divisions were detected in 3 and 4 dpe, respectively (Ahkami *et al.*, 2009; Hartmann *et al.*, 2011).

Actively dividing meristematic cells arrange into the dome-shaped apical meristem that forms the body of the AR primordia, which defines the transition to the expression stage (De Klerk *et al.*, 1999). Subsequent elongation of the cells leaving the meristem allows protrusion of the AR primordia through the stem tissues, while differentiating vascular elements connect developing ARs with the main stele of the stem. The

expression stage ends with emergence of the ARs from the stem base (Kevers *et al.*, 1997). The time needed for emergence of the ARs defines the rate of AR formation and significantly varies between species. ARs emerged in microcuttings of apple tree already in 5 dpe (De Klerk *et al.*, 1999), in leafy cuttings of carnation and petunia first roots appeared in 8 dpe (Vidal *et al.*, 2003; Agulló-Antón *et al.*, 2014), whereas in rose (*Rosa sp.*) first ARs were observed only 3 weeks after excision (Hartmann *et al.*, 2011).

Moreover, performance of AR formation has been shown to vary between closely related species (Ford *et al.*, 2002; Amissah *et al.*, 2008; Pijut *et al.*, 2011) and even within the same plant depending on the state of maturity of the cuttings (Vidal *et al.*, 2003; Díaz-Sala, 2014), highlighting the fact that not only environmental conditions, but also a number of internal factors are involved in the regulation of AR formation.

### 1.3 Essential factors involved in AR formation

AR formation is a complex developmental process associated with a series of physiological transformations accompanying physical recovery of the root system within the base of the cutting. The early events taking place in the cutting are associated with mechanical wounding that causes disruption of existing transport pathways of assimilates and phytohormones within the stem, whereas the following stages are characterized by recovery of metabolic activity and regeneration of the new root system within the rooting zone. Photosynthesis and intensity of various metabolic processes in the cutting, on the other hand, strongly depend on temperature, humidity and light conditions, whereas the rooting medium may serve as a source of the mineral nutrients and other compounds essential for AR formation. Therefore, understanding the role of internal regulators of AR formation as well as environmental factors is crucial to improve rooting performance via manipulation of the rooting conditions or simulating internal signals.

#### 1.3.1 Hormonal regulation of AR formation

The entire process of AR formation, as well as the development of a root *per se*, is regulated by an ensemble of phytohormones and other signaling molecules that tightly integrate various environmental signals into the network of developmental programs. An overview model of the effects of major hormonal regulators of AR formation is summarized in Fig. 4 and described in details in the following Subchapters 1.3.1.1.-1.3.1.4.



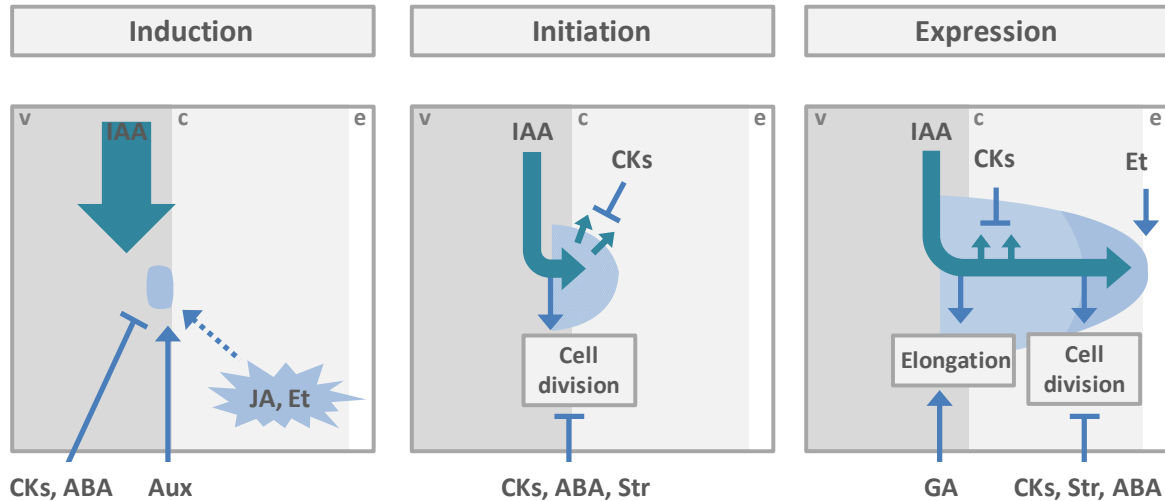


**Fig. 4** Mechanisms for the involvement of major phytohormones in the regulation of adventitious root formation. ABA, abscisic acid; Aux, auxins; CKs, cytokinins; Et, ethylene; GA, gibberellic acid; IAA, indole acetic acid; JA, jasmonic acid; Str, strigolactones.

### 1.3.1.1 Auxin

Auxin appears to regulate various aspects of root development, including early initiation of the primary root in embryogenesis, the meristem patterning, the cell elongation, gravitropic response and formation of LR<sub>s</sub> (Benková *et al.*, 2003; Bliou *et al.*, 2005; Petricka *et al.*, 2012). Unsurprisingly, auxin also takes the central role in AR formation. Since the early discovery of its rhizogenic properties in the cuttings of *Ilex sp.*, *Taxus sp.*, *Acer sp.* (Hitchcock & Zimmermann, 1936) auxin and its synthetic analogs have been intensely used for stimulation of AR formation in a wide range of plant species (Davis & Haissig, 1994; De Klerk *et al.*, 1999; Hartmann *et al.*, 2011).

A significant body of knowledge on the role of auxin in root development comes from the studies on LR formation (Fukaki & Tasaka, 2009; Moreno-Risueno *et al.*, 2011; Peret *et al.*, 2012; Lavenus *et al.*, 2013). However so far, there is no agreement on whether the auxin-mediated signaling network is shared between LR and AR formation. On the one hand, several *Arabidopsis* mutants in auxin transport and signaling demonstrate simultaneous perturbations in LR and AR formation (Fukaki *et al.*, 2002; Gutierrez *et al.*, 2009, 2012). On the other hand, both root types originate from anatomically dissimilar tissues and under different circumstances, that explain identification of certain signaling elements or auxin transporters to be specific only to one type of the roots (Pop *et al.*, 2011; Verstraeten *et al.*, 2014).

Transient increase of auxin levels appears to be the key mechanism for the induction of LR and ARs, however the position of founder cells of LR are developmentally pre-defined already within the root meristem due to the oscillating auxin fluxes (Dubrovsky *et al.*, 2008; Moreno-Risueno *et al.*, 2011). In wound-induced AR formation, severance of the cutting causes disruption of the polar auxin transport (PAT) that leads to the accumulation of the major active auxin form indole-3-acetic acid (IAA) in the stem base, which is considered to be a prerequisite for the induction of the future founder cells (Garrido *et al.*, 2002; Pop *et al.*, 2011; Ahkami *et al.*, 2013). Indeed, high endogenous levels of IAA, at the induction stage have been shown to correlate with an increased rooting response (Blazkova *et al.*, 1997; Caboni *et al.*, 1997), whereas application of PAT inhibitors led to a decreased rooting (Fabijan *et al.*, 1981; Ahkami *et al.*, 2013; Negishi *et al.*, 2014).

As initiation has taken place, externally applied auxins appear to have an inhibitory effect on AR formation, however the endogenous flow of auxin remains essential for the proper patterning of the meristem and subsequent elongation of both LR and AR primordia (Blilou *et al.*, 2005; Swarup *et al.*, 2008; Della Rovere *et al.*, 2013). Although the development of the root is predominately regulated by auxin, a wide range of other phytohormones has been reported to have a direct effect on root development or interfere with auxin distribution and signaling.

### **1.3.1.2 Cytokinins**

Cytokinins (CKs) are often considered to have an antagonistic effect to auxin on root development. Several studies have demonstrated that mutations leading to a decrease in CK levels or interfering with CK signaling enhanced formation of ARs and LR in *Arabidopsis*, tobacco (*Nicotiana tabacum* L.), poplar (*Populus sp.*) and rice (*Oryza sativa* L. (Werner *et al.*, 2001, 2003; Riefler *et al.*, 2006; Ramirez-Carvajal & Davis, 2010; Chang *et al.*, 2013; Gao *et al.*, 2014; Köllmer *et al.*, 2014).

The key mechanism defining the antagonism between CKs and auxin in root development lies in regulation of local auxin distribution via repression of *PIN*-type transporters by CKs (Laplaze *et al.*, 2007; Chang *et al.*, 2015). In the primary root, CKs synthesized at the root apex, have been shown to define the transition from cell division and elongation to differentiation (Dello Ioio *et al.*, 2007; Chapman & Estelle, 2009; Růžicka *et al.*, 2009). Moreover, Chang *et al.* (2015) demonstrated that the local increase in biosynthesis of CKs by founder cells of LR and its surrounding cells was accompanied by

induction of a CK-degrading gene within the founder cell itself, leading to a high auxin/CK ratio only in the founder cell and a low auxin/CK ratio in the surrounding cells. This is proposed to be the key mechanism in the determination of founder cells of LRs following auxin-mediated induction.

The importance of CKs throughout the expression phase of AR formation in *Arabidopsis* was highlighted in the study by Della Rovere *et al.* (2013), where CKs down-regulated the auxin transporters *PIN1* and *LAX3* in the peripheral layers of AR primordia, thus directing the auxin flow toward the tip of AR primordia stimulating the establishment of the quiescent center. Additionally, CKs regulate proliferation and differentiation of vascular cells that is essential for the integrity of the vascular connection between the developing primordia and the stem stele (Kuroha & Satoh, 2007; Caño-Delgado *et al.*, 2010; De Rybel *et al.*, 2015).

### **1.3.1.3 Stress-related phytohormones**

The primary reaction of the severed cutting is associated with wound response and mediated by jasmonic acid (JA). Until now, there is no solid understanding regarding the role of JA in AR formation. Gutierrez *et al.* (2012) have demonstrated that JA negatively regulates AR initiation in *Arabidopsis* hypocotyls, whereas in potato (*Solanum tuberosum* L.) application of JA to microcuttings positively stimulated formation of ARs. Additionally, transgenic petunia plants with knocked-down expression of a key enzyme in JA biosynthesis have shown reduced numbers of ARs and AR primordia in leafy cuttings, suggesting that JAs positively regulate AR formation in this species (Lischweski *et al.*, 2015). Together with the accumulation of auxin, the JA-mediated wound response has been suggested to trigger the establishment of a new carbohydrate sink in the stem base of the cutting (Ahkami *et al.*, 2009).

Abscisic acid (ABA) accumulates in response to various abiotic stresses, and has been shown to inhibit cell cycle progression (Gutierrez, 2009). ABA is considered to be an overall negative regulator of development of LR in *Arabidopsis* and crown roots in rice (De Smet *et al.*, 2003; Steffens *et al.*, 2006), whereas ABA-deficient tomato mutants have been shown to develop a larger number of ARs (Thompson *et al.*, 2004).

Another stress-induced hormone, ethylene, is in close interaction with the biosynthesis, transport and signaling of auxin (Robles *et al.*, 2013), which explains the absence of a universal model describing involvement of this phytohormone in AR

formation. Application of ethylene precursors reduced AR formation in tobacco, sunflower (*Helianthus annuus* L.) and wild cherry (*Prunus avium* L.), whereas in tomato, petunia, grape vine (*Vitis vinifera* L.) and spruce (*Picea abies* (L.) H. Karst.) ethylene treatment promoted rooting (da Costa *et al.*, 2013; Druege *et al.*, 2014; Bellini *et al.*, 2014). Additional evidence for an essential role of ethylene in AR formation has arisen from the studies on ethylene-insensitive tomato and petunia plants, which showed reduced AR formation (Clark *et al.*, 1999). Combined phase-specific treatment with ethylene and auxin in mung bean (*Vigna radiata* (L.) R. Wilczek) suggested that ethylene increased sensitivity to auxin at the induction stage, while having an inhibitory effect on AR formation during the later stages (De Klerk & Hanecakova, 2008). Another possible mechanism for ethylene stimulation of AR formation is related to induced programmed death of epidermis cells located on the site of the emerging primordia in rice, thus facilitating protrusion of ARs through the outer stem tissue (Mergemann & Sauter, 2000; Steffens & Sauter, 2005).

#### **1.3.1.4 Other hormones and signaling molecules**

To date several studies have reported the involvement of a range of other hormones and signaling compounds in the regulation of AR formation, however, the exact mechanisms underlying their effect are still to be clarified. Gibberellins (GAs) play an inhibitory role in AR formation in poplar, tomato and rice (Bellini *et al.*, 2014). Increased expression of GA biosynthetic genes in the vasculature of tobacco suggested a role of stem-derived GA in the regulation of AR elongation (Niu *et al.*, 2013). Recent studies in *Arabidopsis* and pea (*Pisum sativum* L.) demonstrated a negative role of strigolactones in AR formation, which is mediated by inhibition of polar auxin transport (Pandey *et al.*, 2016). Furthermore, an increasing number of studies on the role of other signaling compounds, i.e. polyamines, nitric oxide, hydrogen peroxide and other reactive oxygen species demonstrate their involvement in regulation of AR formation (da Costa *et al.*, 2013; Bellini *et al.*, 2014; Steffens & Rasmussen, 2016).

Taken together, every stage of AR formation is under tight regulation by the complex network of various phytohormones. Whereas induction of AR founder cells should be seen as a unique event characterized by specific regulatory mechanisms, the following stages of AR formation show higher similarity with the overall developmental programs of root formation, that allows transferring the knowledge gained from studies on LR and PR development. Despite an expanding range of the phytohormones and other signaling

molecules, shown to affect AR formation, auxin and cytokinins, however, appear to play a central role in AR morphogenesis as well as throughout the entire life cycle of a plant.

### 1.3.2 Role of photosynthesis and carbohydrate metabolism in AR formation

Carbohydrates serve as a main source of energy and precursors for the synthesis of various structural compounds, both being essential for development of the plant organism and in particular AR formation. Furthermore, sugars have been shown to interact with several hormone signaling pathways, as well as mechanically contribute to root elongation via increasing the cell turgor (Wang & Ruan, 2013). An overview model of the role of carbohydrates as regulators of AR formation is presented in Fig. 5 and described in details below.

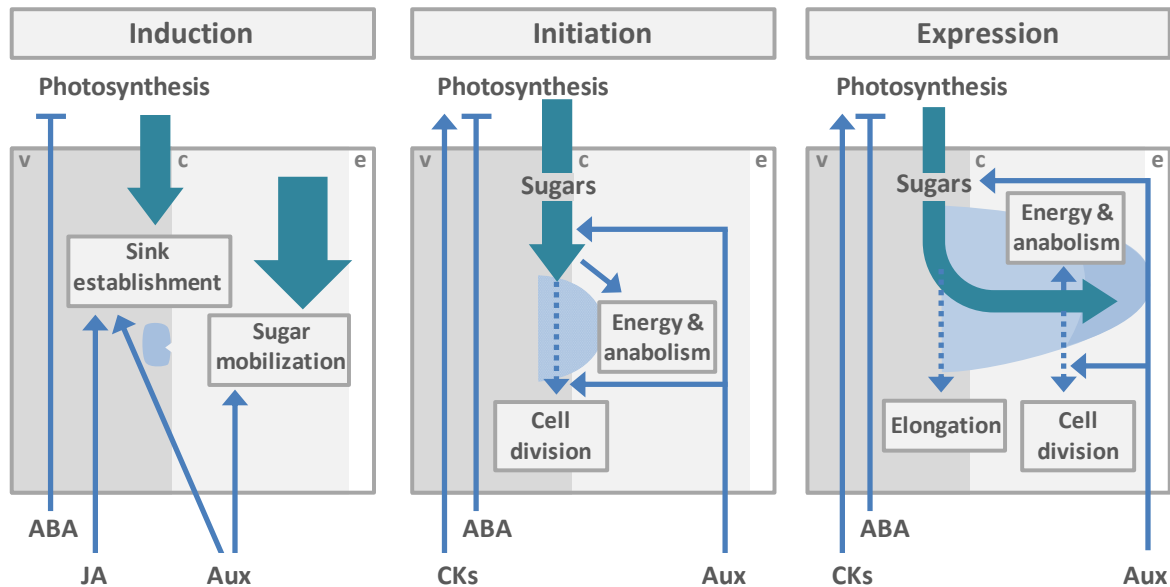


**Fig. 5** Mechanisms for the involvement of carbohydrates and their interaction with major phytohormones in regulation of adventitious root formation. ABA, abscisic acid; Aux, auxins; CKs, cytokinins.

Initially, wounding shock and interruption of water supply as a result of separation of the cutting from the stock plant leads to a decrease in stomatal conductance and inhibition of photosynthetic activity of the cutting, which is observed even under optimized conditions (Svenson *et al.*, 1995; Mesén *et al.*, 1997; Fordham *et al.*, 2001). Described decrease in photosynthetic activity is probably mediated by abiotic stress signals, such as ABA.

Furthermore, studies in petunia have shown a decrease in the levels of the major soluble carbohydrates and intermediates of primary metabolism from 1 dpe, accompanied by an increase in the activity of cell wall invertases, indicating an apoplastic unloading of delivered sucrose (Ahkami *et al.*, 2009). These findings suggest that disruption of existing cell connections by excision interferes with the targeted delivery of the carbohydrates that increases starvation of the rooting zone and leads subsequently to the establishment of a new carbohydrate sink (Ahkami *et al.*, 2009; Druege *et al.*, 2016; Klopotek *et al.*, 2016). Auxin and JA have been proposed as potential regulators of the establishment of the sugar sink in the rooting zone (Ahkami *et al.*, 2009; Agulló-Antón *et al.*, 2011; Druege *et al.*, 2016).

Under conditions of decreased photosynthesis and hampered delivery of assimilates, carbohydrates accumulated by the stock plant before the excision of the cuttings support the starving rooting zone. Indeed, several studies demonstrated that higher levels of stored carbohydrates improved rooting in woody cuttings of *Eucalyptus grandis* W; Hill ex Maiden (Hoad & Leakey, 1996) and mango (*Mangifera indica* L.; Schaesberg & von Ludders, 1993). Moreover, sugar levels in the cutting have been shown to positively correlate with the number of ARs and the survival rate of zonal geranium (*Pelargonium x hortorum* Bailey) cuttings after a period of dark storage, commonly imposed during transportation of the propagation material (Druege *et al.*, 2004; Rapaka *et al.*, 2005). Furthermore, Klopotek *et al.*, (2016) demonstrated a positive effect of dark exposure on subsequent rooting performance of petunia cuttings, highlighting the sink competition between the rooting zone and the shoot apex during the induction stage.

With the progress of AR formation after initiation has taken place, adequate carbohydrate supply from the leaves to the stem base of the cuttings has been shown to improve the rooting performance in pea (Davis & Potter, 1989). Thus, with the onset of the expression phase photosynthesis of the leafy cutting becomes the primary source of assimilates to supply the rooting zone (Jackson, 1986; Ahkami *et al.*, 2009; Hartmann *et al.*, 2011; Agulló-Antón *et al.*, 2011). Studies on <sup>13</sup>C-feeding of larch (*Larix x eurolepis* A. Henry.) cuttings indicated that the main source of carbon accumulated in the rooting zone has been assimilated after the cutting isolation (Pellicer *et al.*, 2000). Besides, net CO<sub>2</sub> exchange in poinsettia cuttings has been shown to increase after primordia formation indicating recovery of the photosynthetic activity (Svenson *et al.*, 1995), which was proposed to be regulated by CKs produced in the developing ARs (Hartmann *et al.*, 2011).

Indeed, CKs have been highlighted among the regulators of the acclimation of the photosynthetic machinery to abiotic stress (Boonman *et al.*, 2007; Shao *et al.*, 2010).

Reestablishment of the cell connections between the phloem and dividing founder cells at the end of initiation stage is an essential step for an improved flux of the leaf-derived carbohydrates toward the rooting zone. In petunia the transition from the cell wall to cytosolic and vacuolar type of invertases in 2 dpe indicated a symplastic delivery of sugars, followed by the recovery of carbohydrate supply (Ahkami *et al.*, 2009). Furthermore, formation of the vascular connections in the developing AR primordia enhanced significantly stomatal conductance and photosynthetic activity in poinsettia cuttings (Svenson *et al.*, 1995) and led to an increase in the levels of intermediates of primary metabolism, major amino acids and total protein in petunia cuttings (Ahkami *et al.*, 2009).

Apart from providing energy and C-skeletons to the developing ARs, recent findings suggest that sugars can regulate the root development via interaction with phytohormones or directly affecting the expression of several key genes (Eveland & Jackson, 2012; Puig *et al.*, 2012; Wang & Ruan, 2013; Lastdrager *et al.*, 2014).

Auxin application has been repeatedly shown to stimulate accumulation of carbohydrates in the rooting zone (Veierskov *et al.*, 1982; Davis & Haissig, 1994; Agulló-Antón *et al.*, 2011), and therefore may modulate the strength of the carbohydrate sink. Glucose, on the other hand, increased the levels of several precursors of IAA biosynthesis in *Arabidopsis*, indicating a positive role of sugars in auxin metabolism (Sairanen *et al.*, 2012). Additionally, LeClere *et al.* (2010) has demonstrated that decreased sugar availability during the kernel formation in maize coincided with a down-regulation of a flavin monooxygenase-like enzyme *YUCCA*, involved in auxin biosynthesis.

Emerging crosstalk between sugar and auxin signaling appears to play a crucial role in the regulation of plant growth and development. Expression of several genes involved in controlling the root development in *Arabidopsis*, e.g. auxin response genes *AUX/IAA*, *LOB* (*LATERAL ORGAN BOUNDARIES*) and *WOX5* (*WUS-RELATED HOMEODOMAIN 5*), has been shown to be regulated by both auxin and sugars (Eveland & Jackson, 2012). Glucose application has been demonstrated to trigger cell proliferation in meristematic tissues by activation of mitotic B-type cyclin and its associated kinase. However glucose alone did not have an effect on cell division and required additional stimulation by auxin (Wang & Ruan, 2013).

Furthermore, two important mechanisms have recently been identified that integrate the metabolic status of the plant into the root developmental program. One is related to the activity of the *TOR* (*TARGET OF RAPAMYCIN*) kinase complex that is expressed in the meristematic tissues, and has been shown to directly promote cell division independently of auxin/cytokinin signaling (Xiong *et al.*, 2013). *TOR* is activated by glucose and triggers phosphorylation of *E2Fa* transcription factor, which promotes progression of the cell cycle in the root meristem of *Arabidopsis* (Xiong *et al.*, 2013).

A second component regulating the growth response by sugars is *SnRK1* (*SNF1-RELATED KINASE 1*) that is highly conserved in all eukaryotes, and has been shown to inhibit plant growth under low carbon availability (Ponnu *et al.*, 2011). Activity of *SnRK1* is repressed by trehalose-6-phosphate, as well as glucose-6-phosphate and glucose-1-phosphate, which accumulate in response to an increased level of sucrose (Lastdrager *et al.*, 2014). Although the downstream mechanism of *SnRK1*-mediated regulation of plant growth is not yet clear, several components of auxin signaling have been shown to interact with *SnRK1*, providing an additional link for sugar and auxin crosstalk (Farrás *et al.*, 2001).

Unexpectedly, activity of several invertases, in addition to their main function in splitting of the sucrose molecule, has also been demonstrated to regulate cell elongation in *Arabidopsis* and rice roots. Vacuolar invertases have been assumed to link vacuole sugar homeostasis with the activity of cell wall-associated kinases that are regulating the cell wall extensibility, whereas cytosolic invertase *AtCIN1*, localized in the nucleus, is suggested to regulate cytoskeleton structure via direct interaction with phosphatidylinositol signaling or via affecting gene expression by signals derived from produced hexoses (Wang & Ruan, 2013).

Taken together, in addition to serving as a source of carbon and energy, carbohydrates are involved in an intricate network of cross-talk between several regulators of plant development, either interfering with a wide range of phytohormones or directly interacting with molecular regulators of cell growth and development, such as *SnRK1*, *TOR* or regulatory invertases. The supply of carbohydrates is a major bottleneck of AR formation, and initially depends on internal resources stored in the cutting, whereas recovered photosynthetic activity takes over the primary role in carbohydrate supply with the onset of the expression phase.



### 1.3.3 Possible involvement of mineral nutrition in AR formation

Roots are the main organs of higher plants facilitating the mineral uptake from the soil. Separation of the cutting from existing root system disturbs the normal flow of the nutrients and thus limits the amount of available mineral elements. To date, information on the role of mineral nutrition in AR formation remains elusive and often the studies are conducted in different growth systems and in various plant species (Bellini *et al.*, 2014; Verstraeten *et al.*, 2014). However, there is an increasing interest in this topic, as commercialization of vegetative propagation have brought a wide use of inert material, which increases the need for better understanding of the role of mineral nutrition in AR formation. An overview model of potential involvement of mineral nutrition in AR formation based on the studies on primary and lateral roots is summarized in Fig. 6 and described in details below.

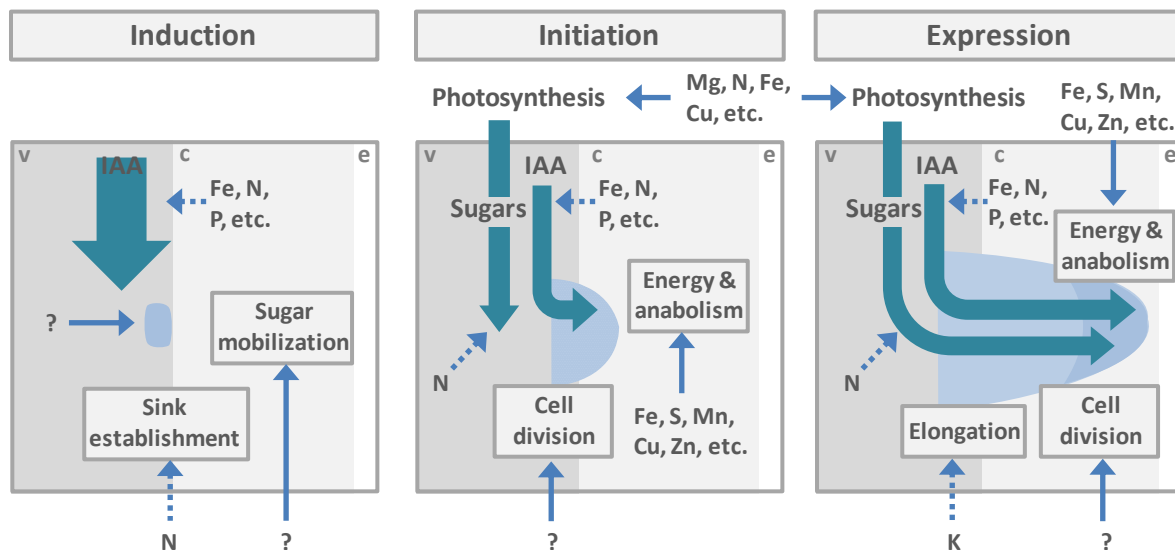


**Fig. 6** Potential mechanisms for the involvement of mineral nutrients in the regulation of adventitious root formation.

Mineral nutrition is tightly associated with nearly every physiological process throughout the entire life cycle of the plant. Essential elements can be divided into two distinct groups based on their abundance in plants: macronutrients (N, P, Ca, Mg, P and S) that are present in relatively high concentrations in plants and micronutrients (Cl, B, Fe, Mn, Zn, Cu, Ni and Mo), which are found in considerably lower concentrations (Marschner, 2012). Deficiency of any of the described elements may potentially affect the development

of the plant including that of the root, by interfering with its physiological functions. On the one hand, lack of several structural elements can interfere with the root growth by affecting synthesis and functions of the proteins (N, S) or fortification of the cell wall (B, Ca, and the beneficial element Si), whereas a decrease in K, required for turgor, may directly affect elongation of the root cells. On the other hand, deficiency of the elements related to photoassimilation and metabolism, i.e. chlorophyll biosynthesis (Mg, Fe), electron transport (Fe, S), energy transfer (P), transpiration and starch synthesis (K) and antioxidant system (Cu, Fe, Mn, Zn, S) would result in an overall negative effect on the energy status of the plant, thus indirectly inhibiting the development of the roots. Furthermore, assimilation of N requires carbon skeletons derived from sugar metabolism (Foyer *et al.*, 2003), and therefore can increase the strength of the carbohydrate sink in the rooting zone. Moreover, some elements may take over specialized functions; for instance, Zn has been shown to increase the concentration of auxin and gibberellins (Mašev & Kutáček, 1966; Sekimoto *et al.*, 1997), which in turn regulate various aspects of AR formation.

Plants are capable of coping with the limitations of the essential nutrients by several mechanisms, involving mobilization of the internal pool of the nutrients and their retranslocation toward the nutrient sinks, modulation of the root system architecture as well as up-regulation of the nutrient acquisition machinery. However, most of the nutrients described above, with the exception of Mn and Ca, are reported to have high to moderate mobility in the phloem, mobilization rates for these elements strongly depend on their physiological properties, stage of ontogenesis and the plant species (Marschner, 2012; Maillard *et al.*, 2015). During the leaf senescence in most of the studied plant species, the rates of retranslocation of N, P, K and Mg have been reported to be higher than those of B, Cu, Fe, S, Mn and Zn, whereas Ca is referred to as a phloem-immobile element (Hocking & Pate, 1977; Himelblau & Amasino, 2001; Moreira & Fageria, 2009; Maillard *et al.*, 2015).

Retranslocation of nutrients may also play an important role in AR formation, where separated cuttings possess a limited amount of mineral elements. In this regard, the nutritional status of the stock plants may play an important role in building up the endogenous pool of nutrients required to support AR formation at the stem base. For this reason, the role of mineral nutrition in AR formation has been studied mainly with respect to the fertilization of the stock plants. Indeed, a high initial N content in cuttings of zonal geranium, chrysanthemum (*Dendranthema x grandiflorum* (Ramat.) Kitam.), New Guinea

impatiens (*Impatiens x hawkeri* Bull.) and poinsettia (*Euphorbia pulcherrima* Willd. ex Klotzsch) has been shown to exert a positive effect on AR formation (Druege *et al.*, 2000, 2004; Gibson, 2003; Zerche & Druege, 2009). Moreover, Dong *et al.* (2004) observed N remobilization in poplar cuttings during AR formation, where approximately 30% of the mobilized N has been allocated toward newly formed roots. Improved rooting performance has been also observed in response to K fertilization of New Guinea impatiens stock plants (Gibson, 2003).

Plants possess a remarkable ability to alter their root system architecture via regulating the length and density of the LR in order to explore the substrate for essential nutrients. Studies on LRs in *Arabidopsis*, demonstrated that localized exposure of a part of the root system to nitrate ( $\text{NO}_3^-$ ), P, or Fe favors LR elongation, whereas the localized supply of ammonium ( $\text{NH}_4^+$ ) stimulated higher-order lateral root branching (Zhang & Forde, 1998; Linkohr *et al.*, 2002; Lima *et al.*, 2010; Giehl *et al.*, 2012). Although the molecular mechanisms underlying the local sensing of specific nutrients remain to be fully elucidated, several lines of evidence suggest that phytohormones, and in particular auxin, act as signals in the nutrient-dependent modification of root morphology (Giehl *et al.*, 2014). In fact, auxin has been shown to regulate LR elongation in response to localized Fe application via induction of the auxin transporter gene *AUX1* (Giehl *et al.*, 2012), whereas the nitrate transporter *NRT1* is also able to transport auxin, allowing immediate integration of nutrient signals with auxin concentration within the LR tip (Krouk *et al.*, 2010). Moreover, P availability has been shown to affect LR development via modulation of auxin receptor *TIR1* and its downstream targets (Perez-Torres *et al.*, 2008).

Partial resemblance of auxin-mediated signaling pathways controlling the induction and the formation of LRs and ARs (Gutierrez *et al.*, 2012; Bellini *et al.*, 2014) suggests that regulatory networks involved in mineral element sensing by LRs can be employed for the stimulation of AR formation. Furthermore, ABA has been shown to inhibit elongation of LRs in response to localized  $\text{NO}_3^-$  (Harris, 2015), whereas cytokinin biosynthetic genes have been reported to be upregulated under high  $\text{NO}_3^-$  supply (Ramireddy *et al.*, 2014).

With the main focus on stock plant fertilization, so far, little attention has been paid to the role of the rooting medium as a potential source of essential nutrients. Empirical trials with *in-vitro* propagated plant material provided evidence for the importance of the mineral composition of the medium for successful formation of ARs (Murashige, 1974). The pioneering study by Schwambach *et al.* (2005) highlighted the importance of balanced

nutrient supply at specific stages of AR formation in microcuttings of *Eucalyptus globulus* Labill. For instance, optimized supply levels of Ca, Zn and  $\text{NO}_3^-$  to the medium increased the number of AR. In another study, Santos & Fisher (2009) showed that application of an N-P-K fertilizer directly to the stem base of petunia cuttings during AR emergence improved rooting, whereas foliar application of nutrients had no effect on AR formation.

Uptake of nutrients in the roots is regulated by the expression of a series of transport proteins in response to nutrient availability (Marschner, 2012). However, little is known on the mechanisms of nutrient uptake in isolated cuttings, before the emergence of the ARs. Transcriptome analysis of AR formation in petunia revealed a substantial increase in the expression of 18 genes involved in the uptake and assimilation of N, P, K, S, Fe and Zn starting from the initiation phase (Ahkami *et al.*, 2014). Moreover, within this period, high transcript abundance was observed for a plasma membrane  $\text{H}^+$ -ATPase, which may energize nutrient uptake. These findings highlight the ability of the cuttings to specifically regulate nutrient uptake and emphasize an increased demand for certain mineral elements in the stem base, suggesting that AR formation may be improved by application of certain nutrients.

Taken together, mineral nutrition appears to be the most unexplored subject in the topic of AR formation. From the function of essential minerals, it can be assumed, that various crucial processes for AR formation, such as energy production, photosynthesis, synthesis of structural components, buildup or loosening of the cell walls, maintenance of the cell turgor, etc. depend on sufficient availability of such elements. On the other hand, knowledge acquired from the studies on PR and LR, suggests that availability of the nutrients significantly affect the morphology of roots, thus highlighting a possible cross-talk with phytohormones. Therefore, a thorough investigation is needed to reveal the limiting elements, essential for the formation of ARs and to understand the mechanisms of their action.

## 1.4 Commercial importance of adventitious rooting

Industrial cultivation of plants often relies on multiplication of a unique genotype that possesses certain desired traits. In this regard, maintenance of the genotypic identity of the propagated plant material is of outstanding importance (Davis & Haissig, 1994; Hartmann *et al.*, 2011). Together with other techniques used for clonal reproduction, such as natural multiplication by tubers or bulbs, fragmentation of rhizomes or stolons, grafting, and more recently developed apomictic seed production, propagation by cuttings remains a common practice in horticulture, agriculture and forestry for multiplication of various important plants (Davis & Haissig, 1994).

AR formation is a major prerequisite for successful propagation by cuttings (Hartmann *et al.*, 2011). Although, modern propagation industry has greatly advanced the control of environmental factors such as humidity, temperature, and light conditions, insufficient rooting is still a major issue resulting in significant economic losses. In addition, an empirical conditioning of the environment cannot overcome the phenomenon of recalcitrant to rooting genotypes occasionally found within the same species. Furthermore, introduction of the inert substrate as soil substitute and increasing attractiveness of tissue culture incites optimization and standardization of the media composition.

With increasing environmental concern in developed countries, application of several synthetic growth stimulating substances may become more restricted. For instance, the highly efficient synthetic auxin,  $\alpha$ -naphthaleneacetic acid, used for stimulation of AR formation in stem and leaf cutting as well as in tissue culture, is a derivative of naphthalene, which has been classified by EPA as a possible human carcinogen (Agency for Toxic Substances and Disease Registry, 2005).

Therefore, a deeper understanding of the physiological and molecular mechanisms of AR formation is essential for the improvement of existing propagation protocols, and will allow avoiding financial losses and introduction of new species for commercial propagation and tissue culture.

## 1.5 Petunia as a model

From its introduction as an ornamental plant approximately two centuries ago, petunia has become a highly important crop in world-wide horticulture. Intense commercial breeding resulted in outstanding diversity of the shape and color of flowers that brings petunia to the top of the list of the best-selling garden plants. Only in the US, the wholesale value in 2015 has reached 133 million for petunia, which makes approximately 10% of total sales in category “annual bedding and garden plants” (Fig. 7, National Agricultural Statistics Service, USDA, 2016).

Furthermore, throughout the last two decades, petunia has been established as a model for a number of traits, which cannot be studied in the standard model *Arabidopsis*. For instance, due to large colored and fragrant flowers, studies on petal pigmentation, floral volatiles, flower and inflorescence development, self-incompatibility and evolution of interactions with pollinators are intensely conducted in petunia (Gerats & Strommer, 2009; Vandenbussche *et al.*, 2016). Moreover, petunia serves as a host for arbuscular mycorrhiza, and its wide ecological adaptation to various environments encourages studies in abiotic stress tolerance.

To date an expanding set of forward and reverse genetic tools has been developed for petunia, such as set of interspecific RIL populations developed in the groups of Dr. Ryan Warner (Dept. of Horticulture, Michigan State University) and Prof. Dr. Cris Kuhlemeier (Institute of Plant Sciences, University of Bern) as well as dTPH1 transposon insertion-mutant collection of the group of Dr. Michiel Vandenbussche (Group of evolution & development of the flower, University of Lyon). Moreover, very recently the genomes of parental species of *P. hybrida*, *P. axillaris* (Lam.) Britton, Stern & Poggenb. and *P. inflata* R.E. Fr. (Bombarely *et al.*, 2016) were published, which opened an opportunity for deep

Wholesale Value (\$ millions), USA, 2015  
Annual Bedding/Garden Plants

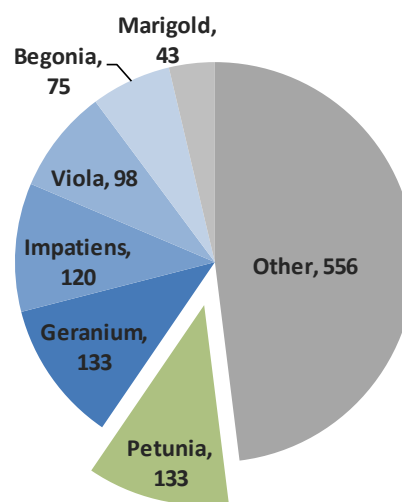


**Fig. 7** Wholesale value (\$ million) for operations with more than \$10,000 sales, in category “annual bedding/garden plants”, USA, 2015 (from National Agricultural Statistics Service, USDA, 2016)

transcriptome studies by RNAseq and implementation of novel approaches for targeted genome editing, such as CRISPR/Cas9 technology.

The described features make petunia a convenient model organism for studies of AR formation compared to Arabidopsis (Ahkami *et al.*, 2009, 2014; Druége *et al.*, 2014). Although a large number of studies on AR formation have been performed in Arabidopsis, this system possesses several drawbacks. Unlike petunia, the stem of Arabidopsis is short and organized in a rosette, thus to achieve stem elongation seedlings are grown in the darkness and the root system is usually not removed (Sorin *et al.*, 2005; Gutierrez *et al.*, 2009, 2012). Furthermore, the anatomical structure of the hypocotyl resembles that of the radicle, retaining the pericycle as a rhizogenous layer, which is different to the stem structures derived from the epicotyl (Scheres *et al.*, 1994; Bennett & Scheres, 2010). Therefore, petunia appears to be an attractive model for a wide spectrum of studies, and in particular studies on AR formation, and provides an appealing opportunity to transfer the obtained knowledge for industrial application.

## 1.6 Aims and approaches of the current work

Based on previous transcriptome studies, emphasizing an increasing demand for certain mineral elements during adventitious root formation in petunia cuttings (Ahkami et al., 2014), it has been hypothesized that a limitation of certain mineral elements in the stem base may pose a physiological bottleneck that restricts the development of ARs. Therefore, the primary aim of this study was to investigate which mineral elements might have a promotive effect on the formation of ARs and how specific elements exert their physiological function during this process. Considering that nutrient application may affect different physiological processes, such as the compensation of nutrient deficiency, the modulation of carbon metabolism in the basal stem zone or changes in the balance of phytohormones, combined morphological, anatomical, biochemical and molecular approaches were employed in order to characterize the influence of selected nutrients throughout AR formation and to investigate their mode of action.

Initially, in order to determine the most limiting nutrients for AR formation, the effect of the withdrawal of nutrient components from the full mineral medium on rooting of petunia cuttings was evaluated in hydroponic culture (see Subchapter 3.1.1). Subsequent experiments were carried out to define the optimal concentration and a period of application for the selected nutrients. Histological examination was performed to assess the dynamics of AR development in response to nutrient supply (see Subchapter 3.1.2).

In order to characterize the nutritional status of the cuttings and to assess the changes in the nutrient demand, a comprehensive elemental analysis was supplemented by analysis of transcript levels of nutrient-deficiency markers (see Subchapters 3.2.1. - 3.2.2).

To investigate the role of nutrient application on metabolic activity and sugar supply of the rooting zone, a metabolite profiling was carried out for the soluble carbohydrates, the primary intermediates of sugar metabolism and proteinogenic amino acids (see Subchapters 3.2.3. - 3.2.5).

In order to elucidate the involvement of phytohormones in nutrient-mediated AR formation, the balance of major phytohormones was analyzed. As auxin is a major factor regulating AR induction and further root growth, expression of auxin-related genes was assessed to deeper analyze the involvement of auxin in nutrient-mediated AR formation. Furthermore, an analysis of auxin responses was carried out in a transgenic petunia line expressing the auxin reporter DR5::GFP/GUS (see Subchapter 3.3).



As the first experiments identified Fe as the major limiting nutrient, the following work has attempted to investigate the mechanisms underlying Fe-mediated promotion of AR formation (Subchapter 3.4). To distinguish whether the positive effect of Fe application on AR formation was achieved by maintenance of the Fe pool in leaves or performance of a specific function in the rooting zone, foliar application of Fe was compared to the application of Fe to the rooting medium. Furthermore, to assess the dynamics of local distribution of Fe during development of AR primordia, a histochemical approach was used to stain Fe in a dissected rooting zone of the cuttings at different developmental stages.

Finally, to evaluate the genotype-dependent variation in Fe-mediated AR formation, rooting performance was assessed in several commercial cultivars derived from different breeding programs (see Subchapter 3.5).

## 2. Materials and methods

### 2.1 Plant material, growth conditions and sampling

#### 2.1.1 Plant growth conditions

Leafy stem cuttings of *Petunia hybrida* cv. Mitchell were used in all experiments, unless otherwise specified. For analysis of genotypic variation in AR formation, 8 commercial cultivars kindly provided by Selecta Klemm GmbH&Co (Stuttgart, Germany) were used. Stock plants were grown in the greenhouse at 22°C and approx. 85 % relative humidity during 10 h of insolation ( $250 \mu\text{mol} \times \text{m}^{-2} \times \text{s}^{-1}$ ), and 20°C and 60 % relative humidity during 14 h of darkness. Excised leafy cuttings with 4-5 leaves were transferred to hydroponic medium with permanent aeration under equal light and temperature condition. The full mineral solution contained 0.1 mM  $\text{KH}_2\text{PO}_4$ , 0.1 mM  $\text{MgSO}_4$ , 0.25 mM  $\text{CaCl}_2$ , 2 mM  $\text{NH}_4\text{NO}_3$ , 0.01 mM Fe-ethylenediamine-N,N'-bis(2-hydroxyphenylacetic acid) (FeEDDHA), 0.05 mM  $\text{H}_3\text{BO}_3$ , 0.005 mM  $\text{MnSO}_4$ , 0.001 mM  $\text{ZnSO}_4$ , 0.001 mM  $\text{CuSO}_4$  and 0.0007 mM  $\text{NaMoO}_4$ . The pH of the medium was adjusted by addition of 1.5 mM 2-(N-morpholino)-ethanesulfonic acid (MES). The standard pH of the medium was maintained at 5.8, unless specifically adjusted to the experimental conditions. Hydroponic solutions were replaced every 5 days.

Influence of individual nutrients was studied by their addition to a nutrient-free solution consisting of 1 mM  $\text{CaSO}_4$  and 1.5 mM MES (pH 5.8). Ammonium ( $\text{NH}_4^+$ ) and nitrate ( $\text{NO}_3^-$ ) were supplied in the form of  $(\text{NH}_4)_2\text{SO}_4$  and  $\text{Ca}(\text{NO}_3)_2$  respectively. Iron was supplied as a FeEDDHA. For the foliar application, 20  $\mu\text{M}$  FeEDDHA was sprayed on the leaf surface twice, immediately after excision and 3 days post excision (dpe).

#### 2.1.2 Sample collection

Samples from 5 mm of the cutting base and 9-mm leaf discs were harvested 0; 0.25 (6 h); 1; 3; 5; and 7 dpe, immediately frozen in liquid nitrogen and stored at -80°C. To collect the phloem exudates, 5-mm fragment above the base of the cutting stem was removed with the razor blade, and cut area was washed with distilled water. The cuttings were incubated in the tubes containing 0.5 ml of 20 mM  $\text{Na}_2\text{-EDTA}$  (pH 7) for 2 h in the plexiglass container at high humidity under standard growth conditions described in the Subchapter 2.1.1. Samples were collected 0; 1; 3; 5 and 7 dpe, vacuum-dried at 40°C and stored at -80°C.

### 2.1.3 Application of auxin regulators

Foliar spraying of the cuttings with 80  $\mu\text{M}$  N-1-naphthylphthalamic acid (NPA, Duchefa) was used to inhibit polar auxin transport in the cuttings according to (Ahkami *et al.*, 2013). In order to inhibit basal auxin biosynthesis 1  $\mu\text{M}$  L-kynurenine (Kyn, Sigma-Aldrich) was added to the hydroponic solution (He *et al.*, 2011). For auxin treatment, 3  $\mu\text{M}$  1-naphthaleneacetic acid (NAA, Sigma-Aldrich) was applied to the rooting medium during 0-2 dpe.

## 2.2 Morphological assessment of AR formation

The performance of AR formation was evaluated according to Agulló-Antón *et al.* (2011). Two days after appearance of the first ARs under control conditions (12-14 dpe) the roots of each cutting (3 replicates, each consisting of 10 cuttings) were counted and assigned to different length classes of 5-mm intervals. The rooting parameters were calculated for each replication as follows:

$$\text{Percentage of rooted cuttings} = N \times 100/10$$

$$\text{Mean root number per rooted cutting} = \sum n_i / N$$

$$\text{Mean root length per rooted cutting} = \sum [\sum (n_x L_x)]_i / \sum n_i$$

where  $N$  is the number of rooted cuttings,  $n$  is the number of roots,  $i$  is each of the 10 cuttings of each replication,  $L_x$  is the assigned length of each root length interval, and  $n_x$  is the number of roots in each length interval. Each experiment was performed in at least two replications.

## 2.3 Histological and histochemical analyses

### 2.3.1 Histological examination

For histological examination 1-mm thick cross-sections of petunia stem cuttings were used for combined conventional and microwave-proceeded fixation, dehydration and resin embedding in a microwave processor (PELCO BioWave34700-230, Ted Pella Inc.) as described in Appendix Table 1.

Semi-thin sectioning and light microscopy was performed according to (Ahkami *et al.*, 2013). 6- $\mu\text{m}$  sections were cut using a microtome (Jung CM 1800, Leica Instruments). Sections were mounted on slides and stained with 0.05 % toluidine blue-O (Serva)

dissolved in 1 % sodium tetraborate decahydrate buffer (Hutchinson et al., 1996). Microscopic analyses were performed using an Axio Imager A1 (Carl Zeiss) microscope in combination with an Axio Cam MRc 5 camera (Carl Zeiss).

### 2.3.2 Quantitative analysis of AR formation

For visualization and calculation of the dynamics of AR formation, fresh 5-mm segments of the cutting base were fixed in a solution containing 1 % (w/v) formaldehyde, 4 % (v/v) glutaraldehyde, in 25 mM phosphate buffer (pH 7). After embedding in 4 % agarose, 100- $\mu$ m-thick transverse sections were made at three different levels using a vibratome (VT-1000S, Leica Microsystems). Obtained sections were mounted on slides and stained for two minutes with 1 % (w/v) methylene blue and 1 % (w/v) azure II before light microscopic examination, using a digital system (VHX-5000, Keyence Deutschland GmbH).

Developing AR initials were divided into 5 classes – I, meristemoids; II, globular meristems; III, AR primordia with dome-shaped meristems; IV, AR primordia with elongated cells and developing vasculature; V, emerged AR. The average number of the defined AR initials was calculated in twelve independent replicates 5, 6, 7, and 9 dpe in control cuttings and cuttings supplied with  $\text{NH}_4^+$ ,  $\text{NO}_3^-$  or Fe.

### 2.3.3 Histochemical detection of Fe

For visualization of Fe deposition the stem bases of cuttings were fixed as described in the Subchapter 2.3.2, followed by dehydration in graded series of ethanol. Embedding was performed using Steedman's polyester wax (Steedman, 1957) consisting of a 9:1 (w/w) mixture of polyethylene glycol 400 distearate (Sigma-Aldrich) and 1-hexadecanol (Sigma-Aldrich). Embedding was carried out at 45°C with graded wax/ethanol series (1:2, 1:1, 2:1, v/v) for 4 h each, followed by incubation in pure wax overnight and transfer into the embedding molds. Specimens were then cut into 20- $\mu$ m sections using a rotary microtome (Jung CM 1800 Leica Instruments). Sections were mounted on poly-L-lysine covered slides (Sigma-Aldrich) and dried overnight at room temperature. Prior to staining procedure, slides were dewaxed in 100 % ethanol and rehydrated in decreasing concentrations of ethanol in Milli-Q water.

The histochemical detection of Fe was carried out by Perls' Prussian blue staining with DAB/H<sub>2</sub>O<sub>2</sub> intensification according to Roschztardt et al. (2009). Briefly, rehydrated samples were incubated in Perls' stain solution consisting of 4 % (v/v) HCl and 4 % (w/v)

K-ferrocyanide (Merk) for 2 h at room temperature. After washing for one minute with Milli-Q water, the samples were incubated in preparation solution, consisting of 0.01 M  $\text{NaN}_3$  (Sigma-Aldrich) and 0.3 %  $\text{H}_2\text{O}_2$  in methanol for one hour, followed by washing three times with 0.1 M phosphate buffer (pH 7.2). Sections were then incubated at room temperature for 10-15 min in the intensification solution containing 0.025 % (w/v) 3,3'-Diaminobenzidine (DAB; Sigma-Aldrich), 0.005 % (v/v)  $\text{H}_2\text{O}_2$ , and 0.005 % (w/v)  $\text{CoCl}_2$  in 0.1 M phosphate buffer (pH 7.2), followed by washing with Milli-Q water. To control the effect of intensification solution, similar procedure was applied to the sections without Perls' staining.

### **2.3.4 Confocal microscopy**

For detection of green fluorescent protein (GFP), hand-cut transverse sections of petunia stem base were first stained in solution consisting of 5 mg  $\text{l}^{-1}$  propidium iodide (PI, Sigma-Aldrich) in 100 mM phosphate buffer (pH 7.0). Sections were analyzed using a laser scanning microscope (LSM780, Carl Zeiss). Fluorescence of GFP was probed with a 488 nm laser line (2.5 % intensity) and fluorescence was recorded between 491 – 535 nm. Combined fluorescence of PI and GFP was visualized by 488 nm laser line (2.5 % intensity) over the range 491-597 nm.

For visualization of nuclei, 20- $\mu\text{m}$  sections, prepared and stained as described in the Subchapter 2.3.3 were additionally stained with 4',6-diamidino-2-phenylindole (DAPI, Sigma-Aldrich). Photospectrometric analysis of sections was performed with a 405 nm laser line (1.8 % intensity) over the range 411-482 nm, after which DAPI-specific fluorescence, corresponding to 461 nm was unmixed. Bright field recordings were taken with a 633 nm laser line using dark field settings.

## **2.4 Biochemical analyses**

### **2.4.1 Analysis of chlorophyll concentration in leaves**

Concentrations of chlorophyll *a* and *b* were analyzed in methanol extracts of leaf samples according to Warren (2008). Chlorophylls were extracted from approximately 50 mg frozen and ground leaf samples by adding 1 ml of methanol and shaking for two minutes at 30 Hz. Samples were centrifuged for two minutes at 15 000 rpm and the supernatant was transferred to a new microcentrifuge tube. The pellet was re-extracted by adding 1 ml of methanol to the pellet, shaking for another two minutes, centrifuging and

removing the supernatant. The pellet was discarded while the two supernatants were pooled and used for measurement of chlorophylls.

Microplate measurements were made by transferring 200  $\mu\text{l}$  of sample (or pure methanol as a blank) into a 96-well flat bottom polystyrol plate (Corning Costar).

Absorbance at 652 and 665 nm was measured using a microplate reader (Infinite 200, Tecan). Chlorophyll concentration was calculated based on conversion of the measured absorbance of 200  $\mu\text{l}$  of sample ( $A_{652, \text{plate}}$ ;  $A_{665, \text{plate}}$ ) into a 1-cm pathlength corrected absorbance ( $A_{652, 1\text{cm}}$ ;  $A_{665, 1\text{cm}}$ ) as described by Warren (2008):

$$A_{652, 1\text{cm}} = (A_{652, \text{plate}} - A_{\text{blank}})/0.51$$

$$A_{665, 1\text{cm}} = (A_{665, \text{plate}} - A_{\text{blank}})/0.51$$

Concentrations of chlorophyll *a* and *b* were calculated according to Ritchie (2006):

$$\text{Chlorophyll } a \text{ } (\mu\text{g/ml}) = -8.0962 A_{652, 1\text{cm}} + 16.5169 A_{665, 1\text{cm}}$$

$$\text{Chlorophyll } b \text{ } (\mu\text{g/ml}) = 27.4405 A_{652, 1\text{cm}} + 12.1688 A_{665, 1\text{cm}}$$

#### 2.4.2 Quantitative measurement of GUS activity

$\beta$ -Glucuronidase (GUS) activity was studied in the cutting base of DR5::GUS/GFP line of *Petunia hybrida* cv. Mitchell as described by Jefferson *et al.* (1987). Approximately 100 mg of homogenized frozen samples of the cutting base was mixed thoroughly with 100  $\mu\text{l}$  extraction buffer containing 10 mM  $\beta$ -mercaptoethanol, 10 mM  $\text{Na}_2\text{EDTA}$ , 0.1 % (w/v) sodium lauryl sarcosine, 0.1 % (v/v) Triton X100 and 140  $\mu\text{M}$  phenylmethylsulfonyl fluoride (Sigma-Aldrich) in 50 mM phosphate buffer, pH 7.0. After centrifugation for 10 min at 4°C at 15 000 rpm, supernatant was transferred into a new microcentrifuge tube and used for the fluorometric assay and protein quantification.

For the fluorometric assay, 10  $\mu\text{l}$  of sample extract was mixed with 130  $\mu\text{l}$  extraction buffer containing 1.2 mM 4-methylumbelliferyl  $\beta$ -D-glucuronide (MUG, Sigma-Aldrich). After 20 min of incubation in the darkness at 37°C, 10  $\mu\text{l}$  of the reaction was mixed with 190  $\mu\text{l}$  of 0.2 M  $\text{Na}_2\text{CO}_3$ . Fluorescence was measured with a microplate reader (Infinite 200, Tecan) at 460 nm when excited at 355 nm. A standard curve corresponding to 50, 25, 5, 2.5, 0.5, 0.25, and 0  $\mu\text{M}$  4-Methylumbelliferone (MU) was used to calculate the amount of MU produced by each sample.

Protein concentrations were determined in Bio-Rad Bradford Protein Assay (Bio-Rad) according to the manufacturer's instructions. Briefly, 10  $\mu\text{l}$  of the sample was transferred to the 190  $\mu\text{l}$  of Bradford Reagent in 96-well flat bottom polystyrene plate (Corning Costar). A series of BSA dilutions (0, 0.05, 0.1, 0.2, 0.4, 0.6, 0.8 and 1.0  $\text{mg ml}^{-1}$ ) were used to build a standard curve. Absorbance was measured at 595 nm with a microplate reader (Synergy HT, BioTEK). Values from the fluorescence GUS assay were standardized by protein concentration and final GUS activity was calculated as  $\text{pmol MU min}^{-1} \text{mg protein}^{-1}$ .

### 2.4.3 Measurement of phytohormones

Extraction of auxin, abscisic acid, cytokinins and their intermediates was performed using Oasis-HLB (30 mg) and Oasis-MCX columns (30 mg, Waters) as described in Kojima *et al.* (2009). Approximately 300 mg of homogenized frozen samples of the cutting base was extracted overnight at  $-20^{\circ}\text{C}$  with 1 ml of buffer, consisting of methanol, formic acid and water in a ratio of 15:1:4 (all solutions used throughout analysis were LC-MS grade). After centrifugation at  $4^{\circ}\text{C}$  for 20 min, the supernatant was transferred to a new 2 ml tube and the pellet was washed with 300  $\mu\text{l}$  of extraction buffer. Samples were vacuum-dried at  $38^{\circ}\text{C}$  and resolved in 1 ml of 0.1 % formic acid. HLB-columns were conditioned with changes of 1 ml acetonitrile and 1 ml methanol, equilibrated with 1 ml of 0.1 % (v/v) formic acid and loaded with the samples, followed by washing with 1 ml of 0.1 % (v/v) formic acid and elution with 1 ml of a solution containing 90 % (v/v) acetonitrile and 1 ml of 0.1 % (v/v) formic acid. Eluted samples were then vacuum-dried at  $38^{\circ}\text{C}$  and resolved in 0.9 ml of 1 M formic acid. MCX-columns were conditioned with changes of 1 ml acetonitrile and 1 ml methanol, and then equilibrated with 1 ml of 1 M formic acid and 1 ml of 0.1 M HCl. Equilibrated columns were loaded with the samples and washed with 1 ml of 1 M formic acid. Elution of the auxins and ABA was performed with 1 ml of methanol, followed by elution of cytokinins with 1 ml of 0.35 M ammonia dissolved in 60 % (v/v) methanol. Samples were then vacuum-dried at  $38^{\circ}\text{C}$  and resolved in 50  $\mu\text{l}$  of methanol.

LC-MS/MS analyses were carried out using the Agilent 1290 Infinity LC system coupled to an Agilent 6490 Triple Quadrupole LC/MS with iFunnel Technology (Agilent). Chromatographic separation was done using an Agilent's ZORBAX Rapid Resolution High Definition (RRHD) analytical column (Eclipse Plus C18, 1.8  $\mu\text{m}$ , 2.1x50 mm). Column temperature was kept at  $40^{\circ}\text{C}$ . The mobile phase consisted of water (A) and methanol (B)

containing both 0.1 % formic acid. The flow rate was kept constant at 0.4 ml min<sup>-1</sup>. Separation of the compounds was achieved by varying mobile phase composition of solvent B from 13.5 % to 70 % in 6 min. Prior to injection of each sample, the column was washed (99 % B) and re-equilibrated (13.5 % B) for another 1 and 2 min, respectively. All solvents used for chromatographic procedures were LC-MS grade (Th. Geyer GmbH).

Mass-spectrometry measurements were performed in an Agilent 6490 Triple Quadrupole LC/MS system at unit resolution in a multiple reaction monitoring (MRM) mode. Both positive and negative ion electrospray modes were used for sample ionization. CKs were analyzed in positive ion mode and ABA in negative ion mode. Parameters for the Agilent Jet Stream ionization source were set as follows: capillary voltage 2000 V (+ve) and 3000 V (-ve), drying gas flow rate 12 l min<sup>-1</sup> and sheath gas temperature of 250°C. The dwell times were set between 20 and 200 s. Collision energies were optimized for each compound (Appendix Table 2). Compounds [<sup>15</sup>N<sub>4</sub>]-*cis*-zeatin, [<sup>2</sup>H<sub>5</sub>]-*trans*-zeatin riboside, [<sup>2</sup>H<sub>6</sub>]-ABA and 3-[<sup>2</sup>H<sub>5</sub>]-indolylacetic acid were used as internal standards and also for testing the stability of the LC-MS instruments by following in time reproducibility of detector's response and retention times. The data were acquired and processed using Agilent MassHunter Workstation and MassHunter Quantitative Analysis software (version B.07.01).

#### 2.4.4 Carbohydrate and amino acid analysis

Carbohydrates and amino acids were extracted with 80 % ethanol at 80°C for 60 min followed by vacuum-evaporation of the supernatant at 50°C and resolving in 250 µl of deionized water.

For analysis of soluble amino acids 20 µl of resolved extract was derivatized by incubation with 20 µl 6-aminoquinolyl-N-hydroxysuccinimidyl carbamate (AQC, Sigma-Aldrich) in 160 µl of 0.2 M boric acid (pH 8.8) at 50°C for 10 min. Separation of amino acids was performed by ultra-high performance liquid chromatography (AcQuity H-Class, Waters GmbH) using fluorescence detection at 473 nm with excitation at 266 nm (PDA eλ Detector). The separation was carried out on a C18 reversed phase column (ACCQ Tag Ultra C18, 1.7 µm, 2.1x100 mm) with a flow rate of 0.7 ml min<sup>-1</sup> and duration of 10.2 min at 50°C. The gradient was accomplished with four solutions prepared from two different buffers purchased from Waters GmbH (eluent A and eluent B for amino acid analysis, Germany). Eluent A was pure concentrate, eluent B was a mixture of 90 % LCMS water



and 10 % eluent B concentrate, eluent C was LCMS water (Th. Geyer GmbH) and eluent D was pure concentrate (eluent B for amino acid analysis). The column was equilibrated with eluent A (10 %) and eluent C (90 %).

Concentrations of glucose, fructose and sucrose were determined in the samples by enzymatic assays according to Ahkami *et al.* (2013).

#### **2.4.5 Analysis of primary metabolites**

Primary metabolites were extracted according to Gullberg *et al.*, 2004 with modifications. Approximately 100 mg of the fresh stem base samples were added to the 1 ml extraction buffer consisting of equal volumes of chloroform and methanol (both solutes were LC-MS grade) and mixed on a vortex at 4°C for 20 min. Subsequently 300 µl of water (HPLC grade) was added to each sample and thoroughly mixed on a vortex for 1 min, followed by centrifugation at 14 000 rpm at 4°C for 10 min. Supernatant was transferred in a new tube, vacuum-dried at 40°C and resolved 200 µl of water (HPLC grade) prior to analysis by ion chromatography coupled to mass spectrometry (IC-MS/MS).

IC-MS/MS analyses were carried out using ICS-5000 system (Dionex) coupled to an Agilent 6490 Triple Quadrupole LC/MS with iFunnel Technology (Agilent). Chromatographic separation was performed using a 250×2 mm AS11-HC column connected to a 10×2 mm AG11-HC guard column and an ATC-1 anion trap column (all columns produced by Dionex). The column was equilibrated with a mixture of 96 % water (HPLC grade) and 4 % KOH, generated by an EGCIII KOH Eluent Generator Cartridge (Dionex) at a flow rate of 0.38 ml min<sup>-1</sup>. The gradient was produced by changes of KOH concentration as follows: 4 % for 4 min; 15 % for 11 min; 25 % for 10 min; 50 % for 3 min; 80 % for 3 min and 4 % for 9 min. The temperature of the column was maintained at 37°C.

Mass-spectrometry measurements were performed in an Agilent 6490 Triple Quadrupole LC/MS system at unit resolution in a multiple reaction monitoring (MRM) mode (Appendix Table 3). Negative ion electrospray modes were used for sample ionization. Electron spray ionization (ESI)-MS/MS condition was as follows: gas temperature 350°C, drying gas flow rate 12 l min<sup>-1</sup>, nebulizer pressure 35 psi, capillary voltage ± 3.5 kV. The fragmentor voltage and collision energies were optimized for each compound. The data were acquired and processed using Agilent MassHunter Workstation and MassHunter Quantitative Analysis software (version B.07.01). <sup>13</sup>C-pyruvate was used to normalize the data and was added to each sample as internal standard before analysis.

### 2.4.6 Mineral element analysis

To analyze major macro- and micronutrients, freeze-dried material was digested in HNO<sub>3</sub> under pressure using a microwave digester (Ultraclave-4; MILESTONE). Elemental analysis was performed using a sector field high-resolution inductively coupled plasma - mass spectrometry (HR-ICP-MS, ELEMENT-2, Thermo Fisher Scientific). Macro elements were analyzed using inductively coupled plasma optical emission spectroscopy technique (ICP-OES, iCAP 6500 dual OES spectrometer; Thermo Fischer Scientific). Total N and C were determined using an elemental analyzer (Euro-EA; HEKAtech).

## 2.5 Analysis of transcript abundance

### 2.5.1 RNA isolation and cDNA synthesis

Total RNA was isolated from the stem base or from mature leaves of at least 8 cuttings according to Logemann *et al.*, (1987). Approximately 100 mg of frozen ground material was extracted with 0.6 µl of Z6-buffer consisting of 8 M guanidine chloride, 20 mM EDTA, 50 mM β-mercaptoethanol, and 20 mM MES (pH 7.5) followed by addition of 500 µl of phenol/chloroform/isoamyl alcohol mixture (w/w/w, 25:1:24, respectively) and incubation on ice for 10 min. Samples were centrifuged at 13 000 rpm for 10 min at 4°C, and the supernatant was transferred into the new tube containing 40 µl of 1 N acetic acid and 500 µl 96 % (v/v) ethanol, mixed thoroughly and incubated over night at -20°C. After incubation, the samples were centrifuged at 13 000 rpm for 10 min at 4°C, and the pellet was washed twice with 500 µl of 3 M sodium acetate and 500 µl of 80 % ethanol. After each wash the supernatant was discarded. The air-dry pellet was resuspended in for 15 min at 65°C 20-30 µl of RNase-free water.

Purified RNA was treated with DNaseI (Qiagen). The first-strand cDNA synthesis was performed using M-MLV reverse transcriptase (Promega) with 1 µg total RNA and 1 pmol poly-A primer at 42°C for 50 min.

### 2.5.2 q(RT)-PCR

Gene expression was analyzed by quantitative real-time (RT)-PCR on a CFX384™ Real-Time System (BioRad) using the SYBR Green Master Mix Kit (BioRad). Gene-specific primers (Appendix Table 4, synthesized by Metabion) were designed to have a melting temperature of 58°C and to result in a PCR product between 150 and 250 bp. The relative transcript abundance of time-course values were determined by the  $2^{-\Delta\Delta Ct}$  method

and related to the initial transcript level (0 dpe). The abundance of *ACTIN7* mRNA was selected as a suitable internal reference based on previous studies (Ahkami *et al.*, 2013, 2014) and a stable expression under all studied conditions throughout the course of experiment compared to *EF1 $\alpha$*  suggested by Mallona *et al.* (2010) as a suitable housekeeping gene for petunia (Appendix Fig. 1). All assays were performed on at least three biological and two technical replicates. Each analysis was repeated at least twice.

## 2.6 Generation of DR5::GFP/GUS auxin reporter petunia plants

### 2.6.1 Standard molecular techniques and bacterial strains

The standard molecular techniques such as polymerase chain reaction, agarose gel electrophoresis and transformation of *Escherichia coli* and *Agrobacterium tumefaciens* strains, were carried out according to Sambrook *et al.* (1989). Digestion with restriction endonucleases and ligation was performed according to the producer's protocol (Thermo Fisher Scientific). Elution and purification of DNA fragments from the gel was carried out using the QIAquick Gel Extraction Kit (Qiagen) according to the manufacturer's protocol. Plasmid DNA purification from *E. coli* and *A. tumefaciens* was carried out using the QIAprep Miniprep Kit (Qiagen) according to the producer's protocol. Oligonucleotides were synthesized and purified by Metabion. All cloning steps were performed using *Escherichia coli* XL1 Blue MRF strain, and transformation of petunia plants was *Agrobacterium tumefaciens* C58C1 pGV2260 (Deblaere *et al.*, 1985).

### 2.6.2 Generation of p9N-DR5-GFP-GUSi construct

Auxin-inducible synthetic promoter DR5 was amplified from pS001:DR5-GFP vector using specific primers containing sites for SpeI (forward) and BamHI (reverse) restriction endonucleases (DR5-TVM-5`SpeI: 5'-AAACTAGTGG AATTCGTCGACGGTATCGCAG-3' and DR5-TVM-3`BamHI: 5'-AAGGATCCTGTAATTGTAATTGTAATAG-3'). The resulting 308-bp fragment was inserted into a multiple cloning site of the intermediate vector pGH183 upstream of *EGFP-GUS* (kindly provided by Dr. Götz Hensel, IPK; Appendix Fig. 2) subsequent to digestion with BamHI and SpeI restriction endonucleases and ligation with T4 ligase. Selected pGH183 vector, with confirmed insertion of *DR5* fragment, was fused using T4 ligase with p9Ndoi-TOCS vector (Appendix Fig. 3) after digestion with SfiI restriction endonucleases. Resulting chimeric vector designated as p9N-DR5-GFP-GUSi (Appendix Fig. 4) was used for the subsequent cloning in petunia plants.

### 2.6.3 Plant transformation

Petunia plants used to collect the explants were grown in tissue culture at 21°C under a 16 h-light/ 8 h-dark period (200  $\mu\text{mol m}^{-2} \text{s}^{-1}$  light; light intensity and photoperiod were unchanged for the following manipulations) on maintenance medium, consisting of Murashige and Skoog basal medium (MS-medium, Duchefa) containing 3 % (w/v) sucrose and 0.9 % (w/v) Phyto agar (Duchefa). Leaf explants approx. 4 x 4 mm in size were cultivated at 24°C for two days on filter paper, immersed in pre-culture medium, consisting of MS-medium (pH 5.7) supplemented with 3 % (w/v) sucrose and 0.1 % (v/v) Gamborg's vitamins (Sigma-Aldrich). Subsequently, explants were inoculated with *Agrobacterium* culture resuspended in pre-culture medium (OD600 approx. 0.5) for 20 min at room temperature with periodic swirling and co-cultivated at 24°C for three days after decanting excess liquid. Following co-cultivation explants were immersed in 5 ml of wash solution consisting of 1/4 strength MS-medium (pH 5.8) and 1 mg L<sup>-1</sup> of ticarcillin (Duchefa) for 15 min at room temperature. Blotted dry explants were then transferred on selection medium, consisting of MS-medium (pH 5.7) supplemented with 3 % (w/v) sucrose, 0.9 % (w/v) Phyto agar (Duchefa), 0.1 % (v/v) Gamborg's vitamins (Sigma-Aldrich), 1  $\mu\text{g l}^{-1}$  6-Benzylaminopurine (Sigma-Aldrich), 0.01  $\mu\text{g l}^{-1}$  NAA (Sigma-Aldrich), 1 mg l<sup>-1</sup> ticarcillin (Duchefa) and 0.2 mg l<sup>-1</sup> kanamycin. The explants with developing calli were subcultured on the fresh selection medium for three times with a period of three weeks. Regenerating shoots were transferred on rooting medium, consisting of MS-medium (pH 5.7) supplemented with 3 % (w/v) sucrose, 0.9 % (w/v) Phyto agar (Duchefa), 0.1 % (v/v) Gamborg's vitamins (Sigma-Aldrich), 1 mg l<sup>-1</sup> ticarcillin (Duchefa) and 0.2 mg l<sup>-1</sup> kanamycin. The presence of the construct in the regenerants has been confirmed by PCR and Southern blot. Selected lines were transferred to the glasshouse with the standard conditions described in Subchapter 2.1.

## 2.7 Statistical analyses

Analysis of variance (ANOVA) provided by the InfoStat<sup>®</sup> software was used for statistical analysis of data. In case of significant impact of the factor, Fisher's LSD or Tukey's HSD were conducted at  $P \leq 0.05$ . Comparison between the treatments and controls was carried out by use of the Student's t-test at  $P \leq 0.05$ .

### 3. Results

#### 3.1 The role of individual nutrients in AR formation

##### 3.1.1 Determination of mineral nutrients essential for AR formation

Rooting has been frequently observed in inert media without any external nutrient supply in leafy cuttings of chrysanthemum, zonal geranium and petunia (Druege *et al.*, 2000; 2004; Ahkami *et al.*, 2009), indicating that the cuttings themselves contain sufficient amounts of nutrients to develop ARs. In the present study, cultivation in full mineral medium significantly improved rooting (Fig. 8), emphasizing the importance and potential role of externally supplied nutrients in AR formation.

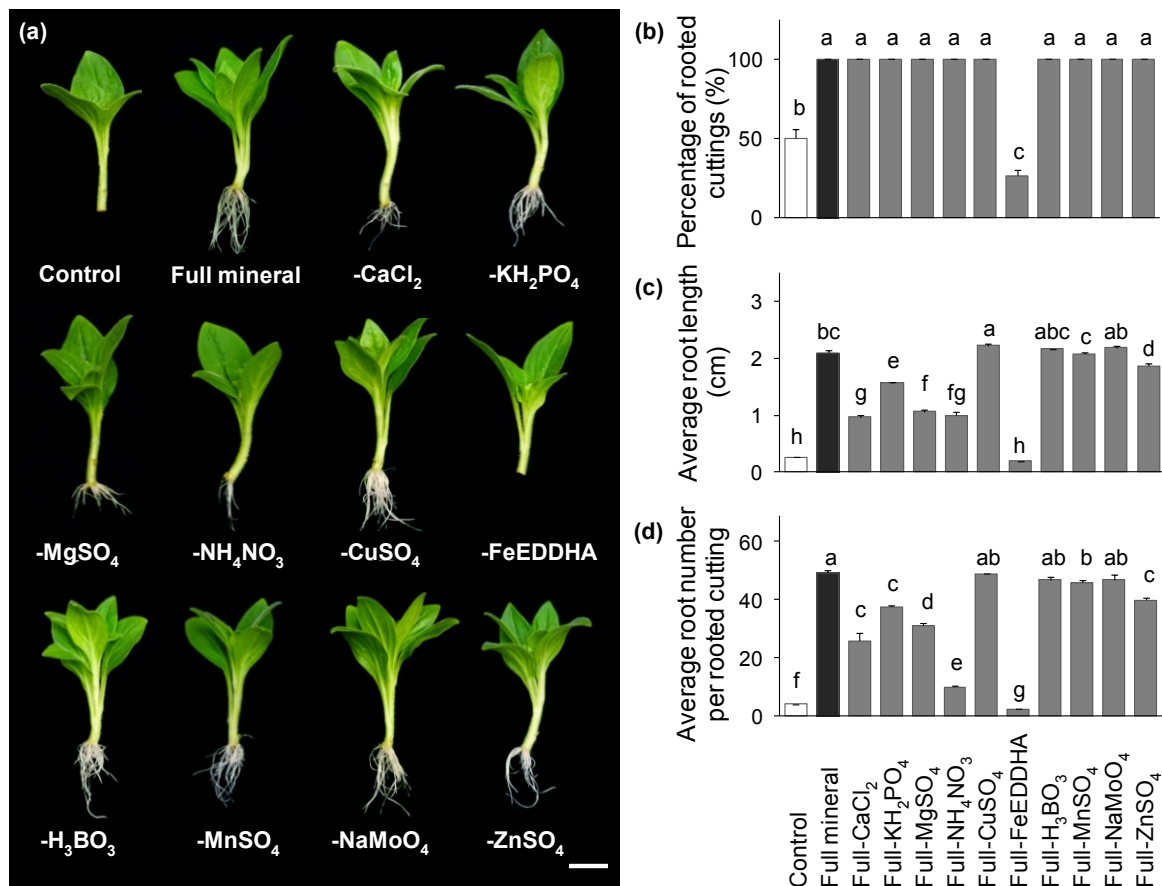


**Fig. 8** Effect of the withdrawal of components from full mineral solution on adventitious root (AR) formation in *Petunia hybrida*. (a) Representative image of rooted cuttings in nutrient-free solution (control), full mineral solution or full mineral solution lacking the indicated nutrients. (b) Percentage of rooted cuttings, (c) average root length and (d) average number of ARs were assessed 14 days post excision. Bars represent means of three independent replicates, each consisting of 10 cuttings + SE. Significant differences between nutrient supplies are indicated by different letters (Fisher's LSD,  $P \leq 0.05$ ). Bar, 1 cm.

To first determine which nutrients limit AR formation, individual elements were withdrawn from the full mineral medium before rooting performance was assessed (Fig. 8). Withdrawal of  $\text{CuSO}_4$ ,  $\text{H}_3\text{BO}_3$ ,  $\text{MnSO}_4$  or  $\text{NaMoO}_4$  from the full mineral medium had no significant effect on the rooting. The average number and the length of ARs decreased significantly in cuttings deprived from  $\text{KH}_2\text{PO}_4$ ,  $\text{MgSO}_4$ ,  $\text{CaCl}_2$  and  $\text{ZnSO}_4$ , however all cuttings still rooted. Omitting  $\text{NH}_4\text{NO}_3$  decreased the average root length by eight times and the average root number by five times compared to the full medium (Fig. 8c,d), which pointed to a potential role of nitrogen in AR formation. The most negative effect on rooting performance was observed by withdrawal of Fe that resulted in poor rooting similar to the control conditions, suggesting that the major promotive effect of the full nutrient supply on AR formation was mainly caused by the presence of Fe (Fig. 8). Based on these results, further investigations of this work were focused on the influence of Fe and N on AR formation.

Initial experiments identified the optimum concentration of Fe supply that leads to significant increase in rooting parameters between 8 and 12  $\mu\text{M}$  (Table 1). The sole application of 10  $\mu\text{M}$  Fe had a positive effect on AR formation, resulting in 100 % rooting that occurred 2-3 days earlier compared to control solution (Fig. 9). The average root length increased three times (Fig. 9c), and thus to a similar level as in full mineral medium, whereas the average AR number increased ten times compared to the control and was approximately 65 % of the values observed in the full medium (Fig. 9d).

**Table 1** Effect of different concentrations of Fe and of N supply on adventitious root (AR) formation in *Petunia hybrida* cuttings

Rooting parameters <sup>1</sup>	Fe EDTA ( $\mu\text{M}$ )				$\text{NH}_4\text{NO}_3$ (mM)			
	4	8	12	16	0.1	0.2	0.5	1.0
Rooting percentage	1.6 $\pm$ 0	1.6 $\pm$ 0	1.7 $\pm$ 0.0*	1.7 $\pm$ 0.0*	1.1 $\pm$ 0.0	1.7 $\pm$ 0.2*	1.5 $\pm$ 0.1*	1.5 $\pm$ 0.1*
Average AR number per rooted cutting	1.5 $\pm$ 0.3	2.1 $\pm$ 0.7*	7.1 $\pm$ 1.0**	6.0 $\pm$ 0.9**	1.2 $\pm$ 0.2	2.9 $\pm$ 0.2**	2.5 $\pm$ 0.3*	2.7 $\pm$ 0.3*
Average AR length	1.4 $\pm$ 0.1**	3.4 $\pm$ 0.2**	9.3 $\pm$ 1.3**	9.0 $\pm$ 1.4**	1.1 $\pm$ 0.2	1.4 $\pm$ 0.1*	1.3 $\pm$ 0.1	1.3 $\pm$ 0.0

<sup>1</sup> Values represent a relative increase in rooting parameters under nutrient application in relation to the control conditions (nutrient application / control). Each value represents the mean of three independent replicates consisting of 8 cuttings  $\pm$  SE. Significant differences to control conditions are indicated by asterisks (t-test; \*,  $P < 0.05$ ; \*\*,  $P < 0.01$ )

The positive effect on the rooting performance of N supplied as  $\text{NH}_4\text{NO}_3$  was most pronounced at a concentration of 0.2 mM (Table 1). In order to distinguish between the influence of different N forms,  $\text{NO}_3^-$  and  $\text{NH}_4^+$  were supplied separately at a concentration of 0.4 mM.  $\text{NH}_4^+$ -supplied cuttings developed 80 % of ARs compared to 43.3 % or 46.7 % in the case of  $\text{NO}_3^-$  application or control conditions, respectively (Fig. 9d). The average number of ARs increased three times in  $\text{NH}_4^+$ - supplied cuttings compared to control conditions, whereas application of  $\text{NO}_3^-$  resulted in values similar to control. However, the number of ARs detected under  $\text{NH}_4^+$  application increased to a lesser extent compared to Fe application and reached only 25 % of the maximal values observed in the full medium (Fig. 9d).

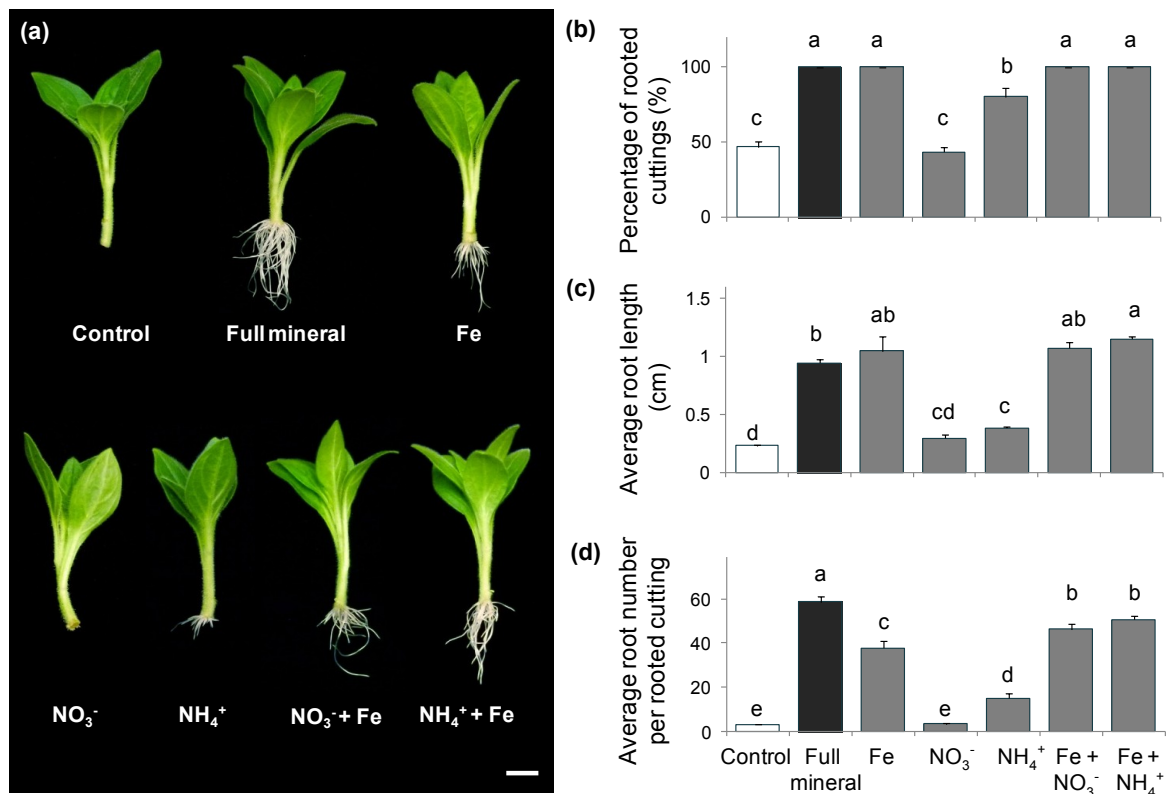


**Fig. 9** Effect of the application of individual elements and their combinations on rooting performance of leafy cuttings of *Petunia hybrida* (a) Representative image of the rooting of the cuttings supplied with iron, nitrate, ammonium and combinations of nitrate with iron and ammonium with iron compared to nutrient free conditions or full mineral supply. (b) Percentage of rooted cuttings, (c) average root length and (d) average number of adventitious roots were assessed 14 days post excision. Bars represent means of three independent replicates, each consisting of 10 cuttings + SE. Significant differences among nutrient supplies are indicated by different letters (Fisher's LSD,  $P \leq 0.05$ ). Bar, 1 cm



Additionally, the influence of a combined application of either  $\text{NH}_4^+$  or  $\text{NO}_3^-$  together with Fe (Fig. 9) was evaluated. The average number of ARs was significantly higher when either of the two N forms was supplied together with Fe than in the sole application of Fe (Fig. 9d), whereas combined application of  $\text{NH}_4^+$  and Fe resulted in 1-day earlier emergence of ARs. To determine the critical developmental stage for nutrient application, Fe,  $\text{NO}_3^-$  or  $\text{NH}_4^+$  were supplied for a period of three days within the first 9 dpe (Fig. 10). Application of Fe during 0-3 and 3-6 dpe significantly improved the rooting, with the higher number and length of ARs being detected in cuttings supplied during 3-6 dpe.

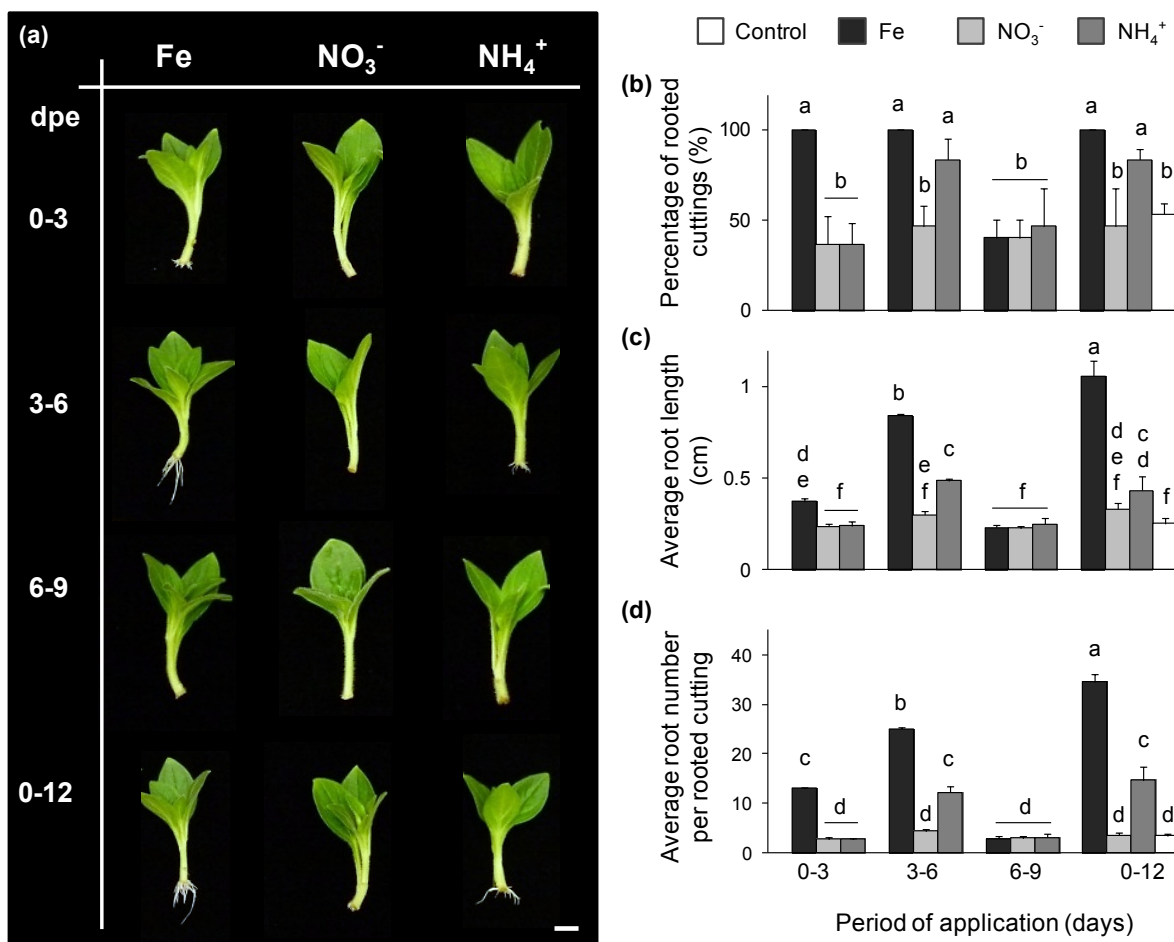


**Fig. 10** Effect of a “pulse application” of individual nutrients on adventitious root (AR) formation in *Petunia hybrida*. (a) Representative image of rooted cuttings in response to a supply of nutrients for a period of three days compared to continuous application of nutrients. (b) Percentage of rooted cuttings, (c) average root length and (d) average number of ARs were assessed 14 days post excision. Bars represent means of three independent replicates, each consisting of 10 cuttings + SE. Significant differences between nutrient supplies and time points are indicated by different letters (Tukey's HSD,  $P \leq 0.05$ ). Bar, 1 cm.



However, root traits still reached highest values in the case of full-time application of Fe. As seen before, AR formation under  $\text{NO}_3^-$  application remained poor (Fig. 10). Application of  $\text{NH}_4^+$  only within 3-6 dpe improved the rooting performance to a similar level as in cuttings supplied with  $\text{NH}_4^+$  during the entire period of cultivation (Fig. 10). Thus, the developmental period between 3-6 dpe appeared to be the most effective to stimulate AR formation.

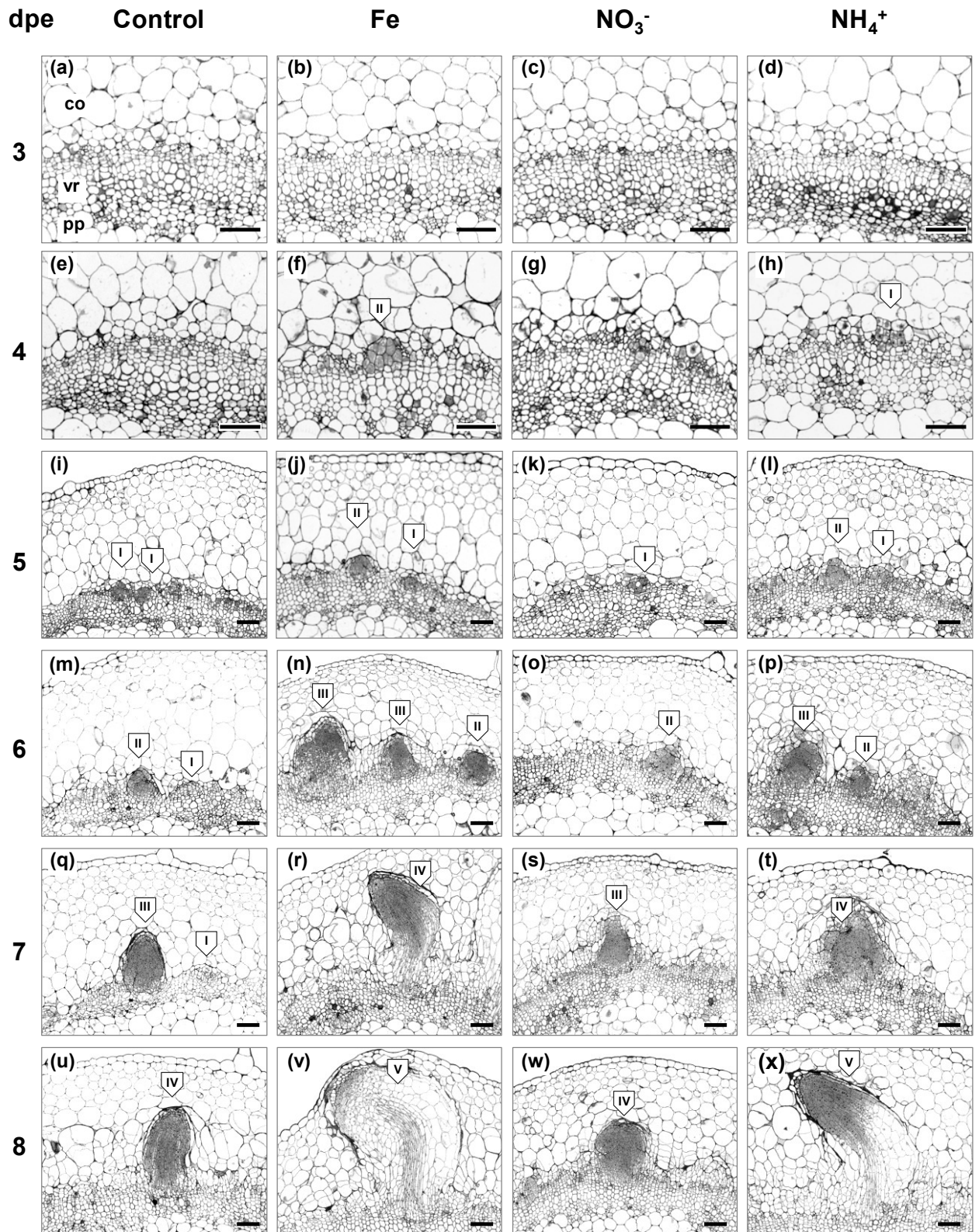
### 3.1.2 Anatomy of AR formation in response to nutrient application

To investigate whether promotion of AR formation by Fe and  $\text{NH}_4^+$  application is accompanied by histological changes in the stem base, a structural analysis using light microscopy was performed.

In this study, the first anatomical structures that were indisputably associated with AR formation were detected in 3 dpe (Fig. 11a-d). The first groups of meristematic cells, characterized by large central nucleus and dense cytoplasm, were observed from 4 dpe in the cambial layer in the rooting zone of the cuttings supplied with Fe and  $\text{NH}_4^+$  (Fig. 11f,h). Moreover, in Fe-supplied cuttings described meristematic cells formed already early meristemoids (Fig. 11f), whereas under control conditions and  $\text{NO}_3^-$  only single dividing cells were detected (Fig. 11e,g). Differences among nutrient applications became more distinct following the progress of AR primordia formation. In the cuttings supplied with Fe and  $\text{NH}_4^+$  the first globular ARs meristems were observed from 5 dpe (Fig. 11j,l), and early AR primordia with dome-shaped meristems were detected in 6 dpe (Fig. 11n,p), whereas in control and  $\text{NO}_3^-$ -supplied cuttings similar formations appeared one day later (Fig. 11m,o,q,s). The first AR primordia with defined elongation zone and developing vasculature were observed in 7 dpe only in the cuttings supplied with Fe and  $\text{NH}_4^+$  (Fig. 11r,t), and one day later in control and  $\text{NO}_3^-$ -supplied cuttings (Fig. 11u,w). The first protrusion of ARs out of the stem cortex occurred in 8 dpe in the cuttings supplied with Fe and  $\text{NH}_4^+$  (Fig. 11v,x).

---

**Fig. 11** (Right) Anatomy of adventitious root (AR) formation in *Petunia hybrida* cuttings in response to nutrient application. Cross sections from 1-4 mm of the stem base are shown in 3-8 days post excision (dpe) in cuttings grown without nutrients or with iron, nitrate or ammonium. Developmental stages of AR initials are indicated in roman numbers – I. meristemoids; II. globular meristems; III. AR primordia with dome-shaped meristems; IV. AR primordia with elongated cells and developing vasculature; V. emerged AR; co. cortex; pp. pith parenchyma; vr. vascular ring. Bar, 100  $\mu\text{m}$ .



To assess the dynamics of AR formation, the number of AR primordia at the above-defined stages was calculated during 5-9 dpe (Fig. 12). The number of total detectable AR initials observed in 5 dpe was higher in the rooting zone of the cuttings supplied with Fe and  $\text{NH}_4^+$ , as compared to control conditions. Moreover, under Fe supply the total number of AR primordia increased gradually during the course of observation. Relative to control conditions, application of  $\text{NO}_3^-$  resulted in a similar number of total AR primordia in 9 dpe, whereas the highest values were observed in the cuttings supplied with Fe, and to a lesser extent with  $\text{NH}_4^+$  (Fig. 12).

The number of meristemoids (Fig. 12) was comparable under all conditions in 5 dpe, followed by a significant decrease at later stages, observed especially upon application of Fe and to a lesser degree  $\text{NH}_4^+$ , which indicated an acceleration of progression through the subsequent stages of AR primordia development in response to supplied nutrients.

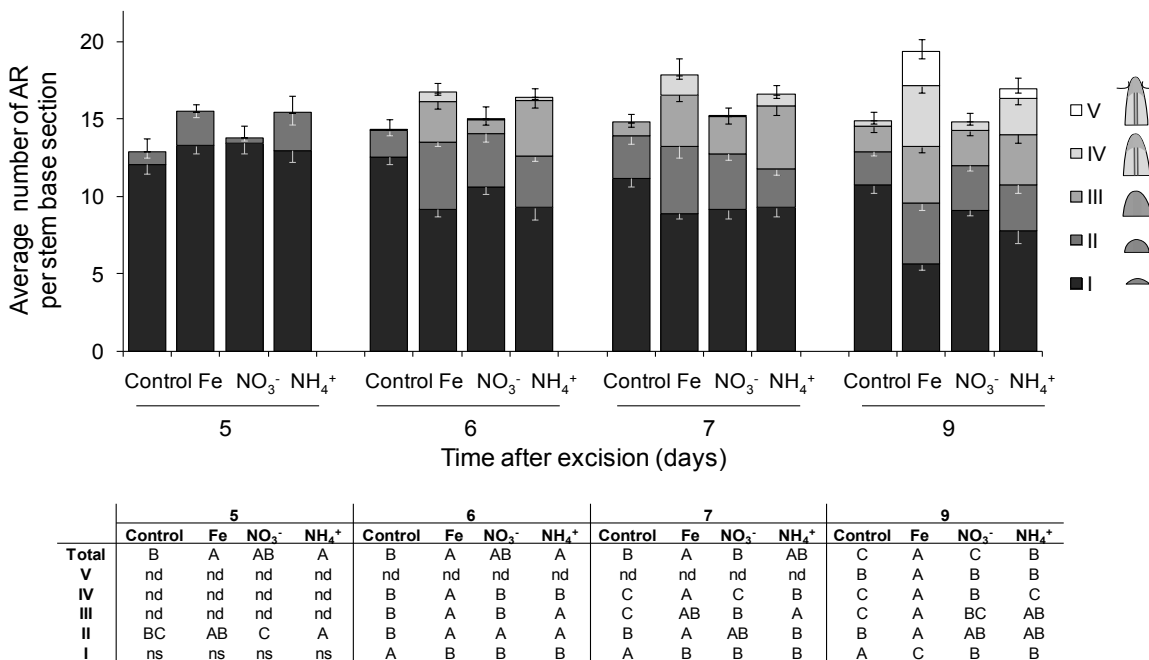


**Fig. 12** Quantitative assessment of the dynamics of adventitious root (AR) formation in *Petunia hybrida* cuttings in response to nutrient application. Developing AR initials were divided into 5 classes – I. meristemoids; II. globular meristems; III. AR primordia with dome-shaped meristems; IV. AR primordia with elongated cells and developing vasculature; V. emerged AR. The average number of the defined AR initials was calculated 5, 6, 7 and 9 days post excision in 100  $\mu\text{m}$  cross sections of the rooting zone at three different levels in cuttings grown without nutrients, with ammonium, nitrate or iron. Bars represent means of twelve independent replicates - SE. The total number of AR initials is represented by the size of the stacked columns + SE. Significant differences between numbers of defined AR initials at specific time point are indicated by different letters (Fisher's LSD.  $P \leq 0.05$ ). nd, structures not detected; ns, difference is not significant.

Taken together, application of Fe resulted in the most distinctive promotion of AR formation in petunia cuttings by enhancing the rate of primordia differentiation and increasing the number of total AR initials. Similar to Fe, application of  $\text{NH}_4^+$ , but not  $\text{NO}_3^-$ , stimulated the development of AR primordia, however the stimulatory effect was less pronounced.

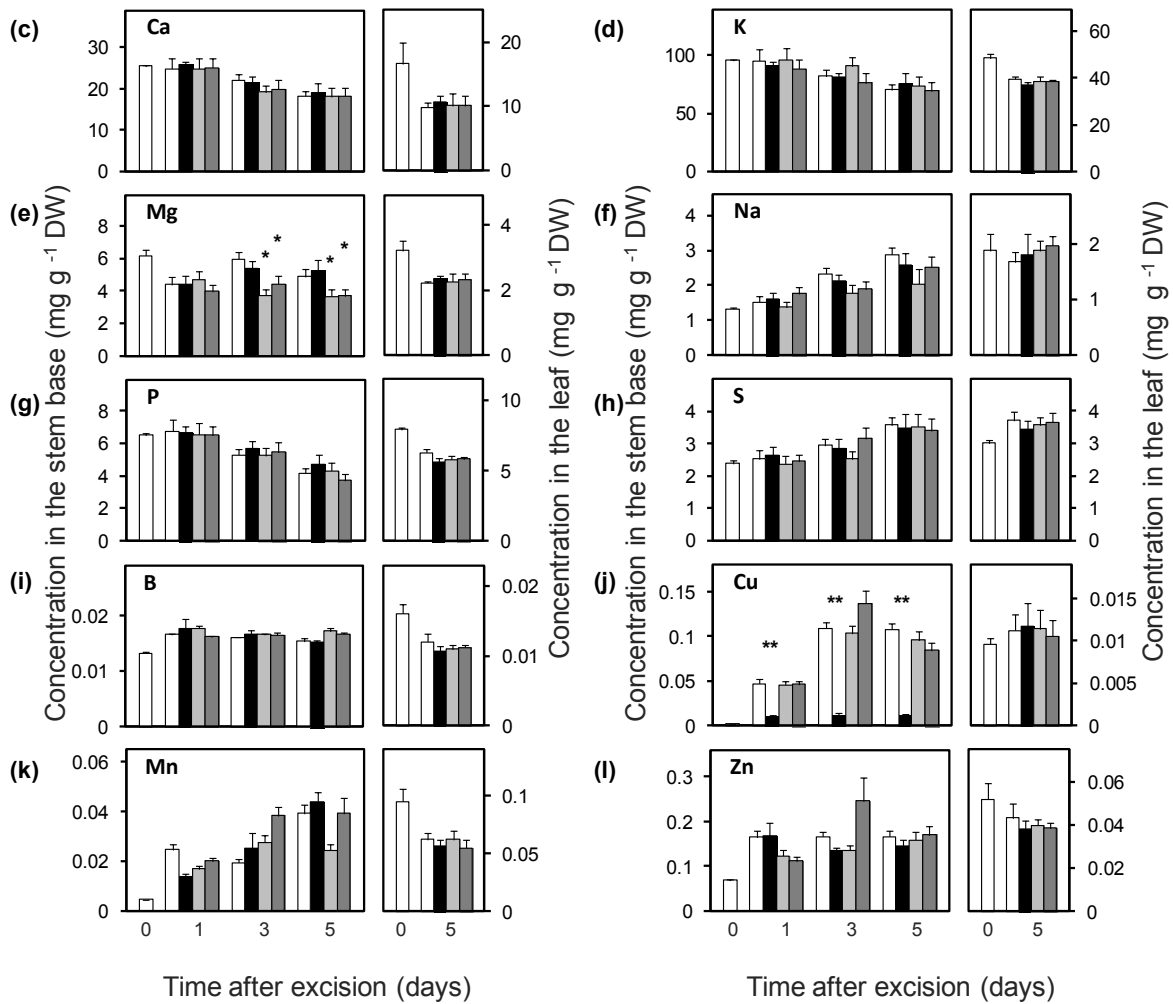
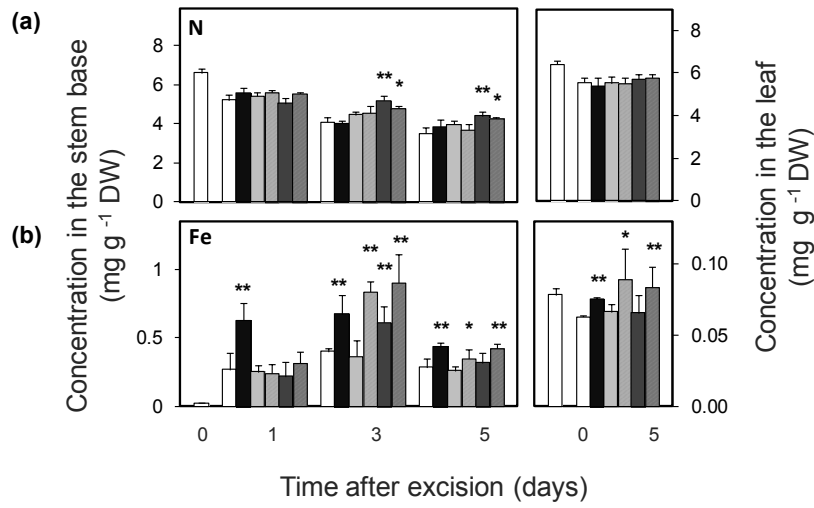
## **3.2 The effect of iron and ammonium on mineral homeostasis and metabolic activity during AR formation**

### **3.2.1 Mineral status during AR formation in response to nutrient application**

In order to assess the status of mineral nutrients within the stem base and leaves of petunia cuttings in response to nutrient application, a comprehensive analysis was conducted (Fig. 13). A gradual decline in the concentration of N has been detected in the stem base throughout the period of measurements (Fig. 13a). However,  $\text{NH}_4^+$ -supplied cuttings maintained a significantly higher level of total N compared to the control and to  $\text{NO}_3^-$  application. In mature leaves the concentration of N slightly declined and was not affected by nutrient application (Fig. 13a).

Under control conditions, the concentration of Fe in the stem base increased ten times already from 1 dpe, whereas application of Fe resulted in a 30-fold increase from the first day post excision (Fig. 13b). The stem base of  $\text{NH}_4^+$ -supplied cuttings accumulated significantly higher levels of Fe in 3 dpe. Within 5 dpe the concentrations of Fe in mature leaves decreased in the control cuttings, while remaining stable under Fe supply. This indicated that an enhanced N level in the stem base was unlikely to explain improved AR formation, whereas enhanced Fe concentrations as observed after Fe and after  $\text{NH}_4^+$  supply coincided with improved AR formation.

To assess the possible effect of N and Fe on the uptake and assimilation of each other, the concentrations of N and Fe were additionally studied in the combined supply of these elements (shown for N and Fe only). In the case of combined application of Fe and  $\text{NH}_4^+$ , N concentrations in the stem base increased similar to application of  $\text{NH}_4^+$  only, whereas application of Fe and  $\text{NO}_3^-$  did not affect the level of N as compared to individual application of these elements (Fig. 13a). Furthermore, combined application of either of the studied N forms with Fe did not alter Fe concentrations in the stem base or in mature leaves, compared to single application of Fe (Fig. 13b).



The concentrations of Ca, K, Mg, and P (Fig. 13c,d,e,g) declined significantly in the stem base and in mature leaves of the cuttings throughout the period of AR formation. The concentrations of Na, Mn and Zn (Fig. 13e,g,i,j) gradually increased in the stem base and decreased in mature leaves of the cuttings. The level of S (Fig. 13e), however, increased slightly in both leaves and stem base samples, which can be explained by the assimilation of possible degradation products of MES, containing a sulfonic group in its structure. The concentration of B did not change significantly in the stem base and decreased four times in mature leaves (Fig. 13i). The mineral status of the described elements (Fig. 13c-l) did not change in response to application of Fe or N. The level of Mg in the stem base remained significantly lower in the N-supplied cuttings, however, despite this change appeared to be specific to N, it did not differ between  $\text{NO}_3^-$  and application. Remarkably, in control conditions the concentration of Cu (Fig. 13l) started to increase from 1 dpe and reached a sixty-fold increase in 3 dpe compared to Fe-supplied cuttings, where the maximum level of Cu was only five-times higher. Additional studies are required in order to investigate the relevance of this element for Fe-mediated improvement of AR formation.

Therefore, the major changes in mineral status of the cuttings in response to nutrient application involved an increase in the level of total N in response to application of  $\text{NH}_4^+$ , whereas Fe accumulated in the rooting zone of the cuttings under all studied conditions already from 1 dpe, and was additionally increased by application of Fe.

### 3.2.2 Effect of nutrient application on iron acquisition and homeostasis genes

As dicotyledonous plant species, petunia acquires Fe via strategy I, which involves the reduction of  $\text{Fe}^{\text{III}}$  to  $\text{Fe}^{\text{II}}$  by the ferric-chelate reductase *FRO2* (*FERRIC REDUCTION OXIDASE 2*) and subsequent  $\text{Fe}^{2+}$  uptake by *IRT1* (*IRON-REGULATED TRANSPORTER 1*; Vert *et al.*, 2002). Under Fe-free conditions, mRNA levels of the petunia *IRT1* homolog increased by five-fold from 3 dpe onwards, whereas in Fe-supplied samples transcripts remained at a basal level (Fig. 14c). Similar patterns of transcript accumulation were recorded for *FRO2* (Fig. 14d).

---

**Fig. 13** (Left) Mineral balance in the stem base and mature leaves of *Petunia hybrida* cuttings during adventitious root formation in response to nutrient application. Concentrations of (a) nitrogen, (b) iron, (f) calcium, (c) potassium, (d) magnesium, (g) sodium, (e) phosphorus, (f) sulfur, (h) boron, (l) copper, (j) manganese, and zink (k). Bars represent means of five independent replicates + SE. Significant differences to control treatments at specified time points after excision are indicated by asterisks (t-test; \*,  $P < 0.05$ ; \*\*,  $P < 0.01$ ).

Transcript levels of the Fe storage protein *FERRITIN* was significantly downregulated in control and  $\text{NO}_3^-$ -supplied cuttings within 7 dpe, whereas Fe application led to a significant increase from 1 dpe, reaching a peak in 3 dpe (Fig. 14f). Interestingly, transcript accumulation of *FERRITIN* under  $\text{NH}_4^+$  application was less pronounced but resembled that observed in Fe-supplied cuttings. Transcript concentration of *NAS* (*NICOTIANAMINE SYNTHASE*), responsible for the synthesis of the intracellular Fe chelator nicotianamine (von Wirén *et al.*, 1999), showed an immediate 10-fold decrease after excision in all studied conditions, followed by a significantly higher accumulation in 3 and 7 dpe in the case of Fe or  $\text{NH}_4^+$  supply (Fig. 14g).

Thus, although only application of Fe prevented transcript accumulation of Fe-acquisition genes, the levels of transcripts associated with Fe-homeostasis were affected by  $\text{NH}_4^+$  and Fe supply in a similar manner.

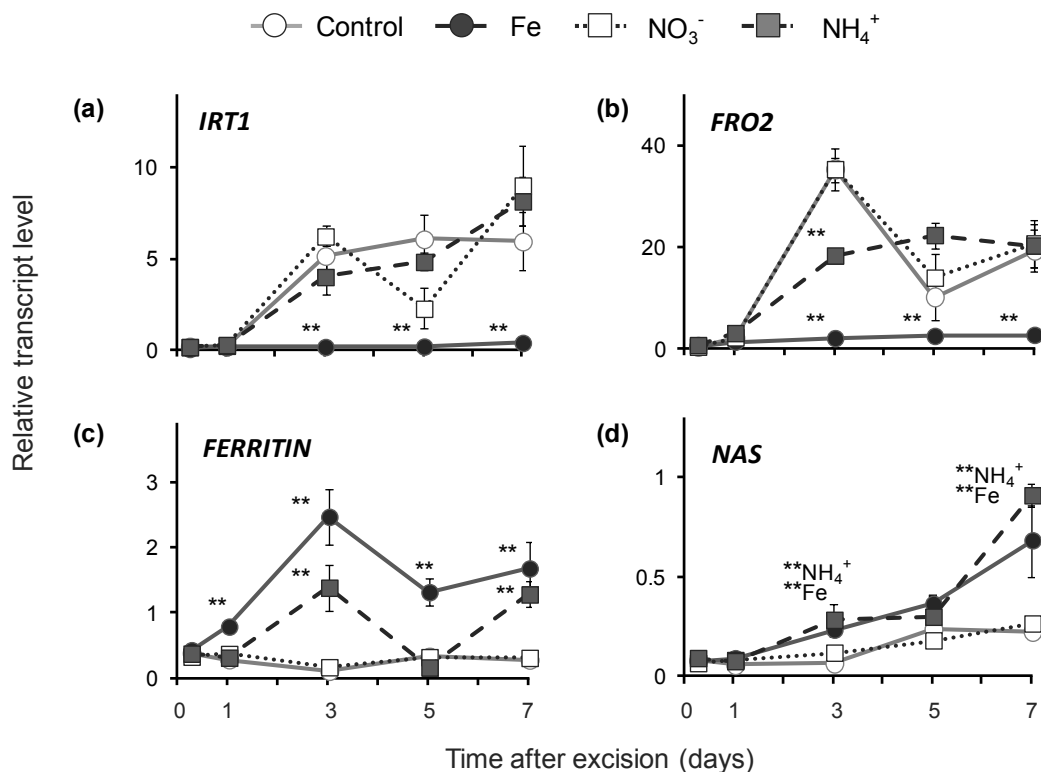


**Fig. 14** Transcript abundance of key Fe-related genes in the stem base of *Petunia hybrida* cuttings during adventitious root formation in response to nutrient application. Transcript abundance of (a) *IRON-REGULATED TRANSPORTER1* (*IRT1*), (b) *FERRIC REDUCTION OXIDASE 2* (*FRO2*), (c) *FERRITIN*, and (d) *NICOTIANAMINE SYNTHASE* (*NAS*). Each data point represents the mean of three independent replicates  $\pm$  SE of the fold-change related to the initial transcript level at the time of excision. Significant differences to control treatments at specified time points after excision are indicated by asterisks (t-test; \*,  $P < 0.05$ ; \*\*,  $P < 0.01$ )

### 3.2.3 The impact of nutrient application on carbohydrate distribution

The concentrations of soluble carbohydrates, reflecting the status of the carbon sink in the stem base (Fig. 15a-c) underwent a significant decrease during 1 dpe followed by a return to the initial levels in 3 dpe. These results were in agreement with the time-dependent pattern of carbohydrate accumulation, previously described for AR formation in petunia (Ahkami et al., 2009).

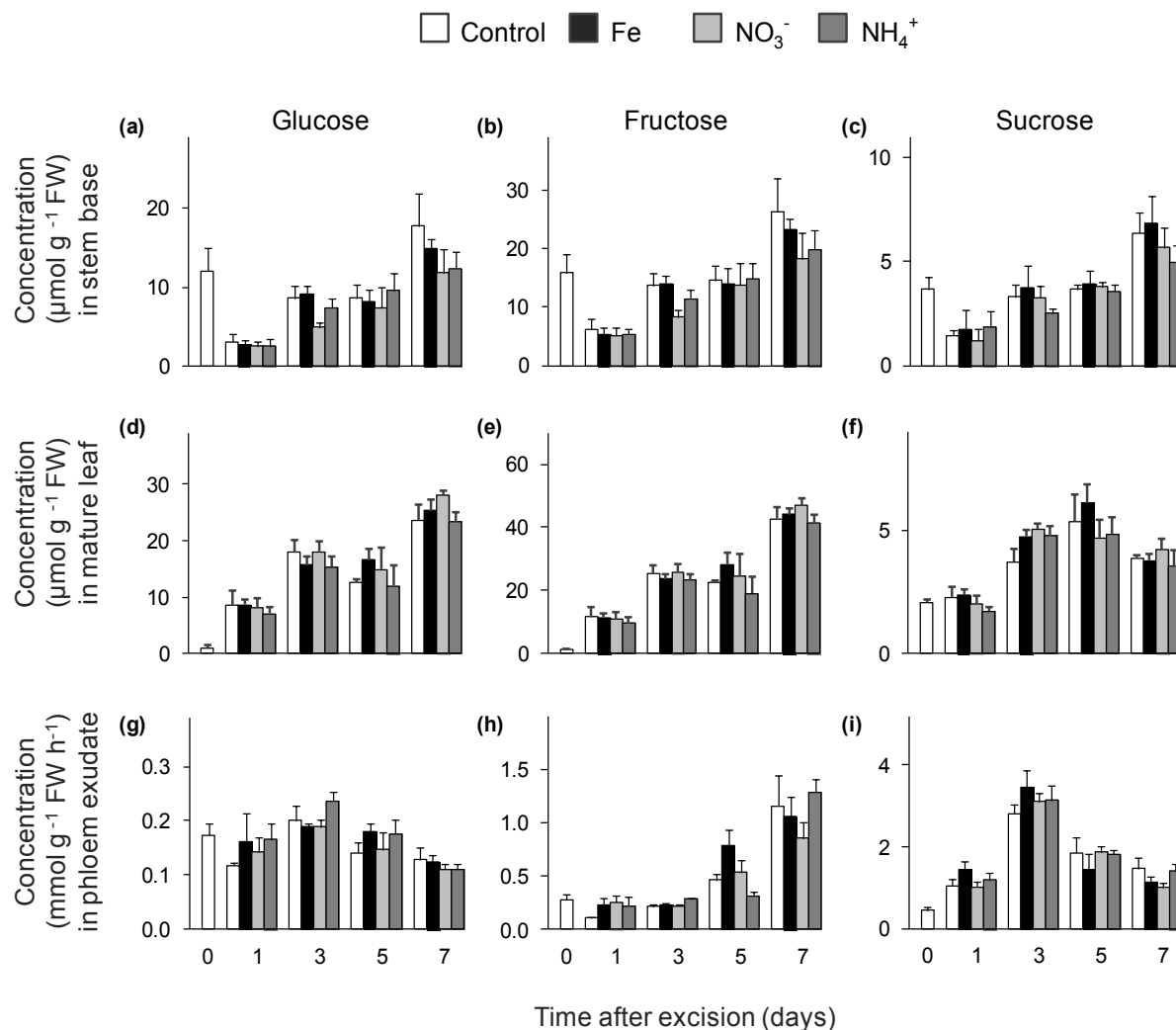


**Fig. 15** Concentrations of soluble carbohydrates in the stem base (a-c), mature leaves (d-f) and phloem exudates (g-h) of *Petunia hybrida* cuttings during adventitious formation in response to nutrient application. Concentrations of (a, d, g) glucose, (b, e, h) fructose, (c, f, i) sucrose. Each value is represented by the mean of five independent replicates + SD.



In mature leaves the concentrations of glucose and fructose (Fig. 15d,c) increased throughout the period of observation up to 40 times compared to the initial values. The concentration of sucrose in the leaves remained unchanged during 1 dpe and increased twofold from 3 dpe (Fig. 15f). Among the analyzed soluble carbohydrates no significant differences in concentrations were detected in response to nutrient application, neither in the stem base nor in mature leaves of the cuttings.

In order to additionally assess the assimilate translocation to the stem base, the concentrations of soluble carbohydrates were analyzed in the phloem exudates of the cutting. The concentration of glucose remained relatively stable within 7 dpe (Fig. 15g). The levels of fructose remained similar to those of glucose during 3 dpe followed by an increase from 5 dpe, reaching approximately five times higher values compared to the initial state (Fig. 15h). The concentration of sucrose increased twice already from 1 dpe, additionally increasing up to three times in 3 dpe followed by return to the values recorded in 1 dpe (Fig. 15i). Therefore, application of the studied nutrients neither affected the carbohydrate translocation to the stem base, nor did it alter the accumulation of sugars in mature leaves throughout the course of AR formation.

### **3.2.4 The effect of nutrient application on primary metabolites and organic acids**

To assess the influence of nutrient application on primary carbon metabolism, a profiling of the primary intermediates of sugar metabolism was carried out using IC-MS/MS (Fig. 16).

The concentrations of glucose 6-phosphate and fructose 6-phosphate (Fig. 16a), 3-phosphoglyceric acid (Fig. 16c) and UDP-glucose (Fig. 16f) underwent a moderate increase throughout the course of analysis, whereas accumulation of glucose 1-phosphate (Fig. 16b) and trehalose 6-phosphate (Fig. 16e) was more pronounced, reaching four- and ten-fold increase in 7 dpe, respectively. The concentration of sucrose 6-phosphate decreased up to 20% with the progress of AR formation (Fig. 16d).

Among the organic acids involved in tricarboxylic acid cycle, the concentration of citrate increased twofold from 3 dpe (Fig. 16g), whereas the maximum levels of cis-aconitate and succinate were detected in 1 dpe (Fig. 16h,k).

The concentration of fumarate (Fig. 16i) remained unchanged during the measurements, and the levels of malate (Fig. 16j) and oxoglutarate (Fig. 16l) decreased from 1 dpe and 3 dpe, respectively. No significant differences in the concentrations of analyzed metabolites were detected in response to nutrient application.

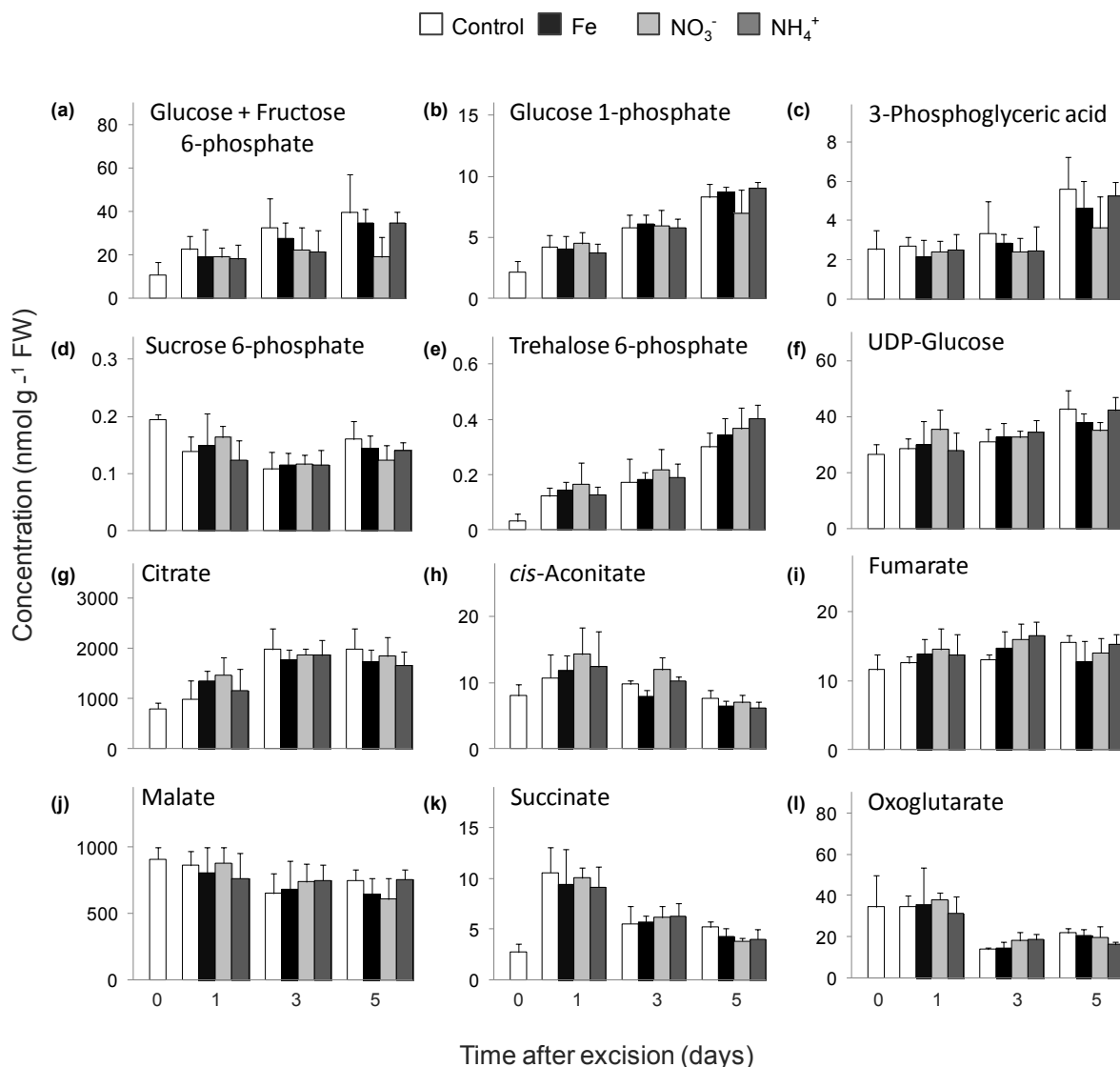


**Fig. 16** Concentrations of primary intermediates of sugar metabolism in the stem base of *Petunia hybrida* cuttings during adventitious root formation in response to nutrient application. Concentrations of (a) glucose 6-phosphate and fructose 6-phosphate, (b) glucose 1-phosphate, (c) 3-phosphoglyceric acid, (d) sucrose 6-phosphate, (e) trehalose 6-phosphate, (f) UDP-glucose, (g) citrate, (h) *cis*-aconitate, (i) fumarate, (j) malate, (k) succinate and (l) oxoglutarate. Bars represent means of five independent replicates + SE.

### 3.2.5 The impact of nutrient application on concentrations of amino acids

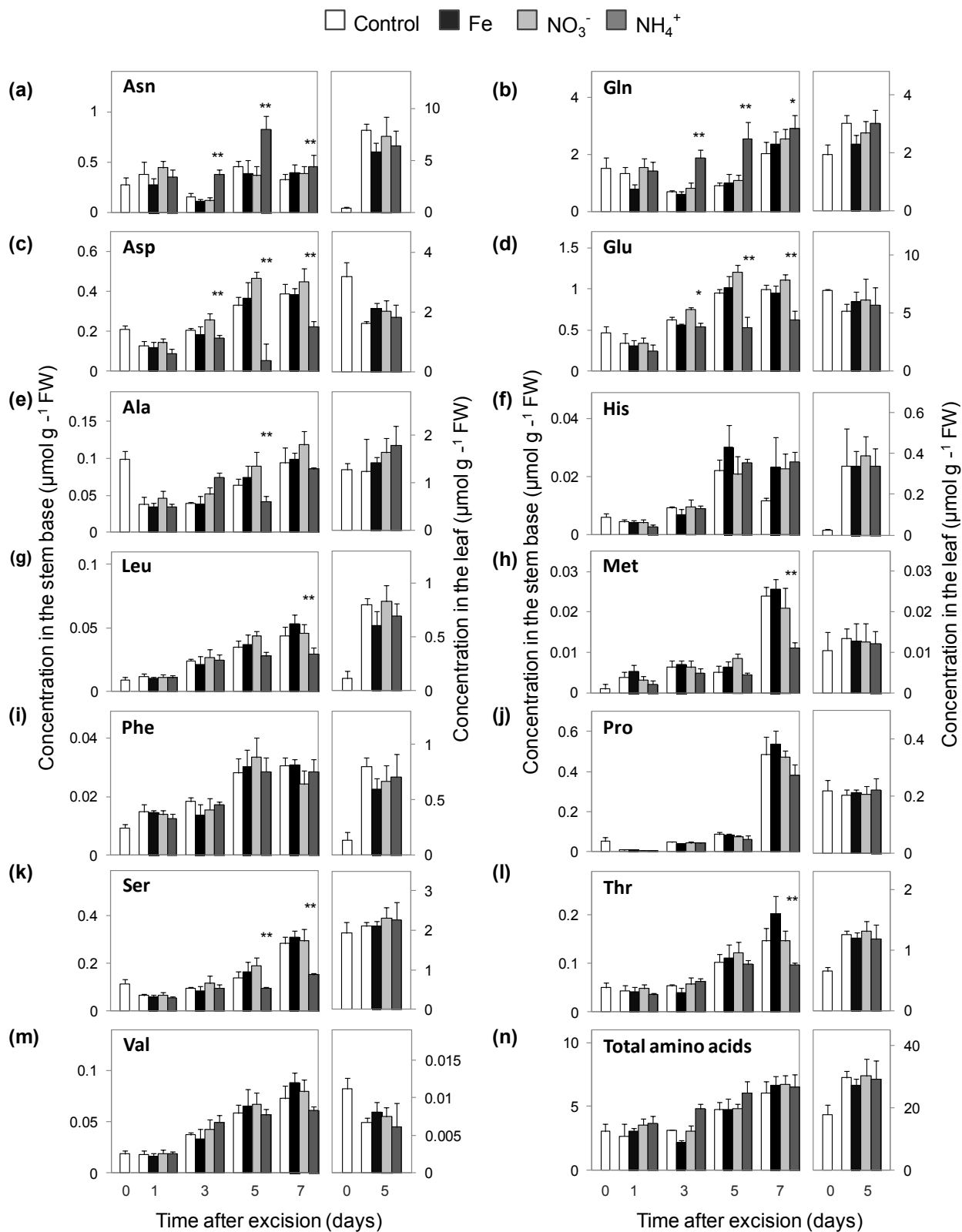
With progressing AR formation the concentrations of the analyzed free amino acids in the stem base of the cutting underwent a gradual increase (Fig. 17). A similar pattern in the accumulation of free amino acids has been observed by Ahkami et al. (2009). Among the prevailing amino acids, the levels of asparagine and glutamine in the stem base decreased significantly from 3 dpe, followed by a recovery to the initial values in 5 dpe (Fig. 17a,b). However, in the stem base of the cuttings supplied with  $\text{NH}_4^+$  the concentrations of asparagine and glutamine increased approximately two-fold from 3 dpe and reached the initial values one day earlier (Fig. 17a,b). Furthermore, the concentrations of aspartic and glutamic acid underwent a simultaneous decrease in the stem base of  $\text{NH}_4^+$ -supplied cuttings starting from 3 dpe (Fig. 17c,d). The levels of alanine, leucine, methionine, serine and threonine showed a significant decrease in 3 dpe in response to the application of  $\text{NH}_4^+$  (Fig. 17e,g,h,k,l).

In mature leaves at 120 hpe the concentrations of aspartic and glutamic acids and valine (Fig. 17a,b,m) were below the initial values. The concentrations of alanine, methionine, proline and serine (Fig. 17e,h,j,k) remained stable in mature leaves of the cuttings, whereas the concentrations of asparagine, glutamine, histidine, leucine, phenylalanine and threonine (Fig. 17c,d,f,g,i,l) were significantly higher than at the time of the cutting excision. The level of the analyzed amino acids in the leaves was not affected by nutrient application.

Therefore, application of  $\text{NH}_4^+$  resulted in an increase of the concentrations of glutamine and asparagine, containing an additional N-atom in their structure compared to their acidic precursors. However, despite an observed decrease in the levels of glutamic and aspartic acid, as well as leucine, methionine, serine and threonine under  $\text{NH}_4^+$ -supply, the concentrations of total analyzed amino acids remained unaffected by nutrient application in the stem base as well as in mature leaves of the cuttings (Fig. 17n).

---

**Fig. 17** (Right) Concentrations of proteinogenic amino acids in the stem base and in mature leaves of *Petunia hybrida* cuttings during adventitious root formation in response to nutrient application. Concentrations of (a) asparagine, (b) glutamine, (c) aspartic acid, (d) glutamic acid, (e) histidine, (f) proline, (g) serine, (h) threonine, (i) alanine, (j) leucine, (k) methionine, (l) phenylalanine, (m) valine and (n) total proteinogenic amino acid. Bars represent means of five independent replicates + SD. Significant differences to control treatments at specified time points after excision are indicated by asterisks (t-test; \*,  $P < 0.05$ ; \*\*,  $P < 0.01$ ).



### 3.2.6 Impact of nutrients on the expression of genes involved in nitrogen metabolism

To assess the response of N-acquisition genes to nutrient application, transcript levels of  $\text{NH}_4^+$  and  $\text{NO}_3^-$  transporters that have been previously shown to be upregulated during AR formation (Ahkami *et al.*, 2014), were selected for the analysis.

Under control conditions, transcript abundance of the N-responsive  $\text{NH}_4^+$  transporter gene *AMT1* (Gazzarrini *et al.*, 1999) showed a twenty-fold increase from 1 dpe and peaking in 3 dpe, followed by a gradual decrease (Fig. 18a). Application of  $\text{NO}_3^-$  did not affect transcript abundance of *AMT1*, whereas  $\text{NH}_4^+$  application led to a significant decrease throughout the major course of analysis (Fig. 18a). The transcript abundance of the petunia  $\text{NO}_3^-$  transporter *NRT1* (Fig. 18b) underwent a significant increase immediately from 1 dpe, reaching maximum values between 3 to 5 dpe. Application of both N forms resulted in decreased levels of *NRT1* mRNA in 3 dpe (Fig. 18b).

To evaluate the influence of nutrient application on the expression of genes involved in N-metabolism, cytoplasmic and plastidic isoforms of *GLUTAMINE SYNTHETASE* (*GS*) and *GLUTAMATE DEHYDROGENASE* (*GDH*) were analyzed in the leaves and the stem base of the cuttings. The transcript abundance of cytosolic *GS1*, shown to play a major role in assimilation of retranslocated N (Miflin & Habash, 2002), increased approximately five times in the stem base and up to three times in mature leaves of the cuttings throughout AR formation (Fig. 18c,d). In contrast to *GS1*, the transcript abundance of the plastidic isoform *GS2*, responsible for primary assimilation of N in chloroplasts (Coruzzi, 2003), was significantly down-regulated immediately after excision in the stem base and leaves, remaining at this level throughout the period of AR formation (Fig. 18e,f). The transcript concentrations of *GDH*, involved in N remobilization (Miyashita & Good, 2008) in the stem base was upregulated already 6 h after excision and continued to gradually increase up to five-fold in 5 and 7 dpe (Fig. 18g). In the leaf samples the level of *GDH* mRNA increased approximately twenty times in 1 dpe followed by a two-fold decrease from 3 dpe (Fig. 18i). No significant differences in the transcript abundance of *GS1*, *GS2* and *GDH* were observed in response to nutrient applications.

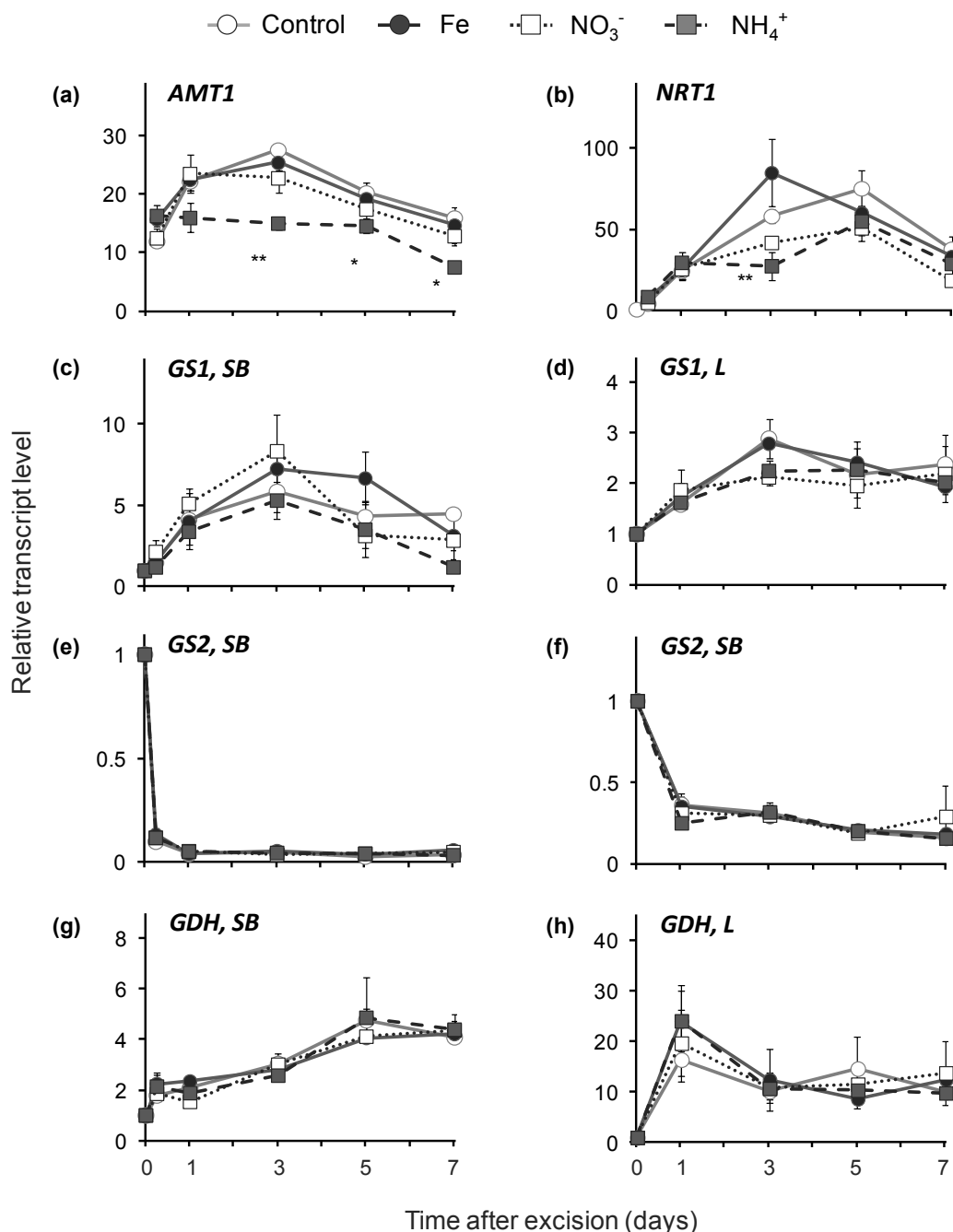


**Fig. 18** Transcript abundance of genes for N transport and metabolism in the stem base (SB; a,b,c,e,g) and mature leaves (L; d, f, h) of *Petunia hybrida* cuttings during adventitious root formation in response to nutrient application. Transcript abundance of (a) *AMT1*, (b) *NRT1*, (c,d) *GLUTAMINE SYNTHASE 1*, (*GS1*; e,f) *GLUTAMINE SYNTHASE 2* and (*GS2*; g,h) *GLUTAMATE DEHYDROGENASE* (*GDH*; g,h). Each data point represents the mean of three independent replicates  $\pm$  SE of the fold-change related to the initial transcript level at the time of excision. Significant differences to control treatments at specified time points after excision are indicated by asterisks (t-test; \*,  $P < 0.05$ ; \*\*,  $P < 0.01$ )

### 3.3 Involvement of phytohormones in nutrient-mediated AR formation

#### 3.3.1 Effect of iron and ammonium application on the phytohormonal balance

To elucidate whether nutrient application affected AR formation via altering the balance of phytohormones, the concentrations of auxin, cytokinins, ABA and related intermediates were analyzed throughout the course of AR formation (Fig. 19).

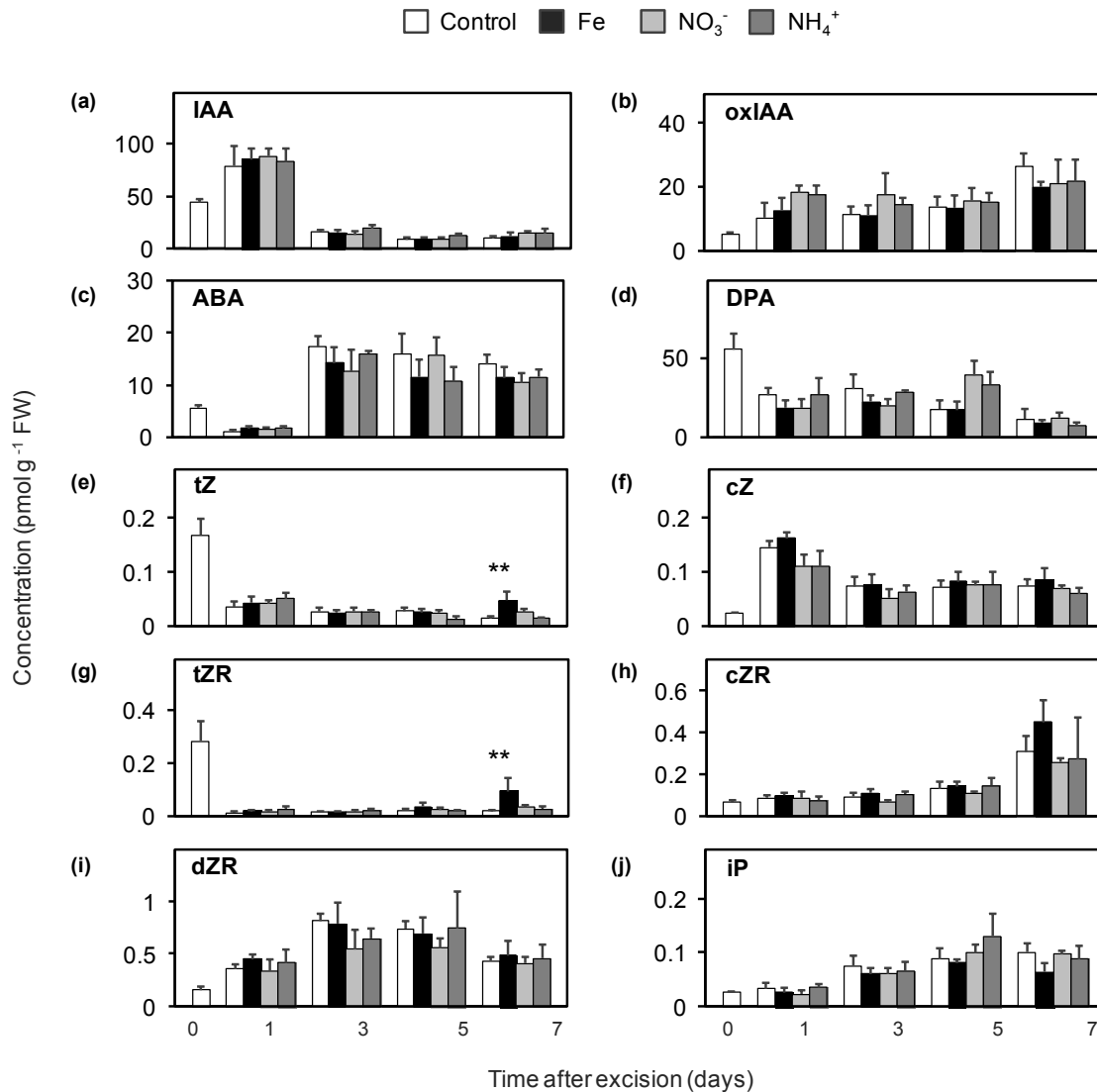


**Fig. 19** Concentrations of major phytohormones and their intermediates in the stem base of *Petunia hybrida* cuttings during adventitious root formation in response to nutrient application. Concentrations of (a) indole-3-acetic acid, (b) 2-oxindole-3-acetic acid, (c) *trans*-zeatin, (d) *cis*-zeatin, (e) *trans*-zeatin riboside, (f) *cis*-zeatin riboside, (g) isopentenyladenine, (h) dihydrozeatin riboside, (i) abscisic and (j) dihydrophaseic acid. Bars represent means of five independent replicates + SD. Significant differences to control treatments at specified time points after excision are indicated by asterisks (t-test; \*, P < 0.05; \*\*, P < 0.01)

The concentration of IAA increased by 100 % within 1 dpe, but dropped to 25 % of its initial value during the following days (Fig. 19a). The concentration of the degradation product of IAA, 2-oxindole-3-acetic acid (oxIAA) underwent a two-fold increase in 1 dpe and continued a gradual increase during the course of analysis (Fig. 19b). Nutrient application revealed no significant impact on the level of IAA and oxIAA.

The concentration of ABA decreased to 25 % from 1 dpe followed by an approximately 15-fold increase at the later stages regardless of nutrient treatments (Fig. 19c). The concentration of ABA catabolite, dihydrophaseic acid (DPA), decreased approximately to a half of initial value in 1 dpe (Fig. 19d). The concentrations of ABA and DPA were not affected by nutrient application.

The concentrations of the major active cytokinin *trans*-zeatin (tZ) and its transport form *trans*-zeatin riboside (tZR) decreased significantly within 1 dpe and remained at a similar level throughout the entire period of development (Fig. 19e,g). The concentration of *cis*-zeatin (cZ) that was almost eight times higher than *trans*-zeatin (tZ) in the intact stem increased seven times during the first day post excision followed by a gradual two-fold decrease in the remaining period of AR formation (Fig. 19f). The concentration of the ribosylated form of *cis*-zeatin (cZR) remained rather stable until 7 dpe (Fig. 19h). While these changes appeared to relate to the separation of the cutting from the stock, nutrient application revealed no significant effect, except for tZ and tZR, which increased significantly in the presence of Fe only from 7 dpe (Fig. 19e,g). The concentrations of the degradation product of CKs, dihydrozeatin riboside (DZR) and another active cytokinin, isopentenyladenine (iP), increased approximately five times after the excision of the cuttings, however were not affected by nutrient application (Fig. 19i,j).

### **3.3.2 Impact of iron and ammonium supply on the activity of the auxin reporter DR5::GFP/GUS**

To deeper analyze the involvement of auxin in nutrient-mediated AR formation, transgenic petunia lines, expressing an ER-targeted GFP/GUS fusion under control of the DR5 promoter, were generated. In addition to spatial information on auxin distribution, this reporter allows to examine also a nutrient-dependent auxin response. First, to assess the local distribution of auxin signal within the rooting zone in response to nutrient application during AR formation, the fluorescence of GFP was visualized using confocal microscopy (Fig. 20).



In the stem base of the cutting at the time of excision a GFP signal was detected in several regions of the inner phloem ring adjacent to the vessels (Fig. 20a,b). Within 1 dpe, the level of GFP-specific fluorescence increased significantly, occupying both outer and inner phloem rings as well as surrounding parenchyma cells of the cortex (Fig. 20c-f).

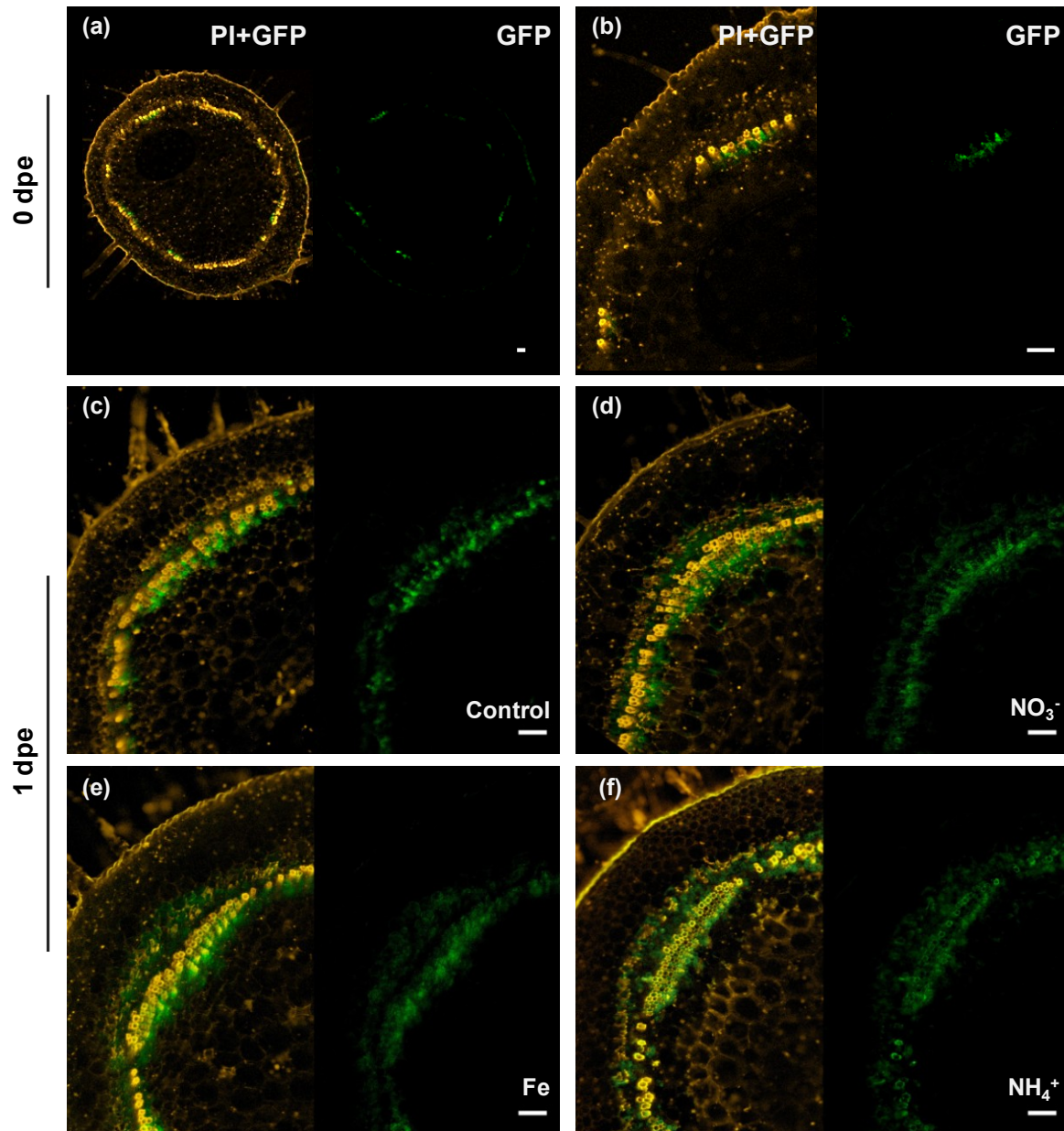
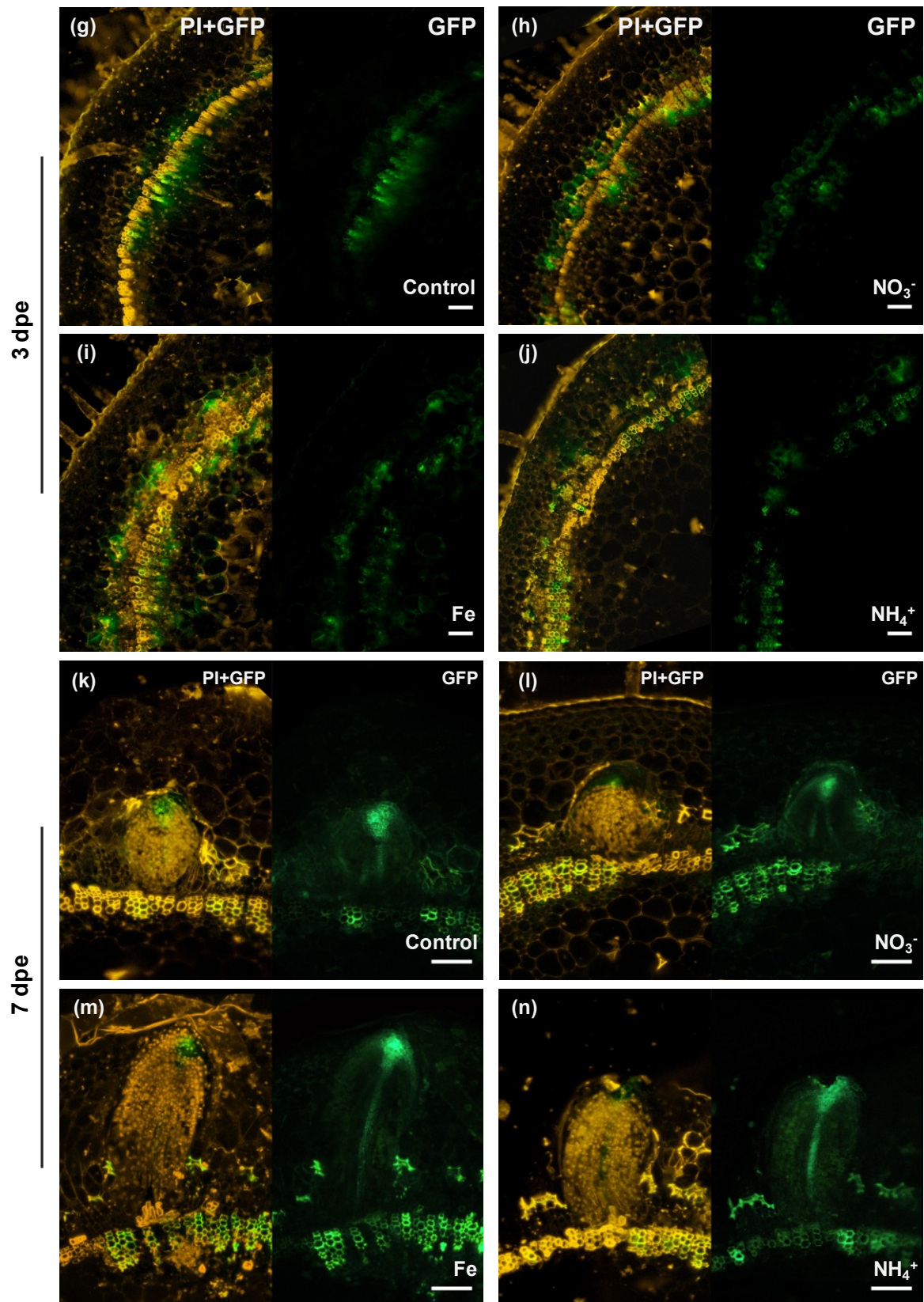


**Fig. 20** Auxin-induced GFP fluorescence in the stem base of *Petunia hybrida* DR5::GUS/GFP reporter line cuttings during adventitious root formation in response to nutrient application. Cross sections from 1-4 mm of the stem base, additionally stained with propidium iodide (PI, yellow color), are shown in 0 dpe (a,b), 1 dpe (c-f), 3 dpe (g-j) and 7 dpe (k-n) in cuttings supplied with iron (e,i,m), nitrate (d,h,l) or ammonium (f,j,n), compared to control conditions without nutrients (c,g,k).



The pattern of GFP fluorescence in 3 dpe under control conditions remained similar to that observed in 1 dpe (Fig. 20,g), whereas in the cuttings supplied with both N forms and in particular with Fe the spots of intense fluorescence appeared on both sides of the vessel ring (Fig. 20h-j). Such accumulation of fluorescence corresponded to dividing meristematic cells of the developing AR primordia, which were most advanced under Fe supply (Fig. 20i).

AR primordia of different developmental stages were observed under all conditions in 7 dpe (Fig. 20, k-n). As it was shown in wild type plants (Fig. 11), the most advanced primordia were found under Fe and  $\text{NH}_4^+$  supply, whereas in control cuttings and under  $\text{NO}_3^-$  supply AR primordia were less elongated. At this time point, GFP fluorescence in the AR primordia resembled the typical “fountain” pattern of the auxin distribution observed in the developed root (Benková *et al.*, 2003) with intense signal in the vasculature and the highest fluorescence detected at the tip of AR primordia (Fig. 20k-l).

To confirm the accumulation of internal auxin in the rooting zone, a fluorometric assay was performed to quantify the activity of the GUS enzyme (Fig. 21). Interestingly, an almost linear increase was detected with the progress of AR formation, without any significant difference in GUS activity in response to nutrient application.

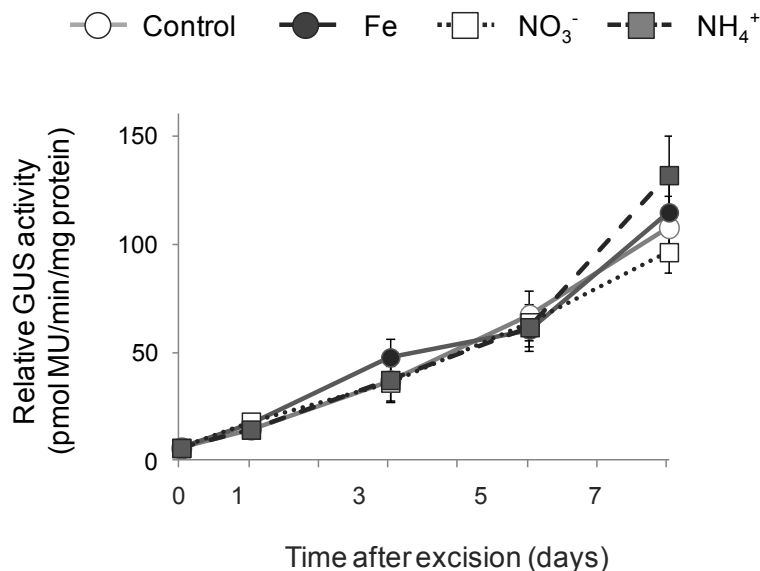


**Fig. 21** GUS activity in the stem base of a *Petunia hybrida* DR5::GUS/GFP reporter line cuttings during adventitious root formation in response to nutrient application. Each data point represents the mean of five independent replicates  $\pm$  SD from one transgenic line.

The described increase in activity could be explained by the high stability of the GUS protein against the plant proteases, leading to constant accumulation of the enzyme even if auxin accumulates only to a minor extent in developing AR.

### 3.3.3 Effect of nutrients application on the expression of genes for auxin transport and biosynthesis

To evaluate the influence of nutrient application on the expression of auxin transporters, members of *PIN*, *AUX/LAX*, and *ABCB* families, previously reported to be upregulated during AR formation, were selected (Xu *et al.*, 2005; Sukumar *et al.*, 2013; Ahkami *et al.*, 2014). Transcript abundance of a *PIN1*-type auxin efflux facilitator increased from 6 h to a maximum in 1 dpe, however, accumulation of this transcript was not altered in response to nutrient supply (Fig. 22a). Relative to control conditions, transcript abundance of a petunia homolog of *LAX1*, encoding an auxin importer, was initially upregulated after 6 hours from excision, followed by another increase in 3 dpe observed in all conditions (Fig. 22b). In contrast, transcript abundance of the other homolog *LAX3* increased significantly from 7 dpe, with highest values recorded in the case of Fe and  $\text{NH}_4^+$  supplies (Fig. 22c). Transcript abundance of an *ABCB*-type auxin transporter increased significantly within 1 dpe reaching the maximum in 3 dpe, without any significant difference in response to supplied nutrients (Fig. 22d).

Among the genes involved in auxin biosynthesis (Ljung, 2013), transcript abundance of a *TAR1* homolog decreased immediately after excision, recovering to the initial levels only in the case of Fe supply (Fig. 22e). Transcript abundance of *TAR4* increased from 7 dpe up to 80 times in the stem base of Fe- and  $\text{NH}_4^+$ -supplied cuttings, compared to only a 45-fold increase under control or  $\text{NO}_3^-$  conditions (Fig. 22f). The level of mRNA of the auxin responsive gene *ARF6*, shown to be a positive regulator of AR formation (Gutierrez *et al.*, 2012), underwent a two-fold increase, returning to the initial levels detected 3 dpe (Fig. 22g). Transcript abundance of *GH3.6*, another gene regulated by auxin signaling, increased immediately 6 h post excision and reached an approximately five-fold increase in 7 dpe in the cuttings supplied with Fe and  $\text{NH}_4^+$ , compared to three-fold increase in control and  $\text{NO}_3^-$  conditions (Fig. 22h).

Taken together, application of Fe and  $\text{NH}_4^+$  supply led to the upregulation of auxin-related genes only at the later time points (7 dpe).

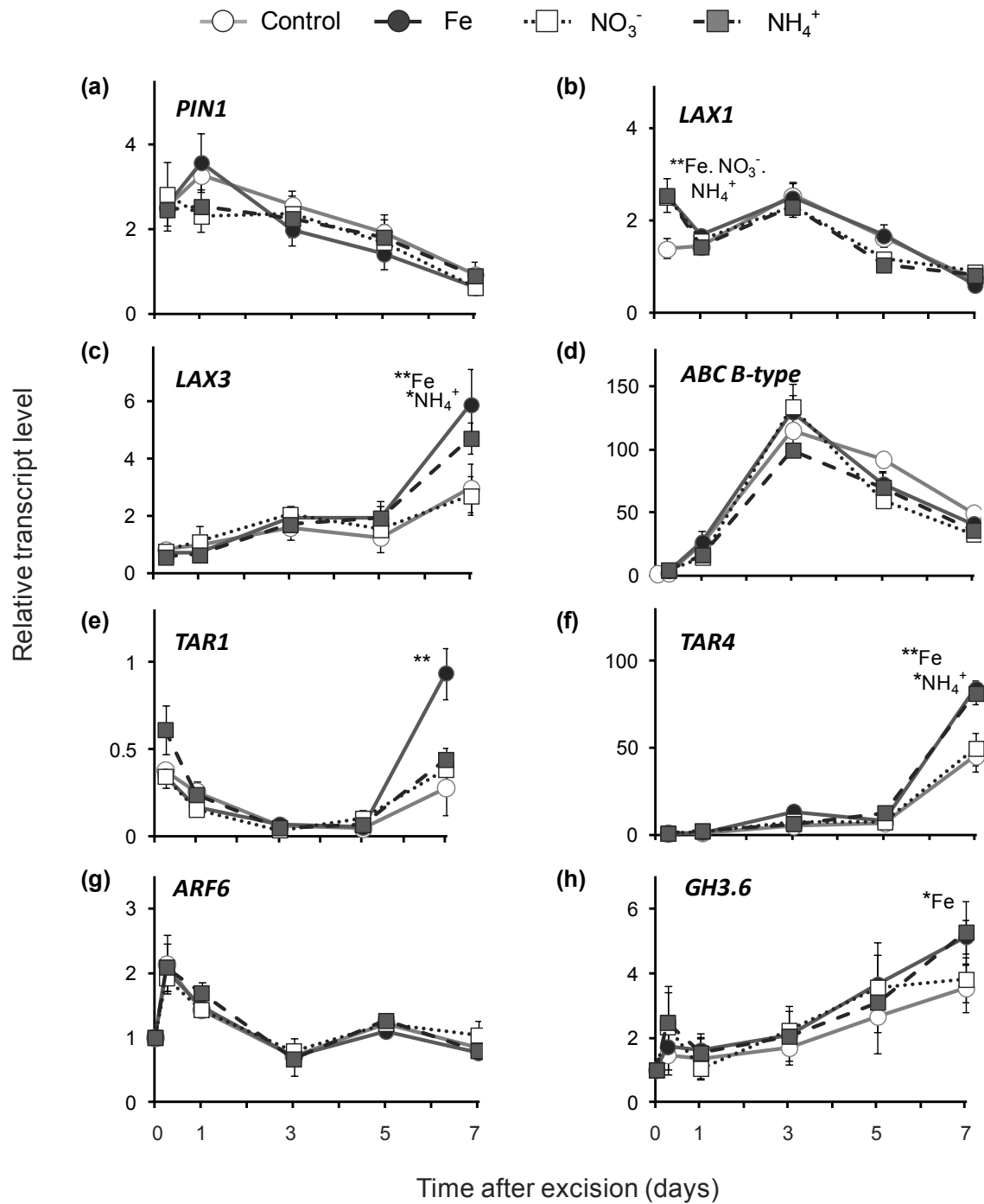


**Fig. 22** Influence of nutrient application on transcript abundance of auxin-related genes in the stem base of *Petunia hybrida* cuttings during adventitious root formation. Transcript abundance of (a) *PIN1*, (b) *LAX1*, (c) *LAX3*, (d) ABC B-type, (e) *TAR1*, (f) *TAR4*, (g) *ARF6*, (h) *ARF8*, (i) *GH3.1* and (j) *GH3.6*. Each data point represents the mean of three independent biological replicates  $\pm$  SE of the fold-change related to the initial transcript level at the time of excision. Significant differences to control treatments at specified time points after excision are indicated by asterisks (t-test; \*,  $P < 0.05$ ; \*\*,  $P < 0.01$ )



### 3.3.4 Impact of nutrient application on the expression of mitotic cyclins

Transcript abundance of the cyclin *CYCB1* gene has been suggested as a marker for mitotic activity (Ferreira *et al.*, 1994; de Almeida Engler *et al.*, 1999). The level of *CYCB1* transcript increased in 3 dpe and was significantly higher in the stem base of Fe-supplied cuttings in 3 and 7 dpe (Fig. 23a). A similar pattern of mRNA accumulation was detected for the G2/mitotic-specific marker *CYC-2* with significantly higher values under  $\text{NH}_4^+$  supply (7 dpe) and under Fe supply (3 and 7 dpe; Fig. 23b).

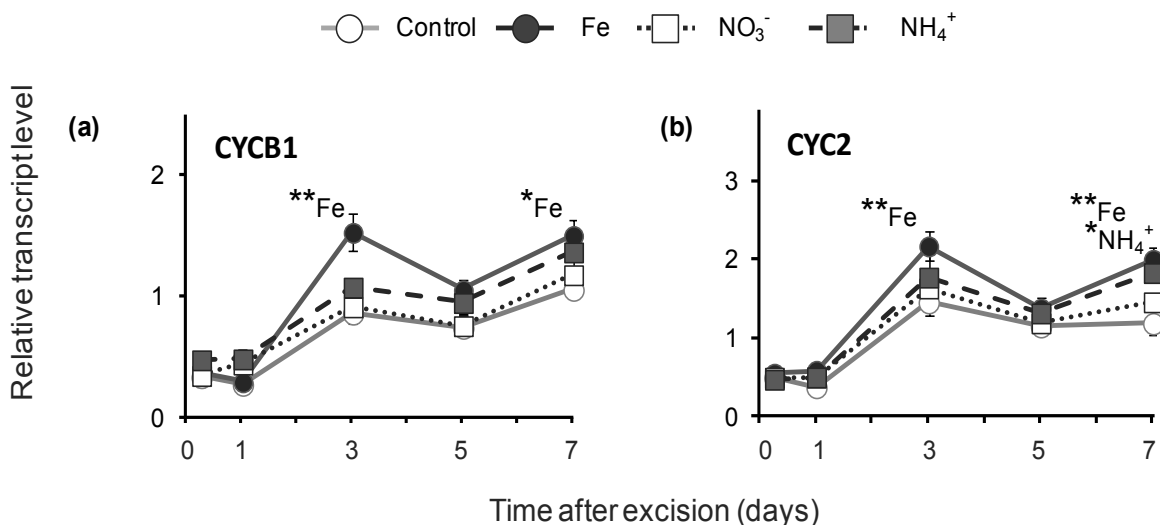


**Fig. 23** Influence of nutrient application on transcript abundance of mitotic cyclins in the stem base of *Petunia hybrida* cuttings during adventitious root formation. Transcript abundance of (a) *CYCLINB1*, (b) G2/mitotic-specific *CYCLIN-2*. Each data point represents the mean of three independent biological replicates  $\pm$  SE of the fold-change related to the initial transcript level at the time of excision. Significant differences to control treatments at specified time points after excision are indicated by asterisks (t-test; \*,  $P < 0.05$ ; \*\*,  $P < 0.01$ )

### 3.3.5 Effect of auxin inhibitors on AR formation in response to nutrient application

Encouraged by several reports emphasizing the involvement of auxin in LR and AR formation (Sánchez *et al.*, 2007; Swarup *et al.*, 2008; Pop *et al.*, 2011; *et al.*, 2012; Gutierrez *et al.*, 2012; Della Rovere *et al.*, 2013) the effect of auxin inhibitors on AR formation in response to nutrient application was assessed. Nutrient-supplied cuttings were treated with 1-naphthylphthalamic acid (NPA) or L-kynurenine (Kyn), which act as inhibitors of polar transport and *de novo* biosynthesis of auxin, respectively.

Application of NPA negatively affected the rooting performance under any of the studied conditions (Fig. 24). In control and  $\text{NO}_3^-$  conditions NPA decreased rooting percentage by almost three-fold with a significant reduction of the average length of ARs compared to non-treated cuttings.

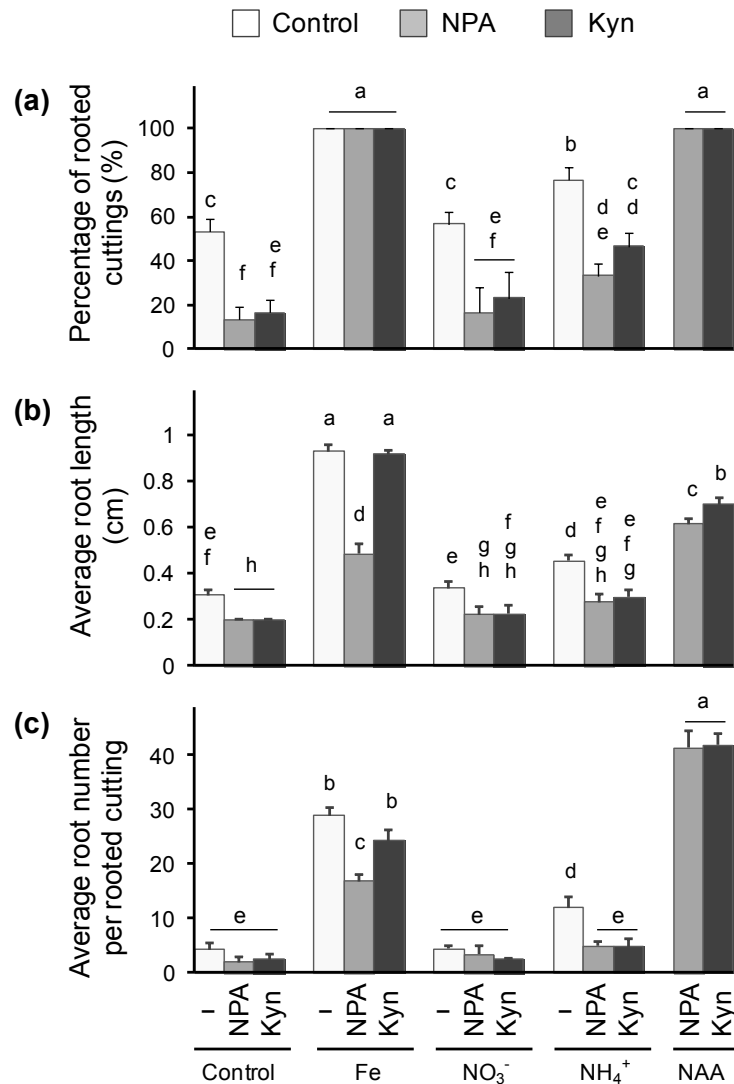


**Fig. 24** Effect of auxin inhibitors on adventitious root (AR) formation in *Petunia hybrida*. Application of the auxin transport inhibitor naphthylphthalamic acid (NPA) or the auxin biosynthesis inhibitor L-kynurenine (Kyn) on AR formation in combination with nutrients. (a) Percentage of rooted cuttings, (b) average root length and (c) average number of ARs were assessed 14 days post excision. Combination of 1-naphthaleneacetic acid (NAA) with NPA or Kyn was used to control the effect of auxin in overcoming the negative effect of studied inhibitors. Each bar represents the mean of three biological replicates, each consisting of 10 cuttings + SE. Significant differences between inhibitor treatments and nutrient supplies are indicated by different letters (Tukey's HSD,  $P \leq 0.05$ )

Rooting percentage and average AR number of  $\text{NH}_4^+$ -supplied cuttings declined by approximately 60 % in response to NPA along with a more than two-fold reduction in average AR length. In contrast to other nutrient applications, all of the Fe-supplied cuttings treated with NPA developed AR. However, the average number and length of ARs decreased by more than 40 % compared to non-treated cuttings.

Treatment with Kyn showed similar negative effects on rooting performance under control and  $\text{NO}_3^-$  conditions, whereas rooting percentage and average AR number of  $\text{NH}_4^+$ -supplied cuttings decreased by approximately 60 % in response to Kyn (Fig. 24). Application of Kyn to Fe-supplied cuttings had no significant effect on the rooting percentage and average AR length, while the average number of ARs decreased by 15 % compared to the non-treated cuttings. Thus, Fe-dependent AR formation was much less affected by inhibition of auxin biosynthesis than  $\text{NH}_4^+$ -dependent AR formation.

### **3.3.6 Impact of auxin application on nutrient-mediated AR formation**

In order to distinguish between the effect of auxin and mineral nutrition on AR formation, the rooting performance was assessed in the cuttings supplied with full mineral elements or Fe alone in combination with NAA during the induction phase (Fig. 25). The effect of additional auxin treatment resulted in significant improvement of rooting in all conditions. In all of the cuttings deprived from nutrients and treated with NAA the rooting percentage reached maximum, whereas the average AR number increased approximately 90% compared to untreated cuttings (Fig. 25b).

Furthermore, the cuttings under control conditions and treated with NAA developed approximately 40% less ARs in comparison to full mineral supply, while NAA application to the cuttings supplied with full mineral elements additionally increased the number of ARs up to 25%. Although Fe-supplied cuttings developed approximately 40% more ARs following NAA-treatment, the resulted value of the average AR number was 15% lower as obtained in the cuttings under full mineral application combined with NAA-treatment, as compared to untreated cuttings (Fig. 25d).



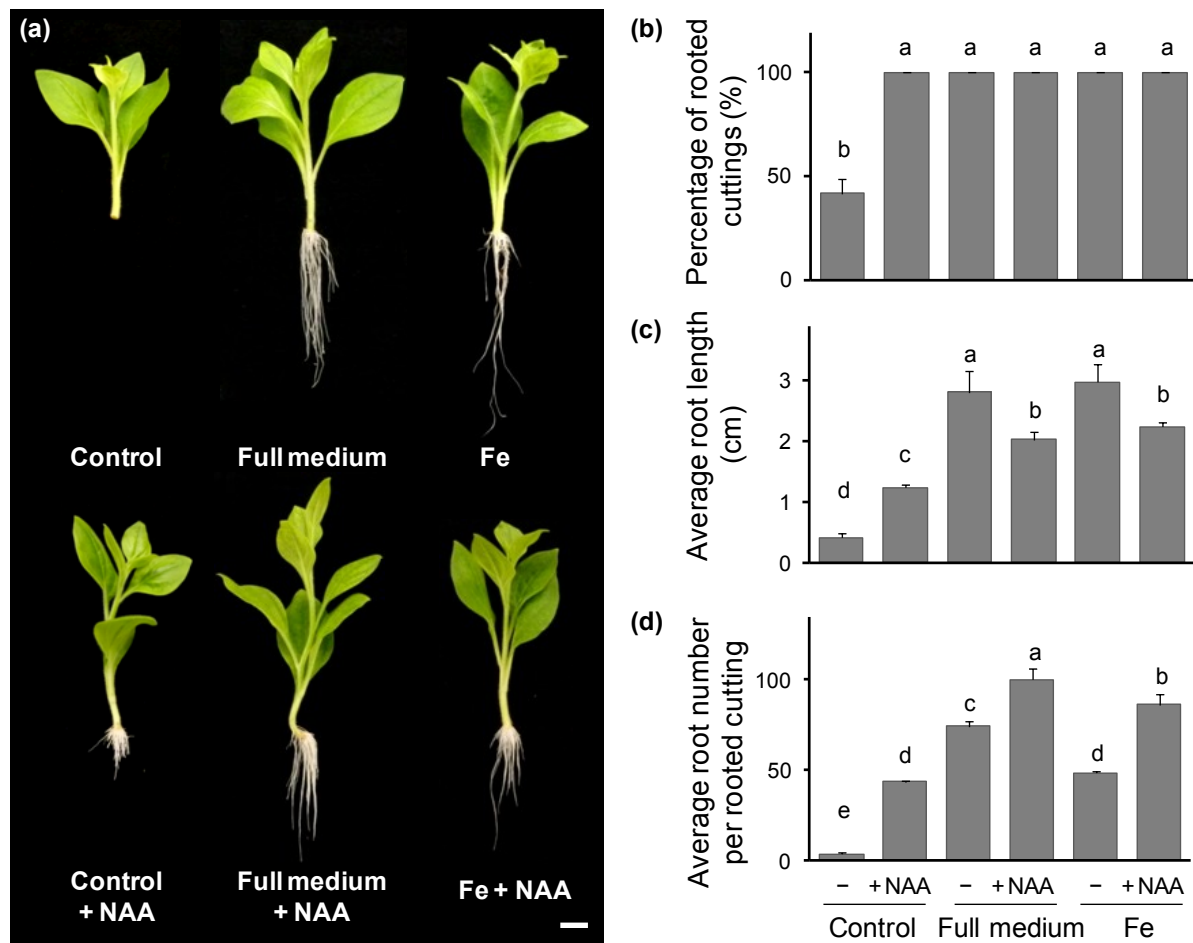


**Fig. 25** Effect of the application of NAA to the cuttings of *Petunia hybrida*, supplied with Fe, full mineral or nutrient-free medium. (a) Representative image of rooted cuttings supplied with Fe, full minerals or nutrient-free medium with or without NAA treatment. (b) Percentage of rooted cuttings, (c) average root length and (d) average number of adventitious roots were assessed 14 days post excision. Bars represent means of three independent replicates, each consisting of 8 cuttings + SE. Significant differences between auxin treatments and nutrient supplies are indicated by different letters (Tukey's HSD,  $P \leq 0.05$ ). Bar, 1 cm.

The lower values of average AR length observed in response to NAA treatment in the cuttings supplied with full mineral elements or Fe alone could be explained by a higher number of protruded ARs. Noteworthy, nutrient-deprived cuttings, treated with NAA, developed a similar number of ARs as compared to Fe application only (Fig. 25d). Therefore, auxin treatment mediated an additional improvement of nutrient-mediated AR formation in petunia cuttings.

### 3.4 The role of Fe distribution and allocation during AR formation

#### 3.4.1 Effect of foliar Fe application on AR formation and chlorophyll concentration

In order to distinguish whether the positive effect of Fe application on AR formation is achieved by maintenance of constant Fe concentration in leaves or performance of a specific function in the rooting zone, foliar application of Fe was compared to the application of Fe to the rooting medium (Fig. 26)

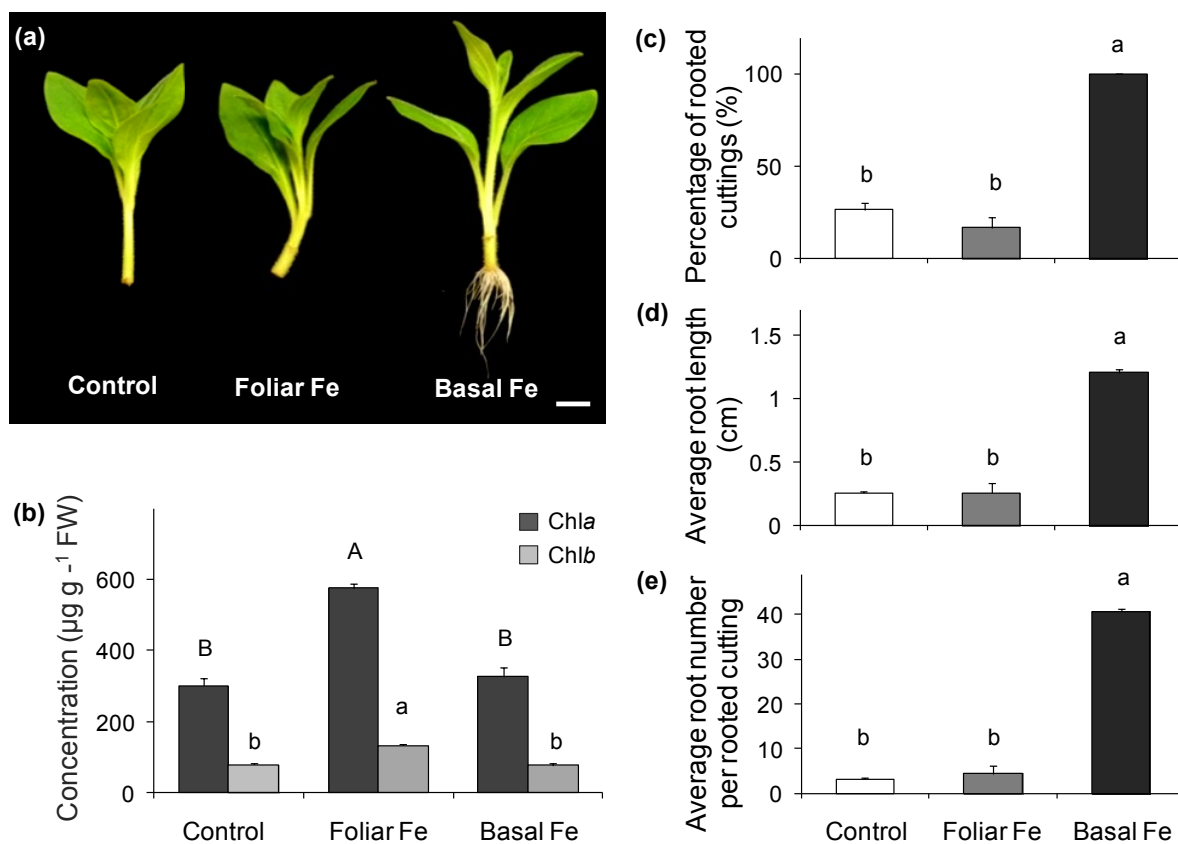


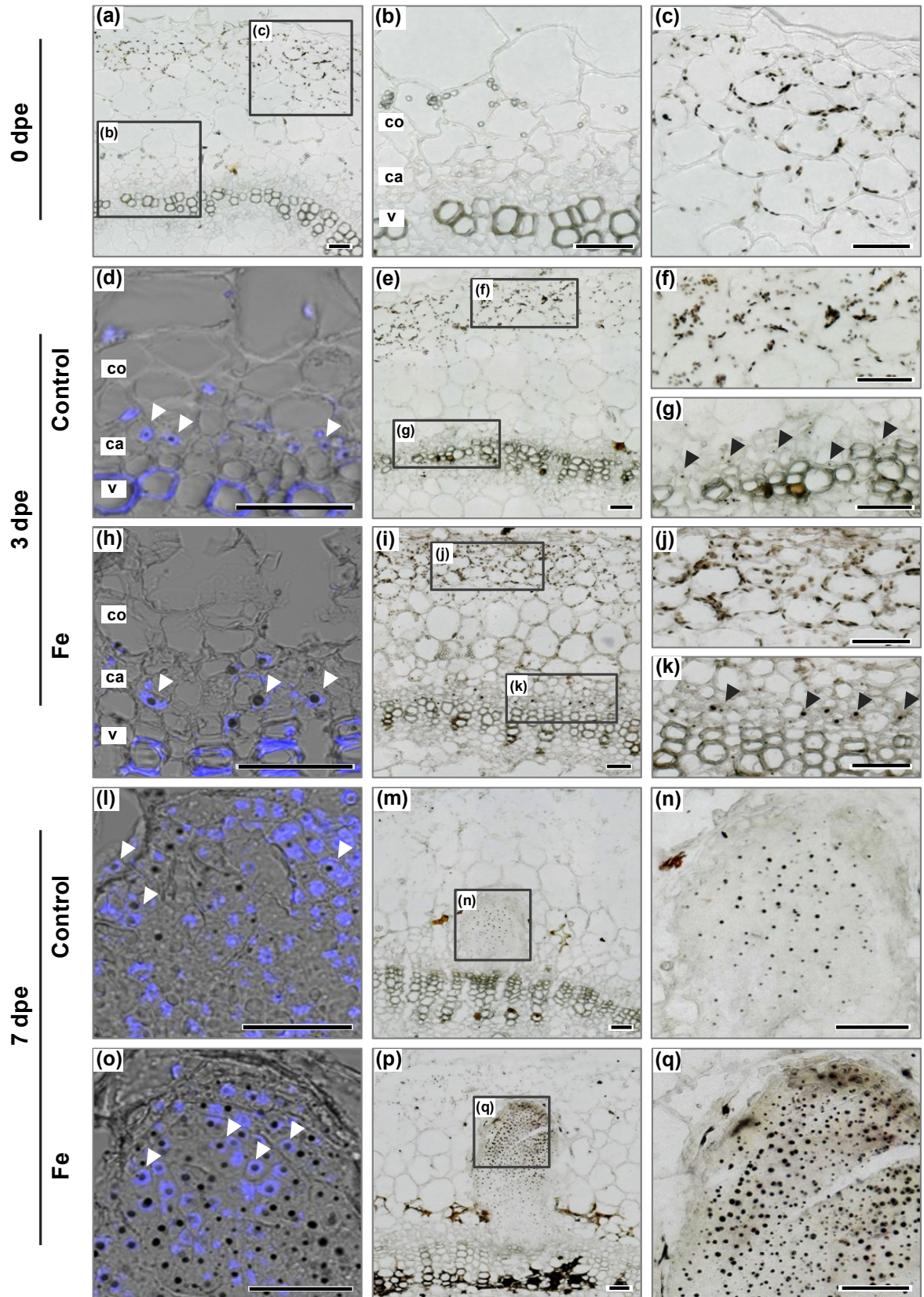
**Fig. 26** Effect of foliar or basal application of iron on adventitious root (AR) formation in *Petunia hybrida*. (a) Representative image of the rooted cuttings in response to foliar or basal application of Fe compared to control conditions. (b) Concentrations of Chlorophyll a or b in mature leaves as represented by the mean of five independent replicates + SE and were analyzed 14 dpe. (c) Percentage of rooted cuttings, (d) average root length and (e) average number of ARs were assessed 14 days post excision. Bars represent means of three independent replicates, each consisting of 10 cuttings + SE. Significant differences between treatments are indicated by different letters of the same case (Fisher's LSD,  $P \leq 0.05$ ). Bar, 200  $\mu\text{m}$ .

Foliar application of Fe increased significantly the concentrations of chlorophyll in mature leaves, as compared to Fe supply to the nutrient solution (Fig. 26b). However, the rooting performance of the leaf-supplied cuttings remained at a similar low level as that observed under nutrient-free conditions. Conversely, only the application of Fe to the cutting base effectively improved AR formation (Fig. 26c-e), indicating that improved AR formation relies on a local rather than a systemic action of the supplied Fe.

### 3.4.2 Cellular localization of iron during AR formation

To assess the dynamics of local distribution of Fe during development of AR primordia, the Perls'/DAB method was used to stain Fe in a dissected rooting zone of the cuttings at different developmental stages (Fig. 27). Right after excision (0 dpe), Fe was stained inside the cortical cells in oval structures located proximal to the surface of the stem. These Fe-containing structures most likely represented chloroplasts of the photosynthetically-active stem tissue (Fig. 27 a,c). A similar pattern of Fe accumulation was observed in 3 dpe under control conditions with appearance of small black dots in the center of the cells adjacent to the vessel ring, corresponding to the cambium and outer phloem (Fig. 27e,g). Under Fe supply, the intensity of the Fe staining in the chloroplasts of the cortex cells was visibly higher. Noteworthy, accumulation of Fe in the central compartment of the phloem cells adjacent to the vessels appeared significantly higher under Fe supply (Fig. 27i,k). The intensity of the Fe staining in 7 dpe in the cortex cells decreased considerably under both conditions with a relatively paler staining observed in control cuttings (Fig. 27m,p). However, the most striking difference in Fe allocation was detected among the developing AR primordia in response to Fe application. While under control conditions Fe was only detected as a small central spot in AR primordia cells (Fig. 27m,n), primordia of Fe-supplied cuttings were entirely and more intensely stained and showed a gradient of Fe accumulation towards the primordial apex (Fig. 27p,q). The clear central spots were visibly larger than under Fe-free conditions and increased in size with proximity to the apex of AR primordia (Fig. 27p,q).

**Fig. 27** (Right) Localization of Fe by Perls'/DAB method in the stem base of *Petunia hybrida* cuttings during adventitious root formation in response to Fe supply. Cross sections from 1-4 mm of the stem base are shown 0 days post excision (dpe, a-c), 3 dpe (a-k) and 7 dpe (l-q) in cuttings grown without nutrients (a-g; l-n) or with Fe (h-k; o-q). Black triangles show Fe localization in cambial cells at 3 dpe. Additional staining with DAPI (d, h, l, o) indicates nuclear localized Fe in meristematic cells (white triangles). co. cortex; ca. cambium; pp. pith parenchyma; v. vessels of xylem. Bar, 50  $\mu$ m.





To investigate, whether discovered central compartment accumulating large amounts of Fe corresponded to the nucleus, DAPI staining was combined with the Perls'/DAB method. Indeed, the observed central allocation of Fe in the phloem cells within 3 dpe and in meristematic cells of AR primordia in 7 dpe co-localized with nuclear-specific DAPI fluorescence (Fig. 27d,h,l,o).

Taken together, these results indicated that Fe is specifically allocated to the nucleoli of meristematic cells as early as 3 dpe, and its concentration is maintained in the apical meristem of the AR primordia. Fe application, on the other hand, additionally increases allocation of this element to the nucleoli of meristematic cells.

### 3.4.3 Effect of the medium pH on AR formation

To assess the potential role of the acidification of the rooting environment in promotion of AR formation, the cuttings were cultivated in the nutrient-deprived conditions at varying pH of the media (Fig. 28).

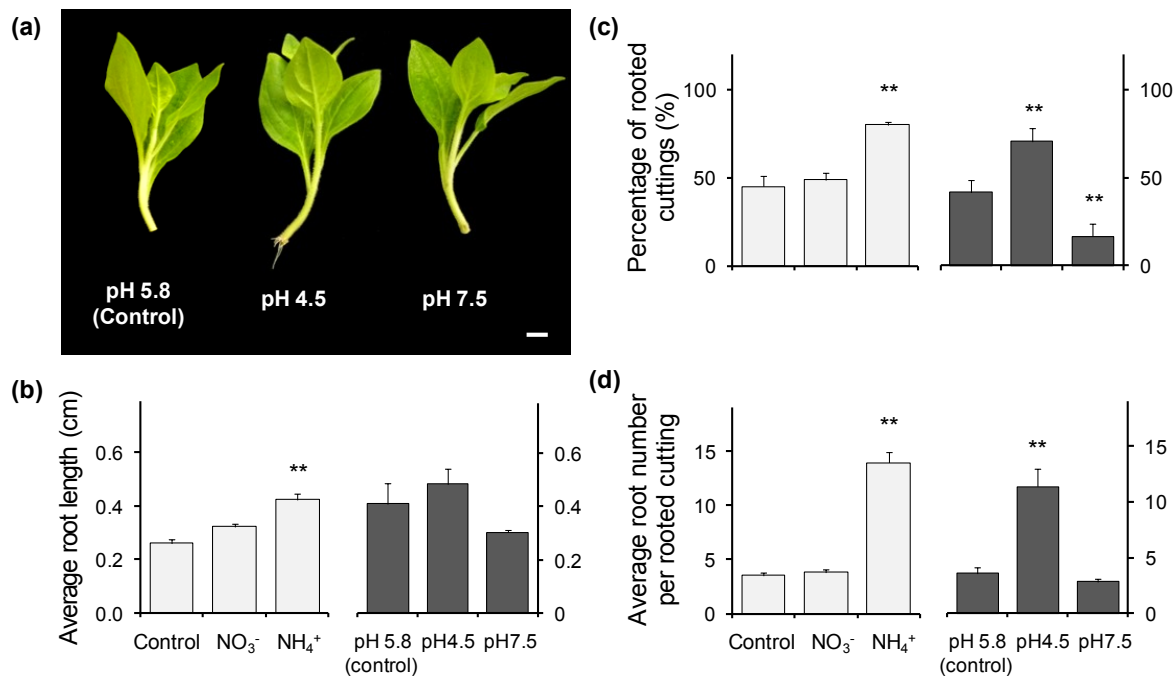


**Fig. 28** Effect of the medium pH on adventitious root (AR) formation in *Petunia hybrida* in comparison to the average rooting performance under ammonium and nitrate supply. (a) Representative image of rooted cuttings in nutrient-free medium under pH 5.8 (control), pH 4.5 and pH 7.5. (b) Percentage of rooted cuttings, (c) average root length and (d) average number of ARs were assessed 14 days post excision. For different pH conditions bars represent means of three independent replicates, each consisting of 8 cuttings + SE. For average ammonium and nitrate supply bars represent means of four independent experiments + SE. Significant differences to control treatments at specified time points after excision are indicated by asterisks (t-test; \*,  $P < 0.05$ ; \*\*,  $P < 0.01$ ). Bar, 1 cm.

Based on the fact that  $\text{NH}_4^+$  nutrition leads to physiological acidification of the rooting environment (Taylor & Bloom, 1998), the effect of medium pH on AR formation was examined. Despite the lack of  $\text{NH}_4^+$  as an N source, all of the rooting parameters were significantly increased when cuttings were cultivated at pH 4.5 as compared to pH 5.8 in control conditions (Fig. 28). In contrast, a pH shift toward more alkaline conditions resulted in a significant decrease of the rooting performance. Thus, a pH drop in apoplastic or rhizosphere pH, as typically observed under  $\text{NH}_4^+$  nutrition, either directly or indirectly promotes AR formation.

### 3.5 Genotypic differences in Fe-dependant promotion of AR formation

To evaluate the genotypic variation in Fe-dependent promotion of AR formation, rooting performance in response to Fe supply was assessed in several commercial cultivars derived from different breeding programs and conventionally propagated by cuttings.

Rooting percentage varied between the analyzed accessions under control conditions as well as in response to Fe supply (Fig. 29a). All cuttings from accessions 7189 and 7137 rooted under both control and Fe supply, whereas only 50% of the cuttings of line 7033 developed roots within 14 dpe regardless of Fe supply. The percentage of the rooted cuttings in control conditions in lines 7026, 7171 and 7048 varied between 30-50% of the values observed under Fe application, similar to the average results from *P. hybrida* "Mitchell". Under control conditions, cultivars 7017 and 7205 did not form ARs within 14 dpe, whereas Fe supply significantly improved rooting percentage. Noteworthy, in the lines 7033, 7171 and 7205 Fe supply could not meet 100%-rooting despite significant improvement of the percentage of rooted cuttings.

The average root length (Fig. 29b) increased in all of the analyzed lines in response to Fe application, except for the line 7033, in which higher root length was observed at a similar rooting percentage, which could be explained by the larger number of shorter protruding roots in response to Fe supply.

In spite of varying rooting percentage and average root length, the average number of ARs increased among all analyzed accessions in response to Fe application. In the lines 7189, 7033, 7026, 7133, 7171 the average AR number increased twice and approximately three-times in the line 7048, whereas lines 7017 and 7205 developed roots

only in response to Fe supply (Fig. 29c). The maximum number of ARs in response to Fe application was observed in the line 7189 and “Mitchell”, however under control conditions the number of ARs was four times higher in the line 7189 than in “Mitchell”.

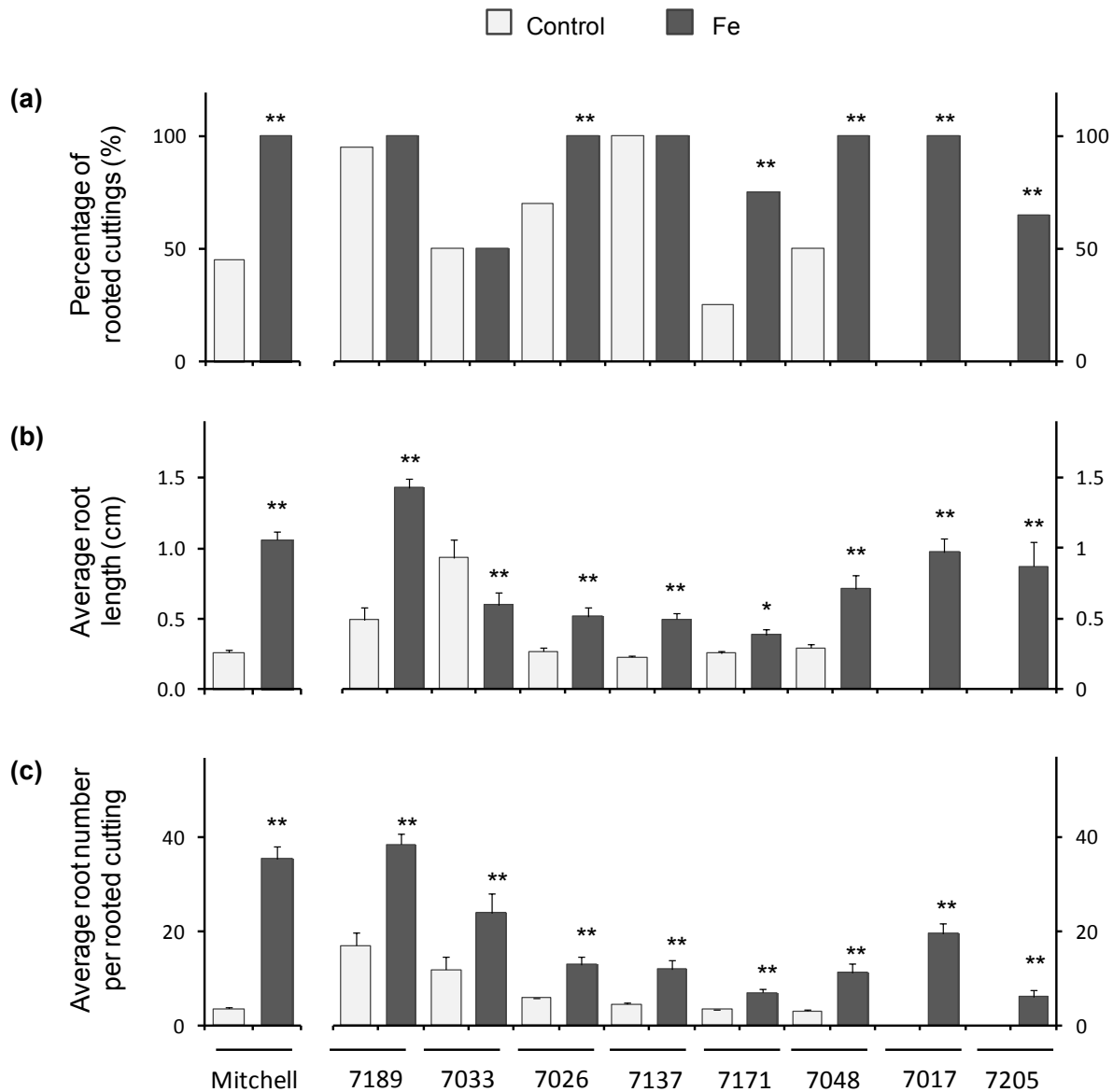


**Fig. 29** Effect of application of Fe on adventitious root (AR) formation in commercial cultivars of *Petunia hybrida* compared to average rooting performance of *P. hybrida* “Mitchell”. (a) Percentage of rooted cuttings, (b) average root length and (c) average number of ARs were assessed 14 days post excision. Bars represent means of 20 independent cuttings + SE for commercial cultivars and means of four independent experiments + SE for “Mitchell”. Significant differences to control treatments are indicated by asterisks (t-test; \*, P < 0.05; \*\*, P < 0.01)

Taken together, the large genetic variability in rooting performance was observed among the tested cultivars in response to Fe application. Therefore, compared to the variety “Mitchell”, at least three distinctive patterns of rooting responses to Fe were found in this study: (i) significant improvement of AR formation by Fe application, with abolished rooting under Fe-free conditions, as observed in the line 7017; (ii) higher rooting performance under control conditions with a similar to variety rooting response to Fe supply as in “Mitchell”; this was seen in the line 7189; (iii) less efficient rooting than in “Mitchell” regardless of Fe application, as detected in lines 7171 and 7033.



## 4. Discussion

The progress of AR formation is associated with several physiological bottlenecks, among which the impact of mineral nutrition remained largely elusive. Previously conducted transcriptome studies highlighted an increasing demand for certain mineral elements during AR formation in petunia cuttings (Ahkami *et al.*, 2014). Assuming that the application of the essential mineral elements might improve rooting performance, AR formation was assessed at different levels in order to investigate the impact of individual nutrients on AR formation. Unexpectedly, this study revealed an outstandingly stimulating role of Fe and a promotive action of  $\text{NH}_4^+$  in AR formation. In addition to immediate benefits for horticultural application, the present study highlights the biological action of these two nutrients in the development of AR.

### 4.1 Promotion of AR formation by iron and ammonium

#### 4.1.1 Ammonium and iron promote different root traits in LR and AR formation

Although in several cultivars of chrysanthemum, zonal geranium and petunia rooting of leafy cuttings is frequently observed in inert media without external nutrient supply (Druege *et al.*, 2000; 2004; Ahkami *et al.*, 2009), cultivation of petunia cuttings in full mineral medium significantly improved rooting performance (Fig. 8), thus emphasizing the importance of external nutrient supply for AR formation.

In the present study, withdrawal of the components from full mineral medium identified Fe and N as limiting nutrients for AR formation in petunia (Fig. 9). Subsequently, the application of individual nutrients indicated a predominant stimulation of AR formation by Fe and a weaker rooting promotion by  $\text{NH}_4^+$ , but not by  $\text{NO}_3^-$ . Worth mentioning that the combination of both N forms together with Fe significantly increased promotion of AR formation compared to single nutrient application, however, remained less efficient as compared to full nutrient supply (Fig. 9).

Studies in *Arabidopsis* on LR formation under localized nutrient supplies demonstrated that Fe and  $\text{NH}_4^+$  promote different root traits. Localized  $\text{NH}_4^+$  supply triggered an increase in the number and density of second-order LRs mostly due to an accelerated LR emergence (Lima *et al.*, 2010; Araya *et al.*, 2015), which is in agreement with a role of  $\text{NH}_4^+$  in stimulating the differentiation of AR primordia and AR emergence

(Figs. 11, 12). In contrast, local application of Fe stimulated LR growth by enhancing cell elongation rather than cell division or cell differentiation (Giehl *et al.*, 2012). This study demonstrated that Fe enhances the growth of ARs in petunia cuttings by stimulating both, the division of early meristematic cells as well as the elongation of developing AR primordia (Figs. 11, 12).

In general, performance of AR formation is determined by two major events, the induction of founder cells and the rate of AR primordia formation (De Klerk *et al.*, 1999; da Costa *et al.*, 2013; Druege *et al.*, 2014). Induction of founder cells in petunia occurs within the first day post excision and predefines the maximum possible number of ARs (Ahkami *et al.*, 2009), whereas the following development of AR primordia depends on the rate of meristem formation and the subsequent elongation and differentiation of meristematic cells. In fact, anatomical studies showed that Fe-supplied cuttings produced AR meristemoids one day earlier than control cuttings and accelerated the progression of AR initials through the different developmental stages (Fig. 12). Hence, the number of AR initials in more developed stages increased, while that in stage I decreased (Fig. 12).

#### **4.1.2 Promotion of AR formation by iron and ammonium is not primarily related to the shoot nutritional status**

A systematic approach by omitting individual nutrients from the nutrient solution demonstrated that AR formation in leafy cuttings of petunia does not improve with the plant nutritional status in general. Instead, only  $\text{NH}_4^+$  and in particular Fe were found to confer a rather specific effect.

Mineral element analysis revealed that petunia cuttings grown in the absence of Fe accumulated Fe in the stem base already after one day (Fig. 13b). As decreasing leaf Fe could be prevented by external Fe supply, it was supposed that Fe retranslocation may stimulate Fe-dependent AR formation. In fact, foliar Fe application could meet the Fe demand of the cutting and prevent a drop of chlorophyll levels in leaves (Fig. 26b), however, none of the rooting parameters improved (Fig. 26c-e). This suggested that Fe takes over a specific role in the rooting zone during AR formation, which cannot be achieved by a long distance translocation of leaf Fe. Moreover, petunia cuttings demonstrated the ability to specifically up-regulate genes involved in Fe acquisition already from 3 dpe. In agreement with a previous transcriptome study (Ahkami *et al.*, 2014), qPCR-based expression analysis revealed a significant down-regulation of *FRO2*

and *IRT1* transcript levels (Fig. 14a,b) in Fe-supplied cuttings, which contained up to three times more Fe in the stem base (Fig. 13b). Taken together, this indicates that the Fe demand relevant for AR formation depends on a local provision of Fe to the stem base rather than on the systemic Fe nutritional status of the stem cutting.

Evidence for a specific role of N during AR formation arrived from studies in chrysanthemum and poinsettia, which showed that the number and length of ARs positively correlated with the initial N concentration in the cuttings (Druege *et al.*, 2000; Zerche & Druege, 2009). In the present study, only  $\text{NH}_4^+$ -supplied cuttings showed a higher concentration of total N (Fig. 13a), which was reflected by elevated concentrations of asparagine and glutamine (Fig. 17a,b) coupled with a simultaneous decrease in glutamic and aspartic acid (Fig. 17c,d). In comparison to  $\text{NO}_3^-$  supply, these results are indicative for a more rapid assimilation of  $\text{NH}_4^+$  directly in the stem base allowing glutamine and maybe other amino acids to decrease transcript levels of N-regulated genes such as *AMT1* homologs (Fig. 18a). Although  $\text{NH}_4^+$ -supplied cuttings had significantly higher N concentrations in leaves than the cuttings from the other treatments (Fig. 13a), N levels in all treatments were not lower than 4 %, which reflects adequate supply (Marschner, 2012). Thus, shoot N metabolism or N accumulation *per se* was most likely not a trigger for AR formation in  $\text{NH}_4^+$ -supplied cuttings.

## 4.2 Phytohormone homeostasis and metabolic activity in nutrient-dependent AR formation

### 4.2.1 Phytohormone homeostasis is not a primary cause of nutrient-dependent stimulation of AR formation

Several phytohormones have been reported to regulate LR formation in response to N and Fe. Auxin with its confirmed role in initiation of AR formation has even been suggested to act as a signal for Fe deficiency (Marschner, 2012; Blum *et al.*, 2014) and shown to mediate LR elongation in response to local Fe application (Giehl *et al.*, 2012). Furthermore, N availability has been reported to regulate auxin homeostasis and signaling at distinct levels. In *Arabidopsis* roots, low N conditions cause auxin accumulation (Kiba *et al.*, 2011), while low  $\text{NO}_3^-$  promotes the auxin transport function of the  $\text{NO}_3^-$  transporter *NRT1.1*, which is prerequisite for LR elongation (Krouk *et al.*, 2010).

In this study, the maximum auxin concentrations in the stem base detected in 1 dpe (Fig. 19a) coincided with the transcript accumulation of a *PIN1* homolog (Fig. 22a). However, neither auxin concentrations nor transcript levels of *PIN1* showed a nutrient supply-dependent response. Moreover, analysis of auxin distribution in a DR5-reporter line revealed no significant differences in the intensity of the auxin response during the induction phase (Fig. 20c-f). Only transcript levels of *LAX3*, *TAR1* and *TAR4* homologs (Fig. 22c,e,f) significantly increased from 7 dpe in response to the application of Fe and  $\text{NH}_4^+$ , whereas the concentration of IAA at this stage remained unaffected by the presence of nutrients (Fig. 19a). Thus, although enhanced auxin levels were most likely required for the early phase of AR initiation, the subtle differences observed in AR formation and auxin-related gene expression were not reflected in gross changes of auxin concentrations in the stem base. Enhanced activity of the auxin reporter in 7 dpe was observed mostly at the tip of AR primordia and in the vasculature (Fig. 20g-j), suggesting that an increased number of advanced AR primordia observed under Fe and  $\text{NH}_4^+$  supply may have went along with the transcript levels of *LAX3*, *TAR1* and *TAR4* homologs (Fig. 22c,e,f). Nonetheless, the role of auxin in development of ARs cannot be entirely disregarded, since the combined effect of auxin inhibitors with nutrient application indicated that stimulation of AR formation by Fe and  $\text{NH}_4^+$  depends on auxin with a major involvement of polar auxin transport (Fig. 24). However, combined application of Fe with synthetic auxin resulted in additional enhancement of rooting performance (Fig. 25), suggesting independent mechanisms of stimulation of AR formation by nutrient application and auxin.

Time-courses of other analyzed hormones revealed a similar pattern for *cis*-zeatin as with auxin (Fig. 19f) but an opposite pattern for ABA (Fig. 19c). While these changes most likely reflected developmental processes, nutrient-dependent changes in phytohormone levels were restricted to minor increases in *trans*-zeatin and *trans*-zeatin riboside from 7 dpe in the rooting zone of Fe-supplied cuttings (Fig. 19e,f). Interestingly, this coincided with an increased abundance of transcripts of homologous genes to *LAX3*, *TAR1* and *TAR4* (Fig. 22c,e,f). Recently, cytokinins have been shown to be involved in regulating auxin distribution via control of the local expression of *PIN1* and *LAX3* in AR primordia, directing the flow of auxin toward the root meristem (Della Rovere *et al.*, 2013). However, whether the observed changes in transcript abundance of *LAX1* at early AR formation or of *LAX3*, *TAR1* and *TAR4* homologs at later developmental stages were the cause or consequence of Fe and  $\text{NH}_4^+$  action requires further analyses.

### 4.2.2 Nutrient-dependent AR formation does not involve changes in primary metabolism

Fe and N are essential elements for a wide range of metabolic processes, such as energy production and protein biosynthesis, which are crucial for development of ARs (Fig 6). Thus, among the initial hypotheses for the involvement of Fe and  $\text{NH}_4^+$  in AR formation, stimulation of metabolic activity in the rooting zone appeared likely. However, the level of soluble sugars as well as analyzed concentrations of primary intermediates of sugar metabolism in the stem base revealed no significant response to nutrient application (Fig. 15a-c, 16). Furthermore, as the concentrations of soluble sugars in mature leaves and phloem exudates (Fig. 15d-i) was not affected by nutrient supply, it was suggested that the observed increase in local N assimilation after  $\text{NH}_4^+$  application did not affect the carbohydrate supply to the sink in the rooting zone. This assumption is supported by the finding that the level of total amino acids (Fig. 17n) remained unchanged under  $\text{NH}_4^+$  supply, despite an increased accumulation of asparagine and glutamine (Fig. 17a,b).

Interestingly, Fe availability in the rooting zone had no significant effect on the levels of organic acids (Fig. 16g-l), known to accumulate in the xylem of Fe-deficient plants (López-Millán *et al.*, 2000). In particular citrate, which serves as a major Fe chelator in the xylem (von Wirén *et al.*, 1999) did not respond to Fe supply (Fig. 16g). These results suggest that control cuttings most likely did not suffer from severe Fe-deficiency, although the demand for this element was indicated by the upregulation of *IRT1* and *FRO2* transcripts (Fig. 14a,b). On the other hand, only a minor portion of the applied Fe has probably been translocated toward the above part of the cutting, as observed by a minor increase in the level of Fe in mature leaves (Fig. 13b).

## 4.3 A local function of iron in the development of AR primordia

### 4.3.1 Developing AR meristems create a sink for Fe

In this study, external application of Fe to the rooting zone stimulated AR formation by enhancing the development of AR primordia (Fig. 11, 12). The most sensitive period for Fe application was within 3-6 dpe (Fig. 10), corresponding to the time of intense cell division of founder cells and formation of meristems in AR primordia. Moreover, this period coincided with an increase in transcript levels of mitotic cyclins, especially under Fe supply (Fig. 23a,b). These findings indicate that a local action of Fe on meristematic cells is

required for enhanced cell division. This view is supported by Fe localization studies, indicating an enhanced allocation of Fe in early dividing cambial cells in 3 dpe (Fig. 27h-k) as well as in apical meristems of AR primordia in 7 dpe, especially under Fe supply (Fig. 27o-q). Despite much weaker intensity, a similar pattern of Fe allocation was observed also under Fe-free conditions (Fig. 27d-g, l-n). This indicates a universal role of Fe in division of meristematic cells which is indicative of a local demand for this element in the rooting zone.

Fe may be delivered to developing ARs in the absence of an external Fe source by several means. First, an increase of Fe in the stem base of control cuttings, revealed as early as 1 dpe (Fig. 13b), could be due to long-distance Fe retranslocation. However, since foliar application of Fe could not improve rooting performance (Fig. 26), Fe is probably translocated from the more proximal parts of the stem above the rooting zone. Second, components of an electron transfer chain of chloroplasts and mitochondria contain a significant amount of Fe. A decrease in Fe staining observed in chloroplasts of the cortical cells in 7 dpe (Fig. 27m,p), suggested that continuous dark exposure leads to the release of Fe from degrading chloroplasts, which may in turn supply the developing AR primordia. Third, increased transcript abundance of a plasma membrane  $H^+$ -ATPase detected in 6 dpe (Ahkami et al., 2014) may have additionally stimulated solubilization of Fe bound to the apoplast. Finally, the increasing demand for Fe may have lead to upregulation of *IRT1* and *FRO2* homologs (Fig. 14a,b), mediating an enhanced acquisition of Fe from the rooting medium. Hence, although the increasing demand for Fe may be partly compensated by mobilization of internal resources, Fe acquisition from the rooting medium is more likely to have served as a major source of Fe for AR formation.

#### 4.3.2 Proposed mechanism for Fe-mediated stimulation of meristematic growth

An increased allocation of Fe to the nuclear compartment of the meristematic cells, as identified in this study (Fig. 27), raises an important question on the possible mechanisms by which Fe stimulates AR formation.

Studies in animals and yeast highlighted a function of numerous iron-containing proteins in the nucleus, such as Fe-S-cluster proteins, hemoproteins or ribonucleotide reductases that are essential for the maintenance of DNA stability, synthesis of deoxyribonucleotides and control of the cell cycle progression (Zhang, 2014). Elimination of Fe from the nuclear area has been shown to impair cell division of animal and yeast

cells (Zhang, 2014). Conversely, Roschztardt *et al.* (2011) have identified a surprisingly high accumulation of Fe in the nucleolus of plant cells, hypothesizing that Fe may be involved in processing of ribosomal RNA and assembly of ribosomes.

Indeed, stabilization of the tertiary structure of catalytic RNAs is achieved by binding to divalent cations, such as  $Mg^{2+}$ , or alternatively  $Fe^{2+}$ , which is similar to  $Mg^{2+}$  in size and coordination geometry (Berens *et al.*, 1998). Furthermore, under anoxic conditions,  $Fe^{2+}$  was shown to increase the ribozyme activity and expand catalytic properties of RNA (Berens *et al.*, 1998; Athavale *et al.*, 2012). These findings have led to the hypothesis that  $Fe^{2+}$  was utilized as a primary cofactor in catalytic RNAs during the early evolution of life on Earth, before  $O_2$  levels increased by photosynthesis and caused the substitution of redox-active  $Fe^{2+}$  by  $Mg^{2+}$  (Athavale *et al.*, 2012; Hsiao *et al.*, 2013). Based on this hypothesis it can be assumed that substitution of  $Fe^{2+}$  by  $Mg^{2+}$  could take place at any point of evolution of living organisms, provided that  $Fe^{2+}$  is isolated from free  $O_2$  to avoid formation of reactive oxygen species (ROS) by the Fenton reaction (Winterbourn, 1995). Exactly the same mechanism has been suggested to cause Alzheimer's disease, where increased levels of redox-active  $Fe^{2+}$  lead to DNA damage and oxidation of rRNA, which is abundant in neurons (Smith *et al.*, 1997; Honda *et al.*, 2005; Castellani *et al.*, 2007).

In this regard, plants must have evolved a specific mechanism to cope with Fe abundance in the nucleus. Two possible strategies to avoid generation of ROS by  $Fe^{2+}$  could be proposed: (i) buffering the free  $O_2$  or (ii) Fe chelation. The first strategy is employed by nitrogen-fixing plants, where leghemoglobins are accumulated in the root nodules to bind free  $O_2$  (Downie, 2005). The second possibility to avoid cytotoxic effects of  $Fe^{2+}$  could be associated with binding to ferritins or forming complexes with Fe-chelators. Fe localization studies in root tips of *Arabidopsis* revealed that the mutation in three ferritin genes abolished the typical accumulation of Fe in central dot-like structures, which are possibly identical to nucleoli described in this work (Reyt *et al.*, 2015). These results suggest that described pattern of Fe allocation is ferritin-dependent. On the other hand, a specific accumulation of flavonoids was observed in nuclei of root cells of *Arabidopsis*, which coincided with the expression of key enzymes of flavonoid biosynthesis, i.e. CHALCONE SYNTHASE and CHALCONE ISOMERASE (Saslowsky *et al.*, 2005). Taking into account antioxidant properties and the ability to chelate  $Fe^{2+}$  (Leopoldini *et al.*, 2006), flavonoids appear to be suitable candidates to buffer and possibly even maintain a reduced state of  $Fe^{2+}$  in the nucleus.

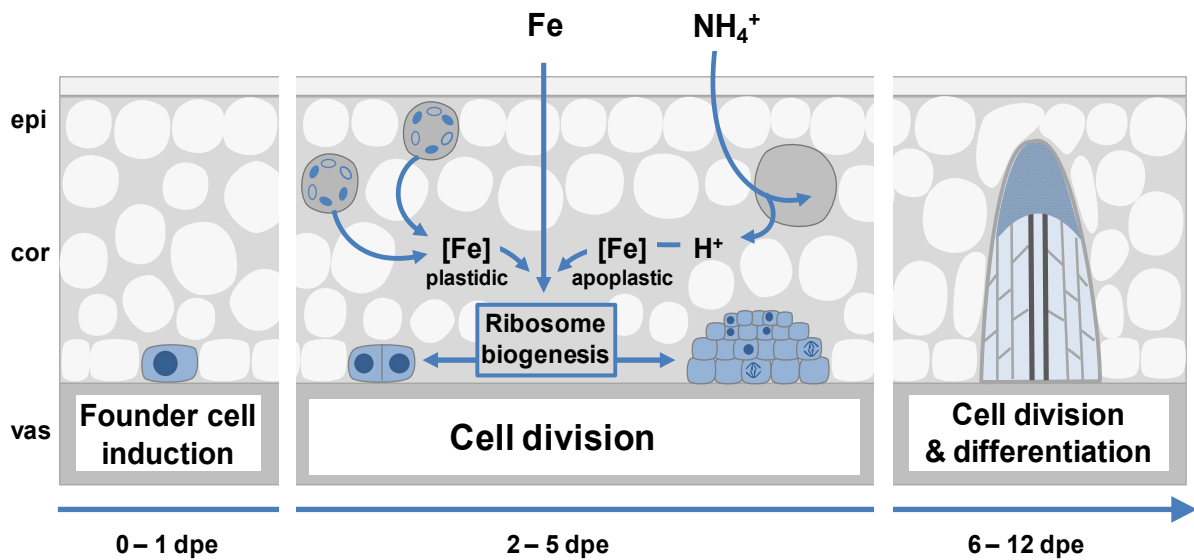


**Fig. 30** Working model for the stimulation of adventitious root (AR) formation by iron and ammonium in *Petunia hybrida*. Fe performs a specific function in the rooting zone by activating the ribosome biogenesis, crucial for growth of the meristematic cells of the developing AR meristems. Under Fe-free conditions Fe is associated with chloroplasts in cortical cell layers and may be released during chloroplast degradation to supply Fe to developing AR meristems. The uptake of  $\text{NH}_4^+$  leads to a local acidification of the apoplast as a consequence of an increased net  $\text{H}^+$  efflux, which in turn facilitates the mobilization of Fe precipitated in the apoplast. cor. cortex; epi. epidermis; vas. vasculature; dpe, days post excision

Although further studies are still required to investigate the detailed mechanisms of Fe functions in the plant nucleolus, involvement of this element in the biogenesis of ribosomes appears the most attractive theory to explain Fe-mediated stimulation of meristematic growth (Fig. 30). This view is further supported by the fact that the rate of ribosome biogenesis appears to become the bottleneck for the cell proliferation, since ribosomes are required for protein biosynthesis and to reach the critical size for cell division, which is a crucial factor in actively dividing meristematic cells (Manzano *et al.*, 2013).



### 4.3.3 Ammonium facilitates iron-mediated AR formation

Several lines of evidence indicated that  $\text{NH}_4^+$  supply promoted AR formation via similar mechanisms as did Fe: i) the phase-specific of  $\text{NH}_4^+$  promoted rooting percentage, average root length and average root number within the same time window as Fe supply (Fig. 10); ii) together with Fe, application of  $\text{NH}_4^+$  caused the formation of AR meristemoids one day earlier as in control conditions or with  $\text{NO}_3^-$  (Fig. 11h) and accelerated progression of AR initials through different developmental stages (Fig. 12); iii) like Fe,  $\text{NH}_4^+$  stimulated transcript abundance of cyclin *CYC2* (Fig. 23b) and the two Fe-related genes *FERRITIN* and *NAS* (Fig. 14c,d) as well as the auxin-related genes *LAX3* and *TAR4* (Fig. 22c,f), and iv)  $\text{NH}_4^+$  supply increased Fe concentrations in the stem base in 3 dpe to a similar extent as Fe supply (Fig. 13b). Regarding all these measures,  $\text{NH}_4^+$  supply just conferred a weaker stimulation than Fe supply, resulting in qualitatively similar dynamics of AR formation as in Fe-supplied cuttings (Fig. 12).

It is therefore proposed that  $\text{NH}_4^+$  supply leads to a local improvement of Fe nutrition at the stem base (Fig. 30).  $\text{NH}_4^+$  uptake is known to cause physiological acidification due to an enhanced net  $\text{H}^+$  efflux (Taylor & Bloom, 1998). Even in buffered solutions apoplastic pH may locally decrease and facilitate solubilization of Fe previously precipitated in the cell walls. Such scenario is in line with the observation that in 3 dpe  $\text{NH}_4^+$  supply increased transcript abundance of *FERRITIN* (Fig. 14c), suggesting that the shoot Fe nutritional status improved, and of *NICOTIANAMINE SYNTHASE* (Fig. 14d), which acts as an intra- and intercellular Fe chelator to facilitate Fe allocation in the stem tissue. A primarily pH-triggered action of  $\text{NH}_4^+$  finds support in another experiment, in which a decreased medium pH enhanced AR formation, similar to  $\text{NH}_4^+$  application (Fig. 28). By contrast,  $\text{NO}_3^-$  supply led in most experiments to similar rooting performance as under control conditions, which is in agreement with a reported physiological alkalization of the apoplast by uptake of  $\text{NO}_3^-$  and thus the lack of an Fe-solubilizing effect (Taylor & Bloom, 1998).

Although the combination of Fe together with either N form had an additive effect on the promotion of AR formation (Fig. 9), the final values did not exceed those observed under the full nutrient supply. Compared to application of  $\text{NH}_4^+$  or  $\text{NO}_3^-$  alone, the combined supplementation with Fe also failed to alter nutrient concentrations in the stem base (Fig. 13a,b). Nonetheless, faster protrusion of the ARs under combined supply of Fe with  $\text{NH}_4^+$  suggested that an increased acidity of the apoplast additionally to stimulating Fe mobilization, also facilitated FRO2-mediated reduction of Fe(III).

#### 4.3.4 Genotypic variability in Fe-mediated improvement of AR formation in petunia

Since the involvement of Fe in stimulating AR formation *a priori* infers to be applied to a wide range of plant species, it was of special interest to assess whether there is genotypic variability in Fe demand during AR formation. Unlike the variety “Mitchell”, which is a doubled haploid backcross of *P. hybrida* to *P. axillaris* and therefore homozygous for all the genes (Gerats & Vandebussche, 2005), analyzed commercial cultivars originated from different breeding programs and thus represent a higher genetic diversity.

Variation in response to Fe application during AR formation could be attributed to (i) different Fe contents in the cuttings, which depends on the ability of the stock plants to acquire and store this element, (ii) variability in Fe mobilization and retranslocation capacity or (iii) differences in the uptake efficiency of Fe from the rooting medium by the cutting.

Petunia is often referred to as an iron-inefficient plant, which is unable to efficiently acquire Fe from soils with pH > 6.0 (Fisher *et al.*, 2003; Wik *et al.*, 2006). Such phenomenon may be explained by lower ability to acidify the rhizosphere, which is essential for Fe uptake in strategy-I plants (Curie & Briat, 2003). Indeed, Fe-efficiency of clover genotypes (*Trifolium subterraneum* L.) has been associated with higher levels of H<sup>+</sup>-excretion, whereas in *Vitis* species, higher acidification of the rhizosphere was achieved by increased exudation of organic acids (Lindberg & Greger, 2002). On the other hand, acidification of the apoplast, as proposed in the current study (Fig 30), plays an important role in the stimulation of AR formation by solubilization of Fe precipitated on the cell walls and by facilitating the reduction of Fe(III) by the plasma membrane-bound reductase. Noteworthy, in preliminary studies, petunia showed toxicity symptoms already at Fe(III)EDTA concentrations slightly above 20 µM (data not shown), which is five times less than used for hydroponic cultivation of Arabidopsis, barley or maize, suggesting that petunia is more sensitive to elevated Fe levels. Therefore, it seems reasonable to assume that petunia plants depend to a large extent on continuous Fe uptake, rather than on mobilization of this nutrient from internal stores.

In this study, three distinctive responses to Fe supply were observed in the analyzed commercial petunia cultivars. Compared to “Mitchell” rooting performance of the line 7189 was significantly higher even under control conditions (Fig. 29), maybe due to improved Fe retranslocation or to other Fe-unrelated mechanisms. In contrast, the line 7017 did not root

at all in the absence of Fe (Fig. 29), suggesting a lower availability of internal Fe. However, both lines responded significantly to addition of Fe to the rooting medium, highlighting an important role of Fe uptake throughout AR formation. Interestingly, Fe supply to the line 7171 demonstrated a much weaker promotion of AR formation than in “Mitchell”, with a similar rooting performance under control conditions (Fig. 29). This suggested that Fe acquisition or remobilization is less efficient in this line.

These findings together with the expanding set of interspecific RIL populations developed in the groups of Dr. Ryan Warner (Dept. of Horticulture, Michigan State University) and Prof. Dr. Cris Kuhlemeier (Institute of Plant Sciences, University of Bern) encourage their utilization in forward genetic approaches in order to identify QTLs and genes responsible for stimulation of AR formation by Fe. Furthermore, additional studies are needed to investigate whether AR formation can be stimulated by Fe in other Fe-inefficient and Fe-efficient plant species.

## 5. Summary

Adventitious root (AR) formation is characterized by a sequence of physiological and morphological processes and is determined by external factors, among which the impact of mineral nutrition remains largely elusive. As indicated in previous transcriptome studies, limitation of certain mineral elements may pose a physiological bottleneck that restricts the development of AR.

With the aim to investigate which mineral elements enhance AR formation, and how stimulatory nutrients exert their physiological function during this process, the present study revealed an unprecedented stimulation of AR formation in petunia cuttings by local Fe supply and a promotive action of  $\text{NH}_4^+$ . The optimal application period for these nutrients corresponded to the early division of meristematic cells in the rooting zone and coincided with increased transcript levels of mitotic cyclins. Fe-localization studies revealed an enhanced allocation of Fe to the nuclei of meristematic cells in AR initials. It was therefore proposed that Fe acts locally by promoting cell division in meristematic cells of AR primordia. Nucleolar localization of Fe supported a role of Fe in ribosome biogenesis, crucial for growth of meristematic cells in developing AR meristems. Under Fe-free conditions Fe disappeared from chloroplasts in cortical cell layers of the stem base and may have served as an Fe source to supply the developing AR meristems.

$\text{NH}_4^+$  supply promoted AR formation to a lower extent than Fe, most likely through increasing the availability of Fe by local acidification of the apoplast. This may be a consequence of an increased net  $\text{H}^+$  efflux, which in turn facilitates the mobilization of Fe precipitated in the apoplast.

In addition to immediate benefits for horticultural application, the present study highlights a specific biological function of Fe in stimulating meristematic cell division. This finding is not only of interest and relevance for the scientific community working on rooting issues of ornamental plants, but also for a larger plant science community interested in developmental processes during *de-novo* organogenesis and root growth. This study will also contribute to establish petunia further as a prime model for genetic and developmental trait investigations and also for studying biological phenomena in a species with different genome organization, biochemistry, development, ecology and evolution.

## 6. Zusammenfassung

Die Bildung von Adventivwurzeln ist durch eine Abfolge physiologischer und morphologischer Prozesse gekennzeichnet, die durch externe Faktoren bestimmt wird, unter welchen der Einfluss von mineralischen Nährstoffen am schwersten definierbar ist. Vorstudien legen nahe, dass die begrenzte Verfügbarkeit einiger mineralischer Elemente einen physiologischen Flaschenhals darstellen könnten, der die Entwicklung von Adventivwurzeln beschränkt.

Angetrieben mit dem Ziel der Untersuchung jener mineralischer Elemente, die die Adventivwurzelbildung fördern, und der Art, wie die stimulierenden Nährstoffe ihre physiologischen Funktionen während dieses Prozesses ausüben, gab diese Studie Aufschluss über eine Stimulation der Adventivwurzelbildung in Petunia Stecklingen durch die lokale Versorgung mit Eisen in einem bislang unerreichten Ausmaß und durch die Versorgung mit Ammonium in einem fördernden Ausmaß. Das optimale Anwendungsfenster für diese Nährstoffe umfasst die frühe Teilungsphase meristematischer Zellen im Wurzelbereich, was sich mit einer gesteigerten Transkription mitotischer Zykline deckt. Eisenlokalisationsstudien ergaben eine verstärkte Anreicherung von Eisen an den meristematischen Zellen der Adventivwurzel-Primordien. Es wurde daher angenommen, dass das Eisen lokal auf eine Verstärkung der Zellteilung meristematischer Zellen in Adventivwurzel-Primordien hin wirkt. Die Lokalisation von Eisen am Nucleolus lässt darauf schließen, dass Eisen eine Rolle in der Ribosom-Biogenese spielt, welche entscheidend für meristematische Zellen bei der Entwicklung von Adventivwurzel-Meristemen ist. Unter eisenfreien Bedingungen verschwand Eisen aus den Chloroplasten der Spindelzellschicht am unteren Sprossende und könnte daher als eine Eisenquelle zur Versorgung sich entwickelnder Adventivwurzel-Meristeme gedient haben.

Ein erhöhtes Angebot an Ammonium verstärkte die Entwicklung von Adventivwurzeln in einem geringeren Maße als Eisen, höchstwahrscheinlich durch eine gesteigerte Verfügbarkeit von Eisen aufgrund einer lokalen Ansäuerung des Apoplasten. Dies könnte die Folge eines gesteigerten netto Ausstroms von Protonen sein, welcher eine Mobilisierung von im Apoplasten ausgefälltem Eisen ermöglichen würde.

Über den unmittelbaren Vorteil für die gärtnerischen Anwendung hinaus, arbeitet die Studie eine spezifische biologische Funktion von Eisen bei der Stimulierung meristematischer Zellteilung heraus. Dies ist nicht nur von Interesse und Relevanz für die wissenschaftliche Gemeinschaft, die am Wurzelwachstum von Zierpflanzen arbeiten, sondern auch für eine größere wissenschaftliche Gemeinschaft, die an den Entwicklungsprozessen während der *de-novo* Organogenese und an Wurzelwachstum interessiert ist. Diese Studie wird ebenfalls dazu beitragen Petunia als weitere Modelnpflanze zu etablieren für die Untersuchung von genetischen Merkmale und Entwicklungsmerkmalen, sowie für das Studium biologischer Phänomene einer Spezies mit unterschiedlicher Genome-Organisation, Biochemie, Entwicklung, Ökologie und Evolution.

## 7. Literature

**Agency for Toxic Substances and Disease Registry. 2005.** *Toxicology profile for naphthalene, 1-methylnaphthalene, and 2-methylnaphthalene.*

**Agulló-Antón MÁ, Ferrández-Ayela A, Fernández-García N, Nicolás C, Albacete A, Pérez-Alfocea F, Sánchez-Bravo J, Pérez-Pérez JM, Acosta M. 2014.** Early steps of adventitious rooting: morphology, hormonal profiling and carbohydrate turnover in carnation stem cuttings. *Physiologia plantarum* **150**: 446–62.

**Agulló-Antón MÁ, Sánchez-Bravo J, Acosta M, Druege U. 2011.** Auxins or sugars: what makes the difference in the adventitious rooting of stored carnation cuttings? *Journal of Plant Growth Regulation* **30**: 100–113.

**Ahkami AH, Lischewski S, Haensch KT, Porfirova S, Hofmann J, Rolletschek H, Melzer M, Franken P, Hause B, Druege U, et al. 2009.** Molecular physiology of adventitious root formation in *Petunia hybrida* cuttings: Involvement of wound response and primary metabolism. *New Phytologist* **181**: 613–625.

**Ahkami AH, Melzer M, Ghaffari MR, Pollmann S, Ghorbani Javid M, Shahinnia F, Hajirezaei MR, Druege U. 2013.** Distribution of indole-3-acetic acid in *Petunia hybrida* shoot tip cuttings and relationship between auxin transport, carbohydrate metabolism and adventitious root formation. *Planta* **238**: 499–517.

**Ahkami A, Scholz U, Steuernagel B, Strickert M, Haensch KT, Druege U, Reinhardt D, Nouri E, von Wirén N, Franken P, et al. 2014.** Comprehensive transcriptome analysis unravels the existence of crucial genes regulating primary metabolism during adventitious root formation in *Petunia hybrida*. *PLoS ONE* **9**: e100997.

**de Almeida Engler J, De Vleeschauwer V, Burssens S, Celenza JL, Inzé D, Van Montagu M, Engler G, Gheysen G. 1999.** Molecular markers and cell cycle inhibitors show the importance of cell cycle progression in nematode-induced galls and syncytia. *The Plant Cell* **11**: 793–808.

**Amissah JN, Paolillo DJ, Bassuk N. 2008.** Adventitious root formation in stem cuttings of *Quercus bicolor* and *Quercus macrocarpa* and its relationship to stem anatomy. *Journal Of The American Society For Horticultural Science* **133**: 479–486.

**Araya T, Kubo T, von Wirén N, Takahashi H. 2015.** Statistical modeling of nitrogen-dependent modulation of root system architecture in *Arabidopsis thaliana*. *Journal of Integrative Plant Biology* **58**: 254–265.

**Athavale SS, Petrov AS, Hsiao C, Watkins D, Prickett CD, Gossett JJ, Lie L, Bowman JC, O'Neill E, Bernier CR, et al. 2012.** RNA folding and catalysis mediated by iron (II). *PLoS ONE* **7**: 1–7.

**Atkinson JA, Rasmussen A, Traini R, Voss U, Sturrock C, Mooney SJ, Wells DM, Bennett MJ. 2014.** Branching out in roots: uncovering form, function and regulation. *Plant Physiology* **166**: 538–550.

**Bellini C, Pacurar DI, Perrone I. 2014.** Adventitious roots and lateral roots: similarities and differences. *Annual Review of Plant Biology* **65**: 639–66.

- Benková E, Michniewicz M, Sauer M, Teichmann T, Seifertová D, Jürgens G, Friml J. 2003.** Local, efflux-dependent auxin gradients as a common module for plant organ formation. *Cell* **115**: 591–602.
- Bennett T, Scheres B. 2010.** Root development—two meristems for the price of one? *Current Topics in Developmental Biology* **91**: 67–102.
- Berens C, Streicher B, Schroeder R, Hillen W. 1998.** Visualizing metal-ion-binding sites in group I introns by iron(II)-mediated Fenton reactions. *Chem Biol* **5**: 163–175.
- Blazkova A, Sotta B, Tranvan H, Maldiney R, Bonnet M, Einhorn J, Kerhoas L, Miginiac E. 1997.** Auxin metabolism and rooting in young and mature clones of *Sequoia sempervirens*. *Physiologia plantarum* **99**: 73–80.
- Blilou I, Xu J, Wildwater M, Willemsen V, Paponov I, Friml J, Heidstra R, Aida M, Palme K, Scheres B. 2005.** The PIN auxin efflux facilitator network controls growth and patterning in *Arabidopsis* roots. *Nature* **433**: 39–44.
- Blum A, Brumbarova T, Bauer P, Ivanov R. 2014.** Hormone influence on the spatial regulation of *IRT1* expression in iron-deficient *Arabidopsis thaliana* roots. *Plant Signaling & Behavior* **9**: e28787.
- Bombarely A, Moser M, Amrad A, Bao M, Bapaume L, Barry C, Bliet M, Boersma M, Borghi L, Bruggmann R, et al. 2016.** Insight into the evolution of the Solanaceae from the parental genomes of *Petunia hybrida*. *Nature Plants* **In press**: 1–9.
- Boonman A, Prinsen E, Gilmer F, Schurr U, Peeters AJM, Voesenek L a CJ, Pons TL. 2007.** Cytokinin import rate as a signal for photosynthetic acclimation to canopy light gradients. *Plant physiology* **143**: 1841–1852.
- Caboni E, Tonelli MG, Lauri P, Iacovacci P, Kevers C, Damiano C, Gaspar T. 1997.** Biochemical aspects of almond microcuttings related to in vitro rooting ability. *Biologia Plantarum* **39**: 91–97.
- Caño-Delgado A, Lee J-Y, Demura T. 2010.** Regulatory mechanisms for specification and patterning of plant vascular tissues. *Annual review of cell and developmental biology* **26**: 605–637.
- Castellani RJ, Moreira PI, Liu G, Dobson J, Perry G, Smith MA, Zhu X. 2007.** Iron: the redox-active center of oxidative stress in Alzheimer disease. *Neurochemical Research* **32**: 1640–1645.
- Chang L, Ramireddy E, Sch Müller T. 2015.** Cytokinin as a positional cue regulating lateral root spacing in *Arabidopsis*. *Journal of Experimental Botany* **66**: 4759–4768.
- Chang L, Ramireddy E, Sch Müller T. 2013.** Lateral root formation and growth of *Arabidopsis* is redundantly regulated by cytokinin metabolism and signalling genes. *Journal of Experimental Botany* **64**: 5021–5032.
- Chapman EJ, Estelle M. 2009.** Cytokinin and auxin intersection in root meristems. *Genome biology* **10**: 210.
- Chen R, Rosen E, Masson PH. 1999.** Gravitropism in Higher Plants. *Plant Physiology* **120**: 343–350.
- Clark DG, Gubrium EK, Barrett JE, Nell T a, Klee HJ. 1999.** Root formation in ethylene-insensitive plants. *Plant physiology* **121**: 53–60.



- Coruzzi GM. 2003.** Primary N-assimilation into amino acids in arabidopsis. *The Arabidopsis Book* **2**: 1–17.
- da Costa CT, de Almeida MR, Ruedell CM, Schwambach J, Maraschin FS, Fett-Neto AG. 2013.** When stress and development go hand in hand: main hormonal controls of adventitious rooting in cuttings. *Frontiers in Plant Science* **4**: 133.
- Curie C, Briat JF. 2003.** Iron transport and signaling in plants. *Annual Review of Plant Biology* **54**: 183–206.
- Davis TD, Haissig BE. 1994.** *Biology of Adventitious Root Formation*. New York: Springer Science+Business Media.
- Davis TD, Potter JR. 1989.** Relations between carbohydrate, water status and adventitious root formation in leafy pea cuttings rooted under various levels of atmospheric CO<sub>2</sub> and relative humidity. *Physiologia Plantarum* **77**: 185–190.
- Deblaere R, Bytebier B, de Greve H, Deboeck F, Schell J, van Montagu M, Leemans J. 1985.** Efficient octopine Ti plasmid-derived vectors for *Agrobacterium*-mediated gene transfer to plants. *Nucleic Acids Research* **13**: 4777–4788.
- Díaz-Sala C. 2014.** Direct reprogramming of adult somatic cells toward adventitious root formation in forest tree species: the effect of the juvenile-adult transition. *Frontiers in plant science* **5**: 310.
- Dolan L, Janmaat K, Willemsen V, Linstead P, Poethig S, Roberts K, Scheres B. 1993.** Cellular organisation of the *Arabidopsis thaliana* root. *Development (Cambridge, England)* **119**: 71–84.
- Dong S, Cheng L, Scagel CF, Fuchigami LH. 2004.** Nitrogen mobilization, nitrogen uptake and growth of cuttings obtained from poplar stock plants grown in different N regimes and sprayed with urea in autumn. *Tree physiology* **24**: 355–359.
- Downie AJ. 2005.** Legume haemoglobins: symbiotic nitrogen fixation needs bloody nodules. *Current Biology* **15**: 196–198.
- Druege U, Franken P, Hajirezaei MR. 2016.** Plant hormone homeostasis, signaling, and function during adventitious root formation in cuttings. *Frontiers in Plant Science* **7**: 1–14.
- Druege U, Franken P, Lischewski S, Ahkami AH, Zerche S, Hause B, Hajirezaei MR. 2014.** Transcriptomic analysis reveals ethylene as stimulator and auxin as regulator of adventitious root formation in petunia cuttings. *Frontiers in Plant Science* **5**: 494.
- Druege U, Zerche S, Kadner R. 2004.** Nitrogen- and storage-affected carbohydrate partitioning in high-light-adapted *Pelargonium* cuttings in relation to survival and adventitious root formation under low light. *Annals of Botany* **94**: 831–842.
- Druege U, Zerche S, Kadner R, Ernst M. 2000.** Relation between nitrogen status, carbohydrate distribution and subsequent rooting of chrysanthemum cuttings as affected by pre-harvest nitrogen supply and cold-storage. *Annals of Botany* **85**: 687–701.
- Dubrovsky JG, Sauer M, Napsucialy-Mendivil S, Ivanchenko MG, Friml J, Shishkova S, Celenza J, Benková E. 2008.** Auxin acts as a local morphogenetic trigger to specify lateral root founder cells. *Proceedings of the National Academy of Sciences of the United States of America* **105**: 8790–8794.

- Eveland AL, Jackson DP. 2012.** Sugars, signalling, and plant development. *Journal of Experimental Botany* **63**: 3367–3377.
- Fabijan D, Yeung E, Mukhejee I, Reid DM. 1981.** Adventitious rooting in hypocotyls of sunflower (*Helianthus annuus*) seedlings. *Physiologia Plantarum* **53**: 578–588.
- Farrás R, Ferrando A, Jásik J, Kleinow T, Okrész L, Tiburcio A, Salchert K, del Pozo C, Schell J, Koncz C. 2001.** SKP1-SnRK protein kinase interactions mediate proteasomal binding of a plant SCF ubiquitin ligase. *EMBO Journal* **20**: 2742–2756.
- Ferreira PCG, Hemeryk AS, de Almeida Engler J, Van Montagu M, Engler G, Inzé D. 1994.** Developmental expression of the Arabidopsis cyclin gene *cyc1At*. *The Plant Cell* **6**: 1763–1774.
- Fisher PR, Wik RM, Smith BR, Pasian CC, Kmetz-gonzález M, Argo WR. 2003.** Correcting iron deficiency in *Calibrachoa* grown in a container medium at high pH. *HortTechnology* **13**: 308–313.
- Ford YY, Bonham EC, Cameron RWF, Blake PS, Judd HL, Harrison-Murray RS. 2002.** Adventitious rooting: Examining the role of auxin in an easy- and a difficult-to-root plant. *Plant Growth Regulation* **36**: 149–159.
- Fordham MC, Harrison-Murray RS, Knight L, Evered CE. 2001.** Effects of leaf wetting and high humidity on stomatal function in leafy cuttings and intact plants of *Corylus maxima*. *Physiologia plantarum* **113**: 233–240.
- Foyer CH, Parry M, Noctor G. 2003.** Markers and signals associated with nitrogen assimilation in higher plants. *Journal of Experimental Botany* **54**: 585–593.
- Francis KE, Spiker S. 2005.** Identification of Arabidopsis thaliana transformants without selection reveals a high occurrence of silenced T-DNA integrations. *Plant Journal* **41**: 464–477.
- Fukaki H, Tameda S, Masuda H, Tasaka M. 2002.** Lateral root formation is blocked by a gain-of-function mutation in the *solitary-root/IAA14* gene of Arabidopsis. *Plant Journal* **29**: 153–168.
- Fukaki H, Tasaka M. 2009.** Hormone interactions during lateral root formation. *Plant Molecular Biology* **69**: 437–449.
- Gao S, Fang J, Xu F, Wang W, Sun X, Chu J, Cai B, Feng Y, Chu C. 2014.** CYTOKININ OXIDASE/DEHYDROGENASE4 integrates cytokinin and auxin signaling to control rice crown root formation. *Plant physiology* **165**: 1035–1046.
- Garrido G, Guerrero JR, Cano EA, Acosta M, Sánchez-Bravo J. 2002.** Origin and basipetal transport of the IAA responsible for rooting of carnation cuttings. *Physiologia Plantarum* **114**: 303–312.
- Gazzarrini S, Lejay L, Gojon A, Ninnemann O, Frommer WB, von Wirén N. 1999.** Three functional transporters for constitutive, diurnally regulated, and starvation-induced uptake of ammonium into Arabidopsis roots. *The Plant Cell* **11**: 937–947.
- Gerats T, Strommer J. 2009.** *Petunia: evolutionary, developmental and physiological genetics* (T Gerats and J Strommer, Eds.). New York: Springer.

- Gerats T, Vandenbussche M. 2005.** A model system for comparative research: Petunia. *Trends in Plant Science* **10**: 251–256.
- Gibson JL. 2003.** Influence of mineral nutrition on stock plant yield and subsequent rooting of stem cuttings of scaevola, new guinea impatiens, and vegetative strawflower.
- Giehl RFH, Gruber BD, von Wirén N. 2014.** It's time to make changes: Modulation of root system architecture by nutrient signals. *Journal of Experimental Botany* **65**: 769–778.
- Giehl RFH, Lima JE, von Wirén N. 2012.** Localized iron supply triggers lateral root elongation in Arabidopsis by altering the *AUX1*-mediated auxin distribution. *The Plant Cell* **24**: 33–49.
- Gullberg J, Jonsson P, Nordström A, Sjöström M, Moritz T. 2004.** Design of experiments: An efficient strategy to identify factors influencing extraction and derivatization of *Arabidopsis thaliana* samples in metabolomic studies with gas chromatography/mass spectrometry. *Analytical Biochemistry* **331**: 283–295.
- Gutierrez C. 2009.** The Arabidopsis cell division cycle. *The Arabidopsis Book* **7**: e0120.
- Gutierrez L, Bussell JD, Pacurar DI, Schwambach J, Pacurar M, Bellini C. 2009.** Phenotypic plasticity of adventitious rooting in Arabidopsis is controlled by complex regulation of *AUXIN RESPONSE FACTOR* transcripts and microRNA abundance. *The Plant cell* **21**: 3119–3132.
- Gutierrez L, Mongelard G, Flokova K, Pacurar DI, Novak O, Staswick P, Kowalczyk M, Pacurar M, Demailly H, Geiss G, et al. 2012.** Auxin controls Arabidopsis adventitious root initiation by regulating jasmonic acid homeostasis. *The Plant Cell* **24**: 2515–2527.
- Harris J. 2015.** Abscisic acid: hidden architect of root system structure. *Plants* **4**: 548–572.
- Hartmann HT, Kester DE, Davies FT, Geneve RL. 2011.** *Hartmann and Kester's plant propagation-principles and practices*. New Jersey: Prentice Hall.
- He W, Brumos J, Li H, Ji Y, Ke M, Gong X, Zeng Q, Li W, Zhang X, An F, et al. 2011.** A small-molecule screen identifies L-kynurenine as a competitive inhibitor of *TAA1/TAR* activity in ethylene-directed auxin biosynthesis and root growth in Arabidopsis. *The Plant Cell* **23**: 3944–3960.
- Himmelblau E, Amasino RM. 2001.** Nutrients mobilized from leaves of *Arabidopsis thaliana* during leaf senescence. *Journal of Plant Physiology* **158**: 1317–1323.
- Hitchcock AE, Zimmermann PW. 1936.** Effect of growth substances on the rooting response of cuttings. *Contr. Boyce Thompson Inst.* **8**: 63–79.
- Hoad S, Leahey R. 1996.** Effects of pre-severance light quality on the vegetative propagation of *Eucalyptus grandis* WW. Hil ex Maiden. *Trees* **10**: 317–324.
- Hochholdinger F, Woll K, Sauer M, Dembinsky D. 2004.** Genetic dissection of root formation in maize (*Zea mays*) reveals root-type specific developmental programmes. *Annals of Botany* **93**: 359–368.
- Hocking PJ, Pate JS. 1977.** Mobilization of minerals to developing seeds of legumes. *Annals of Botany* **41**: 1259–1278.
- Honda K, Smith MA, Zhu X, Baus D, Merrick WC, Tartakoff AM, Hattier T, Harris PL, Siedlak SL, Fujioka H, et al. 2005.** Ribosomal RNA in Alzheimer disease is oxidized by bound redox-active iron. *Journal of Biological Chemistry* **280**: 20978–20986.

- Hsiao C, Chou I-C, Okafor CD, Bowman JC, O'Neill EB, Athavale SS, Petrov AS, Hud N V., Wartell RM, Harvey SC, et al. 2013.** RNA with iron(II) as a cofactor catalyses electron transfer. *Nature Chemistry* **5**: 525–528.
- Dello Ioio R, Linhares FS, Scacchi E, Casamitjana-Martinez E, Heidstra R, Costantino P, Sabatini S. 2007.** Cytokinins determine Arabidopsis root-meristem size by controlling cell differentiation. *Current Biology* **17**: 678–682.
- Jackson M. 1986.** *New root formation in plants and cuttings*. Dordrecht: Martinus Nijhoff Publishers.
- Jefferson RA, Kavanagh TA, Bevan MW. 1987.** GUS fusions:  $\beta$ -glucuronidase as a sensitive and versatile gene fusion marker in higher plants. *The EMBO journal* **6**: 3901–3907.
- Kenrick P, Strullu-Derrien C. 2014.** The origin and early evolution of roots. *Plant Physiology* **166**: 570–580.
- Kevers C, Hausman JF, Faivre-Rampant O, Evers D, Gaspar T. 1997.** Hormonal control of adventitious rooting: progress and questions. *Angewandte Botanik* **71**: 71–79.
- Kiba T, Kudo T, Kojima M, Sakakibara H. 2011.** Hormonal control of nitrogen acquisition: roles of auxin, abscisic acid, and cytokinin. *Journal of Experimental Botany* **62**: 1399–1409.
- De Klerk G-J, Hanecakova J. 2008.** Ethylene and rooting of mung bean cuttings. The role of auxin induced ethylene synthesis and phase-dependent effects. *Plant Growth Regulation* **56**: 203–209.
- De Klerk G-J, Van Der Krieken W, Jong JC De. 1999.** The formation of adventitious roots: new concepts, new possibilities. *In Vitro Cellular & Developmental Biology* **35**: 189–199.
- Klopotek Y, Franken P, Klaering H-P, Fischer K, Hause B, Hajirezaei M-R, Druege U. 2016.** A higher sink competitiveness of the rooting zone and invertases are involved in dark stimulation of adventitious root formation in *Petunia hybrida* cuttings. *Plant Science* **243**: 10–22.
- Kojima M, Kamada-Nobusada T, Komatsu H, Takei K, Kuroha T, Mizutani M, Ashikari M, Ueguchi-Tanaka M, Matsuoka M, Suzuki K, et al. 2009.** Highly sensitive and high-throughput analysis of plant hormones using MS-probe modification and liquid chromatography-tandem mass spectrometry: an application for hormone profiling in *Oryza sativa*. *Plant & cell physiology* **50**: 1201–14.
- Köllmer I, Novák O, Strnad M, Schmölling T, Werner T. 2014.** Overexpression of the cytosolic cytokinin oxidase/dehydrogenase (*CKX7*) from Arabidopsis causes specific changes in root growth and xylem differentiation. *Plant Journal* **78**: 359–371.
- Krouk G, Lacombe B, Bielach A, Perrine-Walker F, Malinska K, Mounier E, Hoyerova K, Tillard P, Leon S, Ljung K, et al. 2010.** Nitrate-regulated auxin transport by *NRT1.1* defines a mechanism for nutrient sensing in plants. *Developmental Cell* **18**: 927–937.
- Kuroha T, Satoh S. 2007.** Involvement of cytokinins in adventitious and lateral root formation. *Plant Root* **1**: 27–33.

- Laplaze L, Benkova E, Casimiro I, Maes L, Vanneste S, Swarup R, Weijers D, Calvo V, Parizot B, Herrera-Rodriguez MB, et al. 2007.** Cytokinins act directly on lateral root founder cells to inhibit root initiation. *The Plant cell* **19**: 3889–3900.
- Lastdrager J, Hanson J, Smeekens S. 2014.** Sugar signals and the control of plant growth and development. *Journal of Experimental Botany* **65**: 799–807.
- Lavenus J, Goh T, Roberts I, Guyomarc'h S, Lucas M, De Smet I, Fukaki H, Beeckman T, Bennett M, Laplaze L. 2013.** Lateral root development in Arabidopsis: Fifty shades of auxin. *Trends in Plant Science* **18**: 1360–1385.
- LeClere S, Schmelz EA, Chourey PS. 2010.** Sugar levels regulate tryptophan-dependent auxin biosynthesis in developing maize kernels. *Plant Physiology* **153**: 306–318.
- Leopoldini M, Russo N, Chiodo S, Toscano M. 2006.** Iron chelation by the powerful antioxidant flavonoid quercetin. *Journal of Agricultural and Food Chemistry* **54**: 6343–6351.
- Li SW, Xue L, Xu S, Feng H, An L. 2009.** Mediators, genes and signaling in adventitious rooting. *Botanical Review* **75**: 230–247.
- Lima JE, Kojima S, Takahashi H, von Wirén N. 2010.** Ammonium triggers lateral root branching in Arabidopsis in an *AMMONIUM TRANSPORTER1;3*-dependent manner. *The Plant Cell* **22**: 3621–3633.
- Lindberg S, Greger M. 2002.** Plant genotypic differences under metal deficient and enriched conditions. In: Prasad MN, Strzałka K, eds. *Physiology and Biochemistry of Metal Toxicity and Tolerance in Plants*. Dordrecht: Springer Science+Business Media B.V, 357–393.
- Linkohr BI, Williamson LC, Fitter AH, Leyser HMO. 2002.** Nitrate and phosphate availability and distribution have different effects on root system architecture of Arabidopsis. *The Plant Journal* **29**: 751–760.
- Lischweski S, Muchow A, Guthörl D, Hause B. 2015.** Jasmonates act positively in adventitious root formation in petunia cuttings. *BMC plant biology* **15**: 229.
- Ljung K. 2013.** Auxin metabolism and homeostasis during plant development. *Development* **140**: 943–50.
- Logemann J, Shell J, Willmitzer L. 1987.** Improved method for the isolation of RNA from plant tissues. *Analytical Biochemistry* **20**: 16–20.
- López-Millán a F, Morales F, Abadía a, Abadía J. 2000.** Effects of iron deficiency on the composition of the leaf apoplastic fluid and xylem sap in sugar beet. Implications for iron and carbon transport. *Plant physiology* **124**: 873–884.
- Maillard A, Diquélou S, Billard V, Laine P, Garnica M, Prudent M, Garcia-Mina J-M, Yvin J-C, Ourry A. 2015.** Leaf mineral nutrient remobilization during leaf senescence and modulation by nutrient deficiency. *Frontiers in plant science* **6**: 317.
- Mallona I, Lischewski S, Weiss J, Hause B, Egea-Cortines M. 2010.** Validation of reference genes for quantitative real-time PCR during leaf and flower development in *Petunia hybrida*. *BMC plant biology* **10**: 4.
- Manzano AI, Larkin OJ, Dijkstra CE, Anthony P, Davey MR, Eaves L, Hill RJ a, Herranz R, Medina FJ. 2013.** Meristematic cell proliferation and ribosome biogenesis are decoupled in diamagnetically levitated Arabidopsis seedlings. *BMC plant biology* **13**: 124.

- Marschner P. 2012.** *Marschner's Mineral Nutrition of Higher Plants*. Boston MA: Academic Press.
- Mašev N, Kutáček M. 1966.** The effect of zinc on the biosynthesis of tryptophan, indol auxins and gibberellins in barley. *Biologia Plantarum* **8**: 142–151.
- Mergemann H, Sauter M. 2000.** Ethylene induces epidermal cell death at the site of adventitious root emergence in rice. *Plant physiology* **124**: 609–614.
- Mesén F, Newton AC, Leakey RRB. 1997.** The effects of propagation environment and foliar area on the rooting physiology of *Cordia alliodora* (Ruiz and Pavon) Oken cuttings. *Trees - Structure and Function* **11**: 404–411.
- Mifflin BJ, Habash DZ. 2002.** The role of glutamine synthetase and glutamate dehydrogenase in nitrogen assimilation and possibilities for improvement in the nitrogen utilization of crops. *Journal of experimental botany* **53**: 979–987.
- Miyashita Y, Good AG. 2008.** Glutamate deamination by glutamate dehydrogenase plays a central role in amino acid catabolism in plants. *Plant Signaling & Behavior* **3**: 842–843.
- Moreira a., Fageria NK. 2009.** Yield, uptake, and retranslocation of nutrients in banana plants cultivated in upland soil of central amazonian. *Journal of Plant Nutrition* **32**: 443–457.
- Moreno-Risueno MA, Norman JM Van, Moreno A, Zhang J, Ahnert SE, Benfey PN. 2011.** Oscillating gene expression determines competence for periodic Arabidopsis root branching. *Science* **329**: 1306–1311.
- Murashige T. 1974.** Plant propagation through tissue cultures. *Annual Review of Plant Physiology* **25**: 135–166.
- National Agricultural Statistics Service, USDA. 2016.** *Floriculture Crops 2015 Summary (April 2016)*.
- Negishi N, Nakahama K, Urata N, Kojima M, Sakakibara H, Kawaoka A. 2014.** Hormone level analysis on adventitious root formation in *Eucalyptus globulus*. *New Forests* **45**: 577–587.
- Niu S, Li Z, Yuan H, Fang P, Chen X, Li W. 2013.** Proper gibberellin localization in vascular tissue is required to regulate adventitious root development in tobacco. *Journal of Experimental Botany* **64**: 3411–3424.
- Pandey A, Sharma M, Pandey GK. 2016.** Emerging roles of strigolactones in plant responses to stress and development. *Frontiers in Plant Science* **7**: 1–17.
- Pellicer V, Guehl J-M, Daudet F-A, Cazet M, Riviere LM, Maillard P. 2000.** Carbon and nitrogen mobilization in *Larix x eurolepis* leafy stem cuttings assessed by dual <sup>13</sup>C and <sup>15</sup>N labeling: relationships with rooting. *Tree physiology* **20**: 807–814.
- Peret B, Swarup K, Ferguson A, Seth M, Yang Y, Dhondt S, James N, Casimiro I, Perry P, Syed A, et al. 2012.** AUX/LAX genes encode a family of auxin influx transporters that perform distinct functions during Arabidopsis development. *The Plant Cell* **24**: 2874–2885.
- Perez-Torres CA, Lopez-Bucio J, Cruz-Ramirez A, Ibarra-Laclette E, Dharmasiri S, Estelle M, Herrera-Estrella L. 2008.** Phosphate availability alters lateral root development in Arabidopsis by modulating auxin sensitivity via a mechanism involving the *TIR1* auxin receptor. *Plant Cell* **20**: 3258–3272.

- Petricka JJ, Winter CM, Benfey PN. 2012.** Control of Arabidopsis root development. *Annual review of plant biology* **63**: 563–590.
- Pijut PM, Woeste KE, Michler CH. 2011.** Promotion of adventitious root formation of difficult-to-root hardwood tree species. *Horticultural Reviews* **38**: 213–251.
- Ponnu J, Wahl V, Schmid M. 2011.** Trehalose-6-phosphate: Connecting plant metabolism and development. *Frontiers in Plant Science* **2**: 70.
- Pop TI, Pamfil D, Bellini C. 2011.** Auxin control in the formation of adventitious roots. *Notulae Botanicae Horti Agrobotanici Cluj-Napoca* **39**: 307–316.
- Puig J, Pauluzzi G, Guiderdoni E, Gantet P. 2012.** Regulation of shoot and root development through mutual signaling. *Molecular Plant* **5**: 974–983.
- Ramireddy E, Chang L, Schmölling T. 2014.** Cytokinin as a mediator for regulating root system architecture in response to environmental cues. *Plant signaling & behavior* **9**: 37–41.
- Ramirez-Carvajal GA, Davis JM. 2010.** Identifying regulators of adventitious rooting. *Plant signaling & behavior* **5**: 281–283.
- Rapaka VK, Bessler B, Schreiner M, Druege U. 2005.** Interplay between initial carbohydrate availability, current photosynthesis, and adventitious root formation in Pelargonium cuttings. *Plant Science* **168**: 1547–1560.
- Raven JA, Edwards D. 2001.** Roots: evolutionary origins and biogeochemical significance. *Journal of experimental botany* **52**: 381–401.
- Reyt G, Boudouf S, Boucherez J, Gaymard F, Briat JF. 2015.** Iron- and ferritin-dependent reactive oxygen species distribution: Impact on arabidopsis root system architecture. *Molecular Plant* **8**: 439–453.
- Riefler M, Novak O, Strnad M, Schmu T. 2006.** Arabidopsis cytokinin receptor mutants reveal functions in shoot growth, leaf senescence, seed size, germination, root development, and cytokinin metabolism. **18**: 40–54.
- Ritchie RJ. 2006.** Consistent sets of spectrophotometric chlorophyll equations for acetone, methanol and ethanol solvents. *Photosynthesis Research* **89**: 27–41.
- Röber R. 1976.** Nitrogen and potassium nutrition of chrysanthemum mother plants and their influence upon quantity and quality of cuttings. *Acta Horticulturae* **64**: 47–53.
- Robles L, Stepanova A, Alonso J. 2013.** Molecular mechanisms of ethylene-auxin interaction. *Molecular Plant* **6**: 1734–1737.
- Roschzttardtz H, Conéjéro G, Curie C, Mari S. 2009.** Identification of the endodermal vacuole as the iron storage compartment in the Arabidopsis embryo. *Plant physiology* **151**: 1329–38.
- Roschzttardtz H, Grillet L, Isaure M-P, Conéjéro G, Ortega R, Curie C, Mari S. 2011.** Plant cell nucleolus as a hot spot for iron. *The Journal of biological chemistry* **286**: 27863–6.
- Della Rovere F, Fattorini L, D’Angeli S, Velocchia A, Falasca G, Altamura MM. 2013.** Auxin and cytokinin control formation of the quiescent centre in the adventitious root apex of arabidopsis. *Annals of Botany* **112**: 1395–1407.

- Růžicka K, Šimášková M, Duclercq J, Petrášek J, Zažimalová E, Simon S, Friml J, Van Montagu MCE, Benková E. 2009. Cytokinin regulates root meristem activity via modulation of the polar auxin transport. *Proceedings of the National Academy of Sciences of the United States of America* **106**: 4284–4289.
- De Rybel B, Mähönen AP, Helariutta Y, Weijers D. 2015. Plant vascular development: from early specification to differentiation. *Nature reviews. Molecular cell biology* **17**: 30–40.
- Sairanen I, Novak O, Pencik A, Ikeda Y, Jones B, Sandberg G, Ljung K. 2012. Soluble carbohydrates regulate auxin biosynthesis via *PIF* proteins in Arabidopsis. *The Plant Cell* **24**: 4907–4916.
- Sambrook J, Fritsch EF, Maniatis T. 1989. *Molecular cloning: a laboratory manual* (J Sambrook, EF Fritsch, and T Maniatis, Eds.). New York: Cold Spring Harbor Laboratory.
- Sánchez C, Vielba JM, Ferro E, Covelo G, Solé A, Abarca D, de Mier BS, Díaz-Sala C. 2007. Two *SCARECROW-LIKE* genes are induced in response to exogenous auxin in rooting-competent cuttings of distantly related forest species. *Tree physiology* **27**: 1459–1470.
- Santos KM, Fisher PR. 2009. Stem versus foliar uptake during propagation of *Petunia x hybrida* vegetative cuttings. *HortScience* **44**: 1974–1977.
- Saslowky DE, Warek U, Winkel BSJ. 2005. Nuclear localization of flavonoid enzymes in Arabidopsis. *Journal of Biological Chemistry* **280**: 23735–23740.
- Schaesberg N, von Ludders P. 1993. Adventitious rooting of mango (*Mangifera indica* L.) cuttings after pretreatment of stock plants. II. N-level and NO<sub>3</sub>/NH<sub>4</sub>-ratio in the nutrition. *Gartenbauwissenschaft* **58**: 280–285.
- Scheres B, Wolkenfelt H, Willemsen V, Terlouw M, Lawson E, Dean C, Weisbeek P. 1994. Embryonic origin of the Arabidopsis primary root and root meristem initials. *Development* **2487**: 2475–2487.
- Schwambach J, Fadanelli C, Fett-Neto AG. 2005. Mineral nutrition and adventitious rooting in microcuttings of *Eucalyptus globulus*. *Tree physiology* **25**: 487–494.
- Seago JL, Fernando DD. 2013. Anatomical aspects of angiosperm root evolution. *Annals of Botany* **112**: 223–238.
- Sekimoto H, Hoshi M, Nomura T, Yokota T. 1997. Zinc deficiency affects the levels of endogenous gibberellins in *Zea mays* L. *Plant and Cell Physiology* **38**: 1087–1090.
- Shao R, Wang K, Shangguan Z. 2010. Cytokinin-induced photosynthetic adaptability of *Zea mays* L. to drought stress associated with nitric oxide signal: Probed by ESR spectroscopy and fast OJIP fluorescence rise. *Journal of Plant Physiology* **167**: 472–479.
- De Smet I, Signora L, Beeckman T, Foyer CH, Zhang H. 2003. An abscisic acid-sensitive checkpoint in lateral root development of Arabidopsis. *The Plant Journal* **33**: 543–555.
- Smith MA, Harris PL, Sayre LM, Perry G. 1997. Iron accumulation in Alzheimer disease is a source of redox-generated free radicals. *Proceedings of the National Academy of Sciences of the United States of America* **94**: 9866–8.
- Sorin C, Bussell JD, Camus I, Ljung K, Kowalczyk M, Geiss G, McKhann H, Garcion C, Vaucheret H, Sandberg G, et al. 2005. Auxin and light control of adventitious rooting in Arabidopsis require *ARGONAUTE1*. *The Plant cell* **17**: 1343–1359.



- Steedman HF. 1957.** Polyester wax: a new ribboning embedding medium for histology. *Nature* **179**: 1345–1345.
- Steffens B, Rasmussen A. 2016.** The physiology of adventitious roots. *Plant Physiology* **44**: 603–617.
- Steffens B, Sauter M. 2005.** Epidermal cell death in rice is regulated by ethylene, gibberellin, and abscisic acid. *Plant Physiology* **139**: 713–721.
- Steffens B, Wang J, Sauter M. 2006.** Interactions between ethylene, gibberellin and abscisic acid regulate emergence and growth rate of adventitious roots in deepwater rice. *Planta* **223**: 604–612.
- Sukumar P, Maloney GS, Muday GK. 2013.** Localized induction of the *ATP-binding cassette B19* auxin transporter enhances adventitious root formation in Arabidopsis. *Plant physiology* **162**: 1392–405.
- Svenson SE, Davies FT, Duray SA. 1995.** Gas exchange, water relations, and dry weight partitioning during root initiation and development of poinsettia cuttings. *Journal of the American Society for Horticultural Science* **120**: 454–459.
- Swarup K, Benková E, Swarup R, Casimiro I, Péret B, Yang Y, Parry G, Nielsen E, De Smet I, Vanneste S, et al. 2008.** The auxin influx carrier *LAX3* promotes lateral root emergence. *Nature cell biology* **10**: 946–54.
- Taylor AR, Bloom AJ. 1998.** Ammonium, nitrate, and proton fluxes along the maize root. *Plant, Cell and Environment* **21**: 1255–1263.
- Thompson AJ, Thorne ET, Burbidge A, Jackson AC, Sharp RE, Taylor IB. 2004.** Complementation of *notabilis*, an abscisic acid-deficient mutant of tomato: Importance of sequence context and utility of partial complementation. *Plant, Cell and Environment* **27**: 459–471.
- Twardowski CM, Crocker JL, Freeborn JR, Scoggins HL. 2012.** Quantity and quality of cuttings as influenced by stock plant nutrition of herbaceous perennials. *HortTechnology* **22**: 89–93.
- United States Department of Agriculture. 2016.** *Floriculture Crops 2015 Summary (April 2016)*.
- Vandenbussche M, Chambrier P, Rodrigues Bento S, Morel P. 2016.** Petunia, your next supermodel? *Frontiers in Plant Science* **7**: 1–11.
- Veierskov B, Andersen AS, Stiumann BM, Henningsen KW. 1982.** Dynamics of extractable carbohydrates in *Pisum sativum*. II. Carbohydrate content and photosynthesis of pea cuttings in relation to irradiance and stock plant temperature and genotype. *Physiologia Plantarum* **55**: 174–178.
- Verstraeten I, Schotte S, Geelen D. 2014.** Hypocotyl adventitious root organogenesis differs from lateral root development. *Frontiers in Plant Science* **5**: 1–13.
- Vert G, Grotz N, Dédaldéchamp F, Gaymard F, Guerinot L, Briat J, Curie C. 2002.** *IRT1*, an Arabidopsis transporter essential for iron uptake from the soil and for plant growth. *The Plant Cell* **14**: 1223–1233.
- Vidal N, Arellano G, San-José MC, Vieitez a M, Ballester a. 2003.** Developmental stages during the rooting of in-vitro-cultured *Quercus robur* shoots from material of juvenile and mature origin. *Tree physiology* **23**: 1247–54.

- Wang L, Ruan Y-L. 2013.** Regulation of cell division and expansion by sugar and auxin signaling. *Frontiers in plant science* **4**: 163.
- Warren CR. 2008.** Rapid measurement of chlorophylls with a microplate reader. *Journal of Plant Nutrition* **31**: 1321–1332.
- Werner T, Motyka V, Laucou V, Smets R, Onckelen H Van, Schmuelling T. 2003.** Cytokinin-deficient transgenic Arabidopsis plants show functions of cytokinins in the regulation of shoot and root meristem activity. *The Plant cell* **15**: 2532–2550.
- Werner T, Motyka V, Strnad M, Schmuelling T. 2001.** Regulation of plant growth by cytokinin. *Proceedings of the National Academy of Sciences of the United States of America* **98**: 10487–92.
- Wik RM, Fisher PR, Kopsell DA, Argo WR. 2006.** Iron form and concentration affect nutrition of container-grown *Pelargonium* and *Calibrachoa*. *HortScience* **41**: 244–251.
- Winterbourn CC. 1995.** Toxicity of iron and hydrogen peroxide: the Fenton reaction. *Toxicology Letters* **82-83**: 969–974.
- von Wirén N, Klair S, Bansal S, Briat J-F, Khodr H, Shioiri T, Leigh R a., Hider RC. 1999.** Nicotianamine chelates both Fe(III) and Fe(II). Implications for metal transport in plants. *Plant physiology* **119**: 1107–1114.
- Xiong Y, McCormack M, Li L, Hall Q, Xiang C, Sheen J. 2013.** *Glc-TOR* signalling leads transcriptome reprogramming and meristem activation. *Nature* **496**: 181–186.
- Xu M, Zhu L, Shou H, Wu P. 2005.** A *PIN1* family gene, *OsPIN1*, involved in auxin-dependent adventitious root emergence and tillering in rice. *Plant and Cell Physiology* **46**: 1674–1681.
- Zerche S, Druege U. 2009.** Nitrogen content determines adventitious rooting in *Euphorbia pulcherrima* under adequate light independently of pre-rooting carbohydrate depletion of cuttings. *Scientia Horticulturae* **121**: 340–347.
- Zhang C. 2014.** Essential functions of iron-requiring proteins in DNA replication, repair and cell cycle control. *Protein & Cell* **5**: 750–760.
- Zhang H, Forde BG. 1998.** An Arabidopsis *MADS* box gene that controls nutrient-induced changes in root architecture. *Science* **279**: 407–410.

## 8. Appendix

Appendix Table 1. Method for combined conventional and microwave-proceeded fixation, dehydration and resin embedding of petunia stem cutting samples.

Process	Reagent	Power, W	Time, sec	Vacuum, mmHg
1. Primary fixation	2 % (v/v) glutaraldehyde and 2 % (w/v) paraformaldehyde in 0.05 M cacodylate buffer (pH 7.3)	150	60	15
		0	60	15
		150	60	15
		0	60	15
		150	60	15
Followed by incubation for 16h on a rotary shaker at RT				
2. Washing	0.05 M cacodylate buffer (pH 7.3) - bidistilled water, repeated two times	150	45	0
		150	45	0
3. Secondary fixation	1% (w/v) OsO <sub>4</sub>	0	60	0
		80	120	15
		0	60	0
		80	120	15
Followed by incubation for 45 min on a rotary shaker at RT				
4. Washing	bidistilled water, repeated three times	150	45	0
5. Dehydration	100 % acetone 30 %, 40 %, 50 %, 60 %, 70 %, 80 %, 90 % acetone in propylenoxide - 100 % propylenoxide	150	45	0
		150	45	0
		150	45	0
		Each step followed by incubation for 20 min on a rotary shaker at RT		
6. Resin infiltration	Spurr's resin in propylenoxide: - 20 % - 40 %, 60 %, 80 % - 100 % Spurr's resin	Incubation on shaker at RT:		
		12 h		
		3h		
		12 h		
7. Polymerization	Transfer of samples into BEEM capsules with fresh Spurr's resin 24 h at 70°C in a heating cabinet			

Appendix Table 2 Settings for MS/MS analysis of phytohormones

Compound	Precursor ion	Product ion	Dwell time	Collision energy	Polarity
<b>Auxins</b>					
<sup>2</sup> H5]-Indole-3-Acetic Acid	181.1	134	20	28	+
	181.1	106	20	28	+
	181.1	80	20	50	+
Indole-3-Acetic Acid	176.07	130	20	28	+
	176.07	103	20	30	+
	176.07	77	20	58	+
Oxindole-3-Acetic Acid	192.07	135	20	22	+
	192.07	107	20	34	+
	192.07	77	20	50	+
<b>Cytokinins</b>					
<sup>15</sup> N4]- <i>cis</i> -Zeatin	224.07	140	20	20	+
	224.07	123	20	20	+
<sup>2</sup> H3]-Dihydrozeatin riboside	357.2	225	20	22	+
	357.2	149	20	50	+
	357.2	137	20	46	+
<sup>2</sup> H5]- <i>trans</i> -Zeatin riboside	357.21	225	20	21	+
	357.21	137	20	41	+
<sup>2</sup> H5]- <i>trans</i> -Zeatin	225.15	148	20	9	+
	225.15	137	20	21	+
<sup>2</sup> H6]-N6-Isopentenyladenine	210.16	137	20	13	+
	210.16	75	20	9	+
<i>cis</i> -Zeatin riboside	352.16	220	20	17	+
	352.16	136	20	45	+
	352.16	119	20	54	+
<i>cis</i> -Zeatin	220.12	136	20	17	+
	220.12	119	20	33	+
Dihydrozeatinriboside	354.18	222	20	21	+
	354.18	148	20	40	+
	354.18	136	20	45	+
N6-Isopentenyladenine	204.13	148	20	9	+
	204.13	136	20	17	+
	204.13	119	20	37	+
<i>trans</i> -Zeatin riboside	352.16	220	20	13	+
	352.16	136	20	41	+
<i>trans</i> -Zeatin	220.12	136	20	13	+
	220.12	119	20	33	+
<b>ABA &amp; Derivatives</b>					
<sup>2</sup> H6]-Abscisic acid	269	210	5.6	20	-
	269	158	5.6	20	-
Abscisic acid	263	219	5.4	10	-
	263	201	5.4	20	-
	263	153	5.4	20	-
Dihydrophaseic acid	281	237	3.3	14	-
	281	171	3.3	18	-
	281	123	3.3	18	-

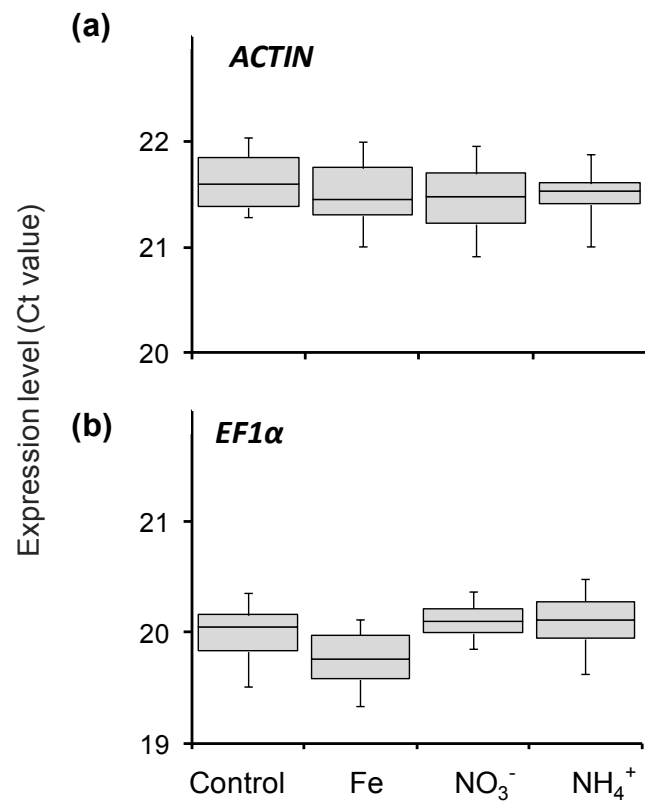
Appendix Table 3 Settings for MS/MS analysis of primary metabolites

Compound	Precursor ion	Product ion	Dwell time	Collision energy	Polarity
<i>cis</i> -Aconitate	173.1	85	20	9	-
	173.1	128.9	20	1	-
Citrate	191	86.8	20	13	-
	191	110.8	20	15	-
Fructose 6-phosphate	259	78.9	20	44	-
	259	96.8	20	9	-
Fumarate	115	70.9	20	1	-
Glucose 1-phosphate	259	78.9	20	44	-
	259	96.8	20	9	-
Glucose 6-phosphate	259	78.9	20	44	-
	259	96.8	20	9	-
Malate	133	71	20	9	-
	133	115	20	5	-
Oxoglutarate	145.1	101	20	5	-
3-Phosphoglyceric acid	185.1	78.8	20	41	-
	185.1	96.8	20	20	-
Succinate	116.9	73	20	5	-
Sucrose 6-phosphate	421	79.1	20	53	-
	421	96.8	20	33	-
Trehalose 6-phosphate	421	139	20	29	-
	421	240.9	20	25	-
UDP-Glucose	565	158.9	20	53	-
	565	322.9	20	25	-

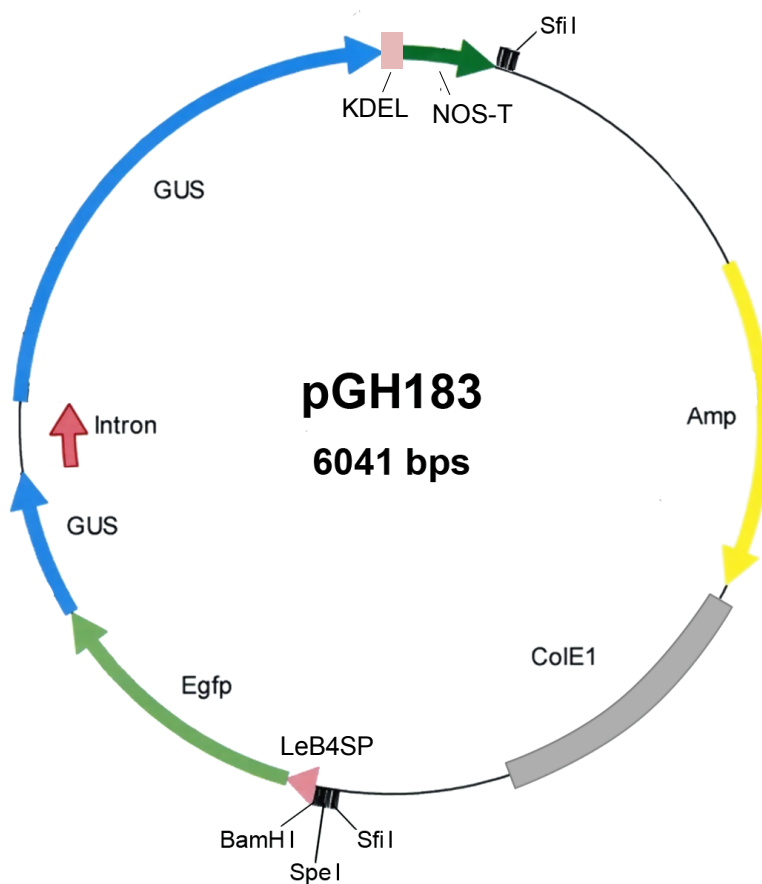
Appendix Table 4. Primers used to study the transcript abundance of marker genes for cell division, nutrient acquisition and auxin homeostasis in *Petunia hybrida*

Primer ID	Sequence ID *	Forward primer (5'-3')	Reverse primer (5'-3')
ABCB	GO_drpoolB-CL9304Contig1	TCAACTGGTGCTGTTTGCTC	AACTAGGCCCAATTGTGCAAG
ACTIN	cn1159	TCAGATTTGCTGGCATGAAG	ATTGTCCAAAAGCAAGGATGG
AMT1	GO_drs12P0011A24_F_ab1	TGCTAAAGGGAGCTATGTGGA	TGGATTATATGTGCCCCCAAG
ARF6	cn8216	CAGAAATGCGGTTATGGGAAC	GGTCATCACCAAGGAGAAGC
CycB1	GO_dr004P0003J17_F_ab1	GGTTACACGTCGTGTTGTTG	TCTGAGCTGCAGGTTTCCTT
Cyc2	GO_drpoolB-CL6689Contig1	ATGTCGAGGAACATGAGGCA	TGGATTCTTTGCATCATCACCA
IRT1	GO_drpoolB-CL5640Contig1	TTGCTCAATGCATCTTCTGC	GGACATTCCACCAGCACCTA
EF1 $\alpha$	cn2411	CCTGGTCAAATTGGAAACGG	GATGCGCTGTCAATCTTGG
FERRITIN	cn442	CAGAACAAGCGTGGTGAAA	ACGTCGTTGTTTTCTGAGGC
FRO2	FN032862	TGTGTGGAAGCAGGTCCATA	TTCAAAAATTGCAATGGCATC
GDH	GO_drpoolB-CL2357Contig1	GGCTTTATGTGGGATGAGGA	CCCATTCCGGAGATCACAGTT
GH3.6	GO_drs13P0001D08_F_ab1	GAGTTGGTGATGTGCTTCGG	TGTGCATCAAAATGGCATCAGA
GS1	cn1768	CCGATCCTTCAAAGCTACCA	CGCACATGACCGAGATATTG
GS2	cn6059	TTCATGGGGAGTTGCTAACC	TAGGGTCCATGTTTGAAGC
LAX1	GO_drpoolB-CL374Contig1	AATTATGCATGCCATGTGGA	GATCTCCGAATGCCCCAGTAA
LAX3	GO_drs31P0009M18_F_ab1	GCGAGCGATGGCTAGACTAC	CATGTGTGCTAAGGCAGGAA
NAS	GO_drpoolB-CL2413Contig1	TGGCTCTTATGAAAACCCCACT	GGAGAGGCGCTGATCCAAATA
NRT1	cn7729	AGCCCATTTGTAACGTATTGC	TAGTATTAGCATCATTTGTCAATCC
PIN1	FN027417	TGTCAGCTGCAATGAACCTT	TGGTTCAGTCAAATGGTGGA
TAR1	cn7627	TTGCTCAAATGACACTGGCT	TGGACAAAAGAGGTGGCAAGA
TAR4	GO_dr001P0018K18_F_ab1	AGCTTACTGGTCATGCTGGA	TGAGATCCCCCATTTTCAGCCA

\* The corresponding sequence ID is given according to EST database previously generated for microarray analysis (Ahkami *et al.*, 2014)

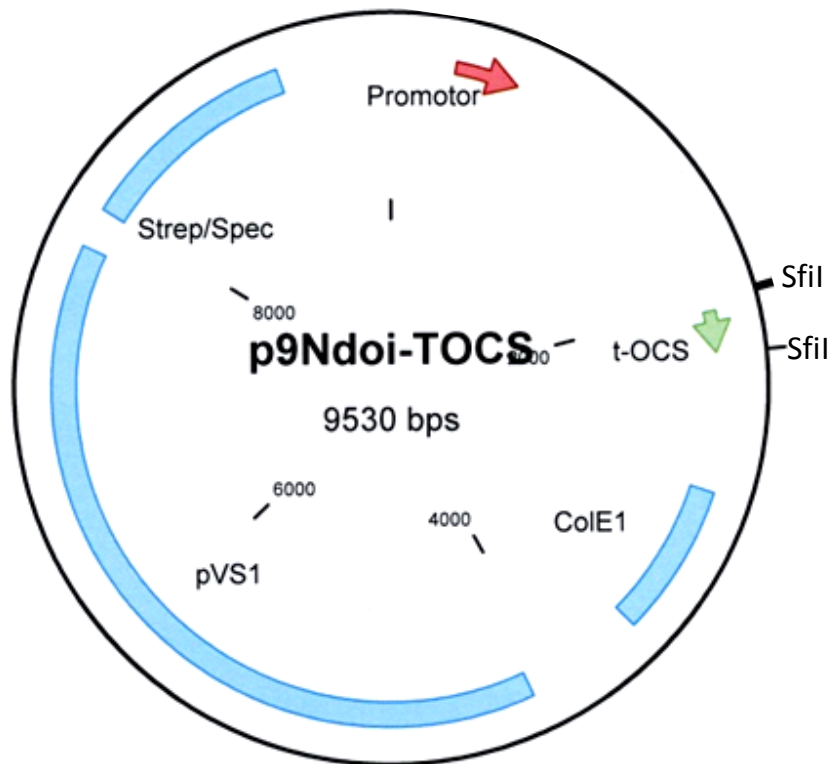


**Appendix Fig. 1** RT-qPCR analysis of transcript abundance of *ACTIN7* (a) gene in comparison to *EF1α* (b) in stem bases of *Petunia hybrida* cuttings supplied with iron, ammonium or nitrate. Global expression levels (Ct values) in 0, 1 and 7 dpe are shown as 25<sup>th</sup> and 75<sup>th</sup> percentiles (top and bottom box borders); median values (middle horizontal line); minimal and maximal values (whiskers).

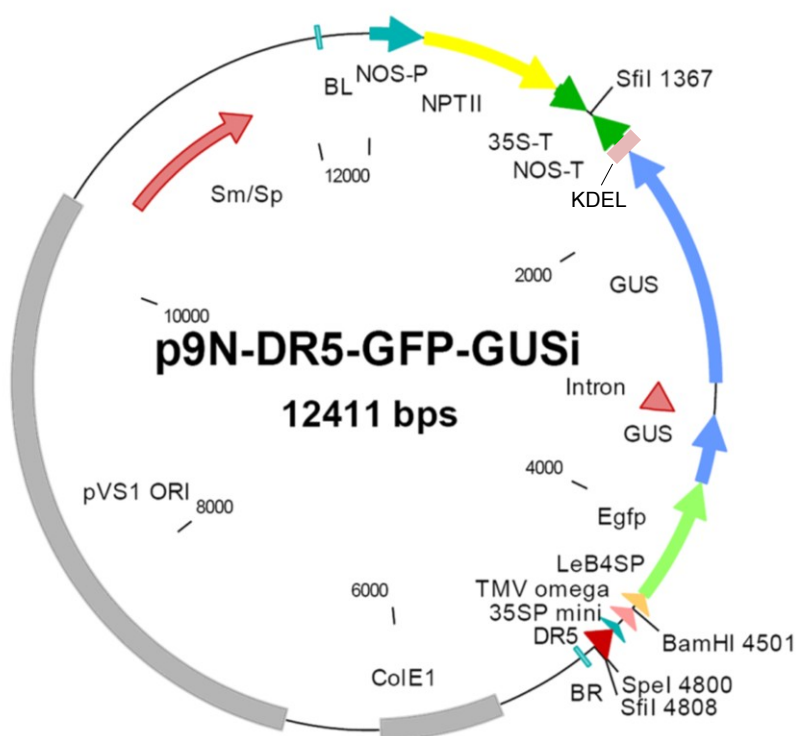


**Appendix Fig. 2** The vector map of pGH183, used for generation of DR5::GFP/GUS auxin-reporter petunia plants. Amp, gene for resistance to ampicillin; ColE1, replication origin; EGFP, enhanced green fluorescent protein; GUS,  $\beta$ -glucuronidase; KDEL, signal peptide for endoplasmic reticulum localization, LeB4SP, legumin B4 signal peptide for endoplasmic reticulum localization; NOS-T, terminator of a nopaline synthase gene. Only restriction sites for BamHI, SfiI and SpeI, used for subsequent cloning procedures, are shown within the multiple cloning sites.





**Appendix Fig. 3** The vector map of p9Ndoi-TOCS, used for generation of DR5::GFP/GUS auxin-reporter petunia plants. ColE1, replication origin from ColE1 plasmid; Strep/Spec, gene for resistance to spectinomycin and streptomycin; pVS1, minimal replication origin of the pVS1 plasmid, t-OCS, terminator of an octopine synthase gene. Only restriction sites for SfiI, used for subsequent cloning procedures, are shown.



**Appendix Fig. 4** The map of the resulting chimeric vector p9N-DR5-GFP-GUSi, used for generation of DR5::GFP/GUS auxin-reporter petunia plants. BR/BL, the left and right border sequences of T-DNA; CoIE1, replication origin; DR5, synthetic auxin-responsive promoter; Egfp, enhanced green fluorescent protein; GUS,  $\beta$ -glucuronidase; KDEL, signal peptide for endoplasmic reticulum localization, LeB4SP, legumin B4 signal peptide for endoplasmic reticulum localization; NOS-P, promoter of a nopaline synthase gene; NOS-T, terminator of a nopaline synthase gene; NPTII, neomycin phosphotransferase gene for kanamycin resistance; pVS1 ORI, minimal replication origin of the pVS1 plasmid; Strep/Spec, gene for resistance to spectinomycin and streptomycin; TMV omega, leader sequence of tobacco mosaic virus; t-OCS, terminator of an octopine synthase gene. Only restriction sites for BamHI, SfiI and SpeI, used for cloning procedures, are shown.

## 9. Publications and proceedings related to the submitted thesis

**Hilo A.**, Shahinnia F., Druége U., Franken P., Melzer M., Rutten T., von Wiren N., Hajirezaei M.-R. 2017. A specific role of iron in promoting meristematic cell division during adventitious root formation (In press)

**Hilo A.**, Shahinnia F., Druége U., Franken P., von Wiren N., Hajirezaei M.-R. 2014. Improvement of adventitious root formation in *Petunia* cuttings by targeted nutrient application at critical developmental stages. *17<sup>th</sup> International Symposium on Iron nutrition and Interactions in Plants (ISINIP'17)*. Gatersleben, Germany. 06 – 10 July 2014. Book of Abstracts, p. 59.

**Hilo A.**, Shahinnia F., Druége U., Franken P., von Wiren N., Hajirezaei M.-R. 2014. Improvement of adventitious root formation in *Petunia hybrida* cuttings by targeted nutrient application. *7<sup>th</sup> International Symposium on Root Development Rooting 2014*. Weimar, Germany. 15 – 19 September 2014. Book of Abstracts, p. 139

**Hilo A.**, Shahinnia F., Druége U., Franken P., von Wiren N., Hajirezaei M.-R. 2015. Improvement of adventitious root formation in *Petunia* cuttings by targeted nutrient application. *14<sup>th</sup> World Petunia Days*. Fribourg, Switzerland. 09 –12 April 2015. Book of Abstracts, p. 9

**Hilo A.**, Shahinnia F., Druége U., Franken P., von Wiren N., Hajirezaei M.-R. 2016. Improvement of adventitious root formation in *Petunia* cuttings by targeted application of iron and ammonium. *18<sup>th</sup> International Symposium on Iron nutrition and Interactions in Plants (ISINIP'18)*. Madrid, Spain. 30 May – 3 June 2016. Book of Abstracts

**Hilo A.**, Hajirezaei M.-R. 2016. Improvement of adventitious root formation in *P. hybrida* cuttings by targeted nutrient application. *15<sup>th</sup> World Petunia Days*. Wittenberg, Germany. 9 – 11 September 2016. Book of Abstracts, p. 9

## 10. Declaration

I hereby declare that this thesis has been written by me without having used other than mentioned references and resources. This thesis has been submitted in neither its original nor similar form for the purpose of academic examination.

Hiermit erkläre ich, dass ich diese Arbeit selbständig und nur unter Zuhilfenahme der angegebenen Hilfsmittel und Literatur angefertigt habe. Ich versichere, dass diese Arbeit von mir bisher weder der Naturwissenschaftliche Fakultät I - Biowissenschaften der Martin-Luther- Universität Halle-Wittenberg noch einer anderen wissenschaftlichen Einrichtung zum Zweck der Promotion eingereicht wurde.

Gatersleben, den .....

---

Alexander Hilo

## 11. Curriculum vitae

### **Personal information:**

Name: Alexander Hilo

Address: 06466, Hans-Stubbe Str. 18, Gatersleben, Germany

Phone / E-mail: +4915168174743; [hilo@ipk-gatersleben.de](mailto:hilo@ipk-gatersleben.de); [hilo.alexander@gmail.com](mailto:hilo.alexander@gmail.com)

Date of Birth: February 17, 1986

Place of Birth: Molodechno, Minskaja Woblasz, Belarus

### **Academic education:**

**Ph.D.**; Plant Molecular Physiology, Martin Luther University, Halle, Germany (Mar. 2013 – Feb. 2017), Thesis prepared at: Leibniz Institute of Plant Genetics and Crop Plant Research (IPK), Molecular plant nutrition group, Gatersleben, Germany

Thesis title: The specific role of iron in promoting adventitious root formation in petunia cuttings

**Diploma** (Sep. 2004 – July 2009) Belarusian State University, Faculty of Biology, Department of Genetics, Minsk, Belarus.

Thesis title: Characterization of native Gram-positive naphthalene-utilizing bacteria.

### **Employment:**

**2013 – 2017** Ph.D. student at Leibniz Institute of Plant Genetics and Crop Plant Research (IPK), Molecular plant nutrition group, Gatersleben, Germany. Project: Improvement of adventitious root formation in Petunia cuttings by targeted nutrient application at critical developmental stages.

**2010 – 2013** Junior research fellow at Republican Research Center for Epidemiology and Microbiology, Laboratory of natural reservoir infections, Minsk, Belarus. Projects: Genetic diversity of epidemically significant non-polio Enteroviruses in Belarus. Development of ELISA diagnostic kit for detection of anti-Enterovirus IgM.

**2009 – 2010** Junior research fellow at Institute of Microbiology, National Academy of Sciences, Laboratory of Xenobiotic Degradation and Bioremediation of Natural and Industrial Media, Minsk, Belarus. Project: Characterization of biosurfactant production by oil-degrading bacteria.

**2008 – 2009** Research assistant at Belarusian State University, Faculty of Biology, Department of Genetics, Minsk, Belarus.